Ann. Naturhist. Mus. Wien	110 A	313–329	Wien, Jänner 2009

PROCEEDINGS
1st Correlation of Cretaceous Micro- and Macrofossils Meeting

New biostratigraphic ammonite data from the Jurassic/Cretaceous boundary at Nutzhof (Gresten Klippenbelt, Lower Austria)

By Alexander LUKENEDER[1]

(With 3 plates and 4 figures)

Manuscript submitted on September 4th 2008,
the revised manuscript on October 16th 2008

Abstract

Upper Jurassic to Lower Cretaceous ammonites were collected at the Nutzhof locality in the eastern part of the Gresten Klippenbelt in Lower Austria. The cephalopod fauna from the Blassenstein Formation, correlated with micro- and nannofossil data from the marly unit and the limestone unit, indicates Early Tithonian to Middle Berriasian age (*Hybonoticeras hybonotum* Zone up to the *Subthurmannia occitanica* Zone). According to the correlation of the fossil and magnetostratigraphic data, the entire succession of the Nutzhof section embraces a duration of approx. 7 million years (approx. 150–143 Ma). The deposition of the limestones, marly limestones and marls in this interval occurred during depositionally (e.g. tectonics) unstable conditions.

The ammonite fauna comprises 6 different genera, each apparently represented by a single species. The occurrence at the Nutzhof section is dominated by ammonites of the perisphinctid-type. Ammonitina are the most frequent component (60 %; *Subplanites* and *Haploceras*), followed by the Phylloceratina (25 %; *Ptychophylloceras* and *Phylloceras*), and the Lytoceratina (15 %; represented by *Lytoceras* and *Leptotetragonites*). The ammonite fauna consists solely of Mediterranean elements.

Keywords: Ammonites, Jurassic/Cretaceous boundary, Gresten Klippenbelt, Lower Austria

Zusammenfassung

Ober-Jurassische und Unter-Kretazische Ammoniten der Lokalität Nutzhof im östlichen Teil der Grestener Klippenzone Niederösterreichs wurden untersucht. Die Cephalopoden Fauna der Blassenstein Formation zeigt unteres Tithonium bis mittleres Berriasium an (*Hybonoticeras hybonotum*-Zone bis *Subthurmannia occitanica*-Zone). Der Korrelation von Fossilien und magnetostratigraphischen Daten zufolge umfasst das gesamte Profil Nutzhof eine Dauer von an die 7 Millionen Jahre (ca. 150–143 Mio. J.). Die Kalke, mergeligen Kalke und Mergel dieses Abschnitts lagerten sich während instabiler (tektonisch) Ablagerungsbedingungen ab. Die Ammoniten Fauna zeigt 6 unterschiedliche Gattungen, von welchen jede durch nur eine Art vertreten ist. Das Vorkommen am Nutzhof wird durch Ammoniten vom Typ *Perisphinctidae* dominiert. Die Ammonitina stellen das häufigste Faunenelement dar (60 %; *Subplanites* und *Haploceras*), gefolgt von

---

[1] Natural History Museum Vienna, Geological-Palaeontological Department, Burgring 7, 1010 Vienna, Austria; e-mail: alexander.lukeneder@nhm-wien.ac.at

der Gruppe der Phylloceratina (25 %; *Ptychophylloceras und Phylloceras*) und den Lytoceratina (15 %; *Lytoceras* und *Leptotetragonites*). Die Ammoniten Fauna setzt sich ausschließlich aus mediterranen Elementen zusammen.

Schlüsselworte: Ammoniten, Jura/Kreide-Grenze, Grestener Klippenzone, Niederösterreich

1. Introduction

Jurassic and Lower Cretaceous pelagic sediments are well known to form a major element of the northernmost tectonic units of the Gresten Klippenbelt. In this Klippenbelt, Tithonian to Berriasian cephalopod-bearing deposits are recorded in 2 different facies, the Stollberger Schichten (KÜPPER 1962; GOTTSCHLING 1965) and the Blassenstein Formation (KÜHN 1962; DECKER 1990; DECKER & RÖGL 1988; PILLER et al. 2004). Upper Jurassic (Tithonian) sediments of the lower part of the Blassenstein Formation comprise marls, marly limestones and limestones (intercalated), whereas the upper part of the Blassenstein Formation at Nutzhof (Tithonian to Valanginian) is composed of very pure limestones (up to 97 % $CaCo_3$). The stratigraphy of the Lower Cretaceous sediments around the investigated area is mainly based on microfossils. The first study of the lithology and stratigraphy of this area was provided by CŽJŽEK (1852), followed a century later by KÜPPER (1962). The presented cephalopod fauna was collected in limestones and marly sediments of the Blassenstein Formation of the Gresten Klippenbelt.

Biostratigraphic data on the Stollberger Schichten of the Gresten Klippenbelt (Lower Austria) are remarkably scarce (CŽJŽEK 1852; KÜPPER 1962). This reflects the rare occurrence of identifiable ammonoid fauna as well as the absence or bad preservation of relevant microfossils. The discussed lithological (marls versus limestones) and biostratigraphic (Jurassic versus Cretaceous) boundary, however, is extraordinarily important for reconstructing pieninic geodynamics. They mark the initial siliciclastic input into the basin, reflecting the phase of the Penninic Ocean opening. The newly discovered outcrop at Nutzhof (fig. 1) in the heart of Lower Austria now fills the above gap. That section revealed, for the first time, the critical interval in an environment comprising extraordinarily rich accumulations of radiolaria, calpionellids, saccocomids, nannofossils and, in parts of the log, ammonites.

1.1 The history of the opening Penninic Ocean

The Penninic Ocean was initiated in the Late Triassic by rifting and disjunction of the Austroalpine microcontinent from the southern European Plate margin (SCOTESE 2001; STAMPFLI & MOSAR 1999). It was the eastern prolongation of the North Atlantic Rift-System, which effected the final disintegration of the Permotriassic Pangea Supercontinent (e.g. FAUPL 2003). The formation of the oceanic crust and the sea floor spreading lasted from the Middle Jurassic to the Early Cretaceous, terminating with the introduction of its southward-directed subduction beneath the northern Austroalpine plate margin (FAUPL & WAGREICH 2000; MANDIC & LUKENEDER). This tectonic mega-event is reflected by the lithological change in the middle part at the Nutzhof section. An increasing deepening, detected by the formation of different sediments (e.g. allodapic limestones and microturbidites), of the succession at Nutzhof marks the beginning of the opening of the Penninic Ocean. The pelagic carbonate sedimentation, which already started in the Late Jurassic, therefore changes within several meters of the section from a siliciclastic into pure limestone-dominated sedimentation. The history of the Penninic Ocean persisted from the Upper Jurassic through almost the whole Lower Cretaceous.

1.2. Depositional and tectonic setting

The studied section at Nutzhof includes the distal slope succession of the Gresten Klippenbelt, representing an independent and scarcely known part of the southern Rhenodanubian Flysch system. The Gresten Klippenbelt is tectonically intercalated within the

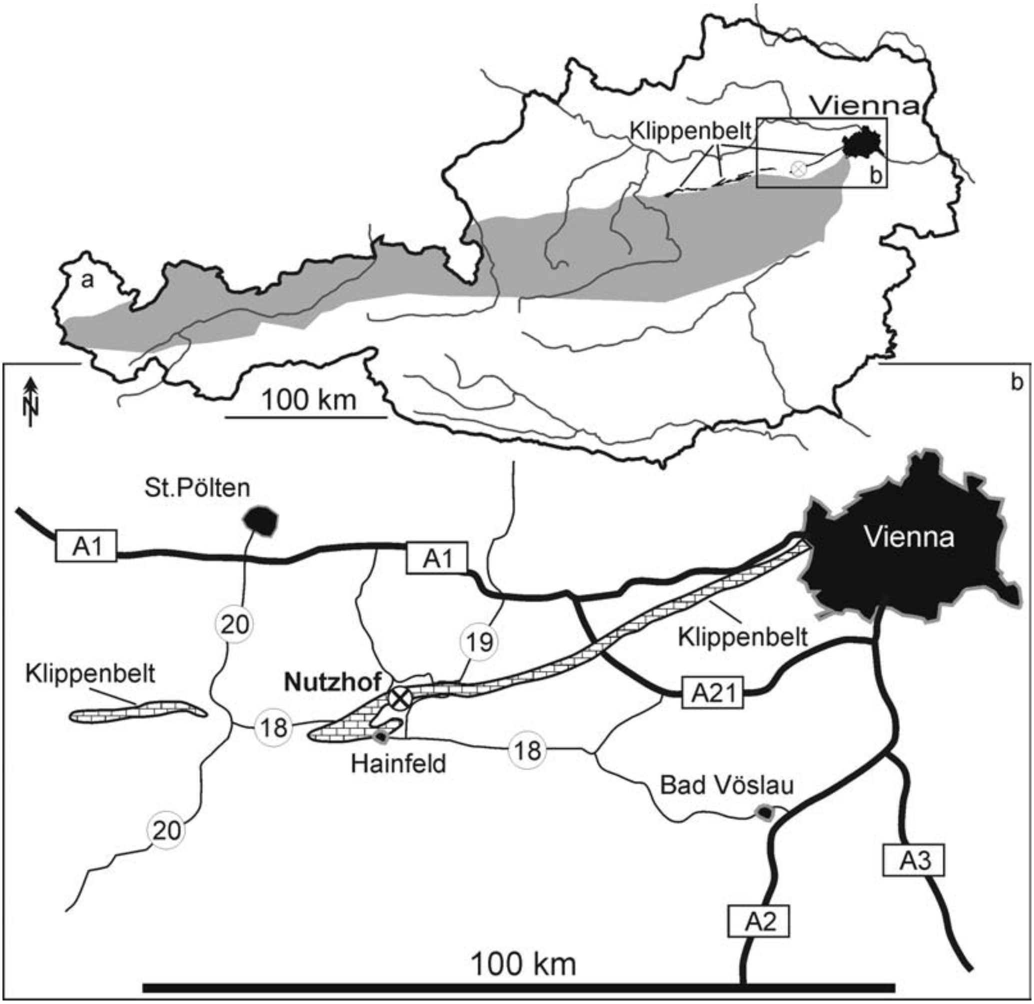

Fig. 1a: Locality map of Austria with indicated position of the Gresten Klippenbelt in Lower Austria. 1b: Detailed map of the area around Nutzhof showing the outcrop of Upper Jurassic – Lower Cretaceous sediments from the Gresten Klippenbelt (brick-structure).

latter zone as a thin, long, east-west striking marly and calcareous succession. The Upper Jurassic to Lower Cretaceous pelagic sediments of the Gresten Klippenbelt at Nutzhof represent a major sedimentation cycle. The significant depositional change from the siliciclastic to the carbonate depositional system is reflected in the boundary between the lower marly part and the upper calcareous part. Accordingly, the older (Tithonian) marly part features typically dark, laminated pelagic marls and marly limestones with intercalated limestone beds whose formation was triggered by erosion and intensive redeposition (e.g. allodapic limestones and microturbidites). This is comparable to the formation of the younger (Aptian) siliciclastic and marly Tannheim Formation (WAGREICH 2003). The younger part (limestones), on the other hand, represents the phase of autochthonous pelagic sedimentation with the light-colored, chert- and aptychi-bearing nannoconid limestones. The macro-invertebrate fauna of the Berriasian limestone succession is very sparse, comprising rare ammonites, aptychi, belemnites and brachiopods. The macro-invertebrate fauna of the Tithonian marl-limestone succession is rich in saccocomids accompanied by rare bivalves (inoceramids) and, in parts, abundant ammonites. The microfauna is in contrast abundant, with dominating calpionellids and radiolarians in the limestone succession and saccocomid blooms within the marl-limestone succession.

2. Geographical setting

The outcrop is situated in the Gresten Klippenbelt in Lower Austria. The exact position is about 20 km south of Böheimkirchen and 5 km north of Hainfeld (600 m, ÖK 1:50000, sheet 56 St. Pölten; fig. 1a). The outcrop is located in an abandoned quarry in the southeastern-most part of the northeast-southwest Gresten Klippenbelt, running between the Kasberg (785 m) to the east and the vicinity of the Nutzhof (550 m) to the west. The surrounding area is called Kleindurlas and the locality itself Nutzhof, nearby the farming house Nutzhof.

The dark and light grey succession, comprising the ammonite-bearing beds, is located on the northern side of the Kasberg ridge (approx. 785-500 m). The ammonite-occurrence is exposed on the left side (eastern) of the quarry. The exact position of the ammonite-occurrence as determined by GPS (global positioning system) is N 48°04’49’’ and E 15°47’36’’ (fig. 1).

3. Material, preservation and methods

During the course of this study, 46 ammonite specimens (NHMW 2008z0264/0001-0021) and 238 lamellaptychi were examined. Four brachiopods and 3 inoceramids as well as a single belemnite specimen were collected. Ammonites are preserved as steinkerns and most are moderately well preserved. No shell is present. The phragmocones are mostly flattened, whereas the body chambers are better preserved because of early sediment infilling. The fragmentation is due to preburial-transport, sediment compaction and considerable tectonic deformation, which influences the precise determination of most cephalopods with chambered hard-parts (e.g. ammonites and belemnites).

Calcium carbonate contents ($CaCO_3$) were determined using the carbonate bomb technique. Total carbon content was determined using a LECO WR-12 analyser. Total organic carbon (TOC) contents were calculated as the difference between total carbon and carbonate carbon, assuming that all carbonate is pure calcite. All the chemical analyses were carried out in the laboratories of the Department of Forest Ecology at the University of Vienna.

4. Geological setting and biostratigraphy

Setting. The Gresten Klippenbelt is in this area a small band of Upper Jurassic to Lower Cretaceous sediments from 200-500 m width. It is surrounded by thick sediments of the Rhenodanubian Flysch Zone. Tectonically, the outcrop is situated only 5 km north of the main border of the Rhenodanubian Flysch Zone to the more southern Northern Calcareous Alps. The section at Nutzhof contains 18 m of inverse, cm to dm beds showing the Jurassic-Cretaceous boundary at meter 7 (Nu 7.0).

The succession at Nutzhof was deposited in an unstable slope setting to the north of the Penninic Ocean characterized by thick stratigraphic units that reflect transgressive histories punctuated by tectonic events (shown by the deposition of allodapic limestones).

The entire section at Nutzhof is inversely bedded, and the beds dip 45-60° to the southeast. At this outcrop the lower part comprises a series called Blassenstein Formation with dark marls and intercalated limestone beds; the upper part consist solely of limestones with sometimes cherty areas (Nu 5.0-7.0).

Lithology. The Nutzhof section apparently consists of two different parts (fig. 2). The lower part (Tithonian, 18.0-10.0 m) with dark-grey marls with rhythmically intercalated

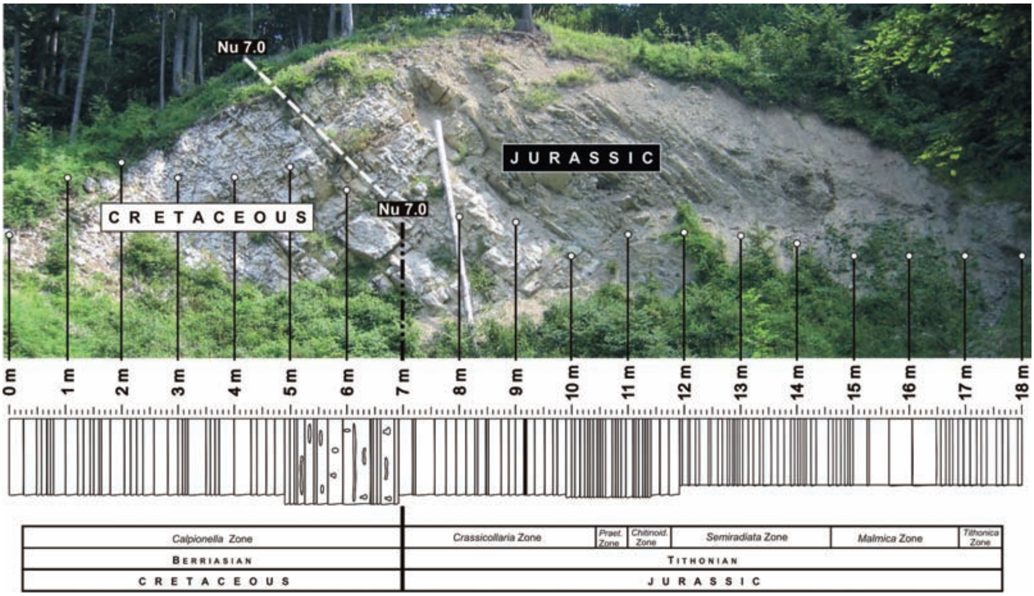

Fig. 2: Exposure of the investigated detailed log with indicated position of the outcrop at the Nutzhof section (Gresten Klippenbelt) and Jurassic-Cretaceous boundary, located at meter 7.0.

limestone beds, and the upper part (Berriasian, 10.0-0.0 m) with light-grey limestones. The strong lithological change at Nu 10.0 does not coincide with the Jurassic/Cretaceous boundary at bed Nu. 7.0. Sediments occur as wacke-, pack- or mudstones.

The $CaCO_3$ (calcium carbonate contents, equivalents calculated from total inorganic carbon) vary in the lower and upper part of the log. The lower part shows variations from 89.03 % (Nu 12.0) to 40.72 % (Nu 13.4), whereas the more constant upper part displays values ranging from 86.16 (Nu. 9.6) up to the maximum log value of 97.4 % (Nu 3.6).

The total sulphur content is positively correlated to the $CaCO_3$ values. The maximum sulphur amount (0.59 %) in the lower part corresponds to bed Nu 12.0 and the minimum value in this part, as for $CaCO_{3,}$ is at Nu 13.4 with 0.30 %. In the upper part the maximum value is at bed Nu 9.0 (0.58 %) and the minimum (0.5 %) corresponds to bed Nu 0.0.

The weight % TOC values (total organic carbon) show no positive correlation, either to S or to $CaCO_3$. TOC values oscillate throughout the log. They vary from 0.91 % (Nu 11.2) to 0.001 % (numerous beds) in the lower part and from 1.07 % (Nu 3.4) to 0.001 % (numerous beds).

Fauna. The invertebrate fauna consists of ammonites, aptychi (*Lamellaptychus*), rhyncholites, belemnites (*Hibolithes* gr. *semisculcatus*), serpulids, echinoderms (*Phyllocrinus*), bivalves (*Inoceramus*), brachiopods (*Triangope*), ophiurids, crinoids (*Saccocoma*), benthic and planktonic foraminifera and radiolarians (fig. 3; see also REHAKOVA et al. 2009; this volume). The only benthic macrofossils observed in the ammonite beds are bivalves and brachiopods. The rare but generally well-preserved cephalopods are dominated by members of the Perisphinctidae. The fairly fossiliferous part of the section is at Nu 14.0-Nu 18.0 m.

Biostratigraphy. According to microfossil (calcareous dinoflagellates, calpionellids) and palaeomagnetic data (more details in PRUNER et al. 2009; this volume), the association indicates that the cephalopod-bearing beds of the Nutzhof section belong to the *Carpistomiosphaera tithonica*-Zone of the Early Tithonian up to the *Calpionella* Zone of the Middle Berriasian (figs 2 & 3). This interval corresponds to the ammonite zones from the Early Tithonian *Hybonoticeras hybonotum*-Zone up to the Middle Berriasian *Subthurmannia occitanica*-Zone.

The biostratigraphically indicative cephalopods are: *Subplanites fasciculatiformis* sp. nov., *Ptychophylloceras ptychoicumm*, *Leptotetragonites honnoratianus*, *Haploceras elimatum*, *Hibolithes* (gr.) *semisulcatus* and some lamellaptychi.

Although zonal index ammonites are missing, the typical ammonite association, in correlation with the micro- and nannofossil data, allows a precise evaluation of the age. The stratigraphic investigation of the micro- and nannofauna revealed that the Nutzhof section comprises sedimentary sequence of Early Tithonian to Middle Berriasian age. Microfossils from the *Tithonica*-Zone up to the *Calpionella*-Zone were detected. The nannofossil zonation shows the *Conusphaera mexicana mexicana* Zone up to the *Nannoconus steinmannii steinmannii* Zone (for more details see REHAKOVA et al. 2009; this volume).

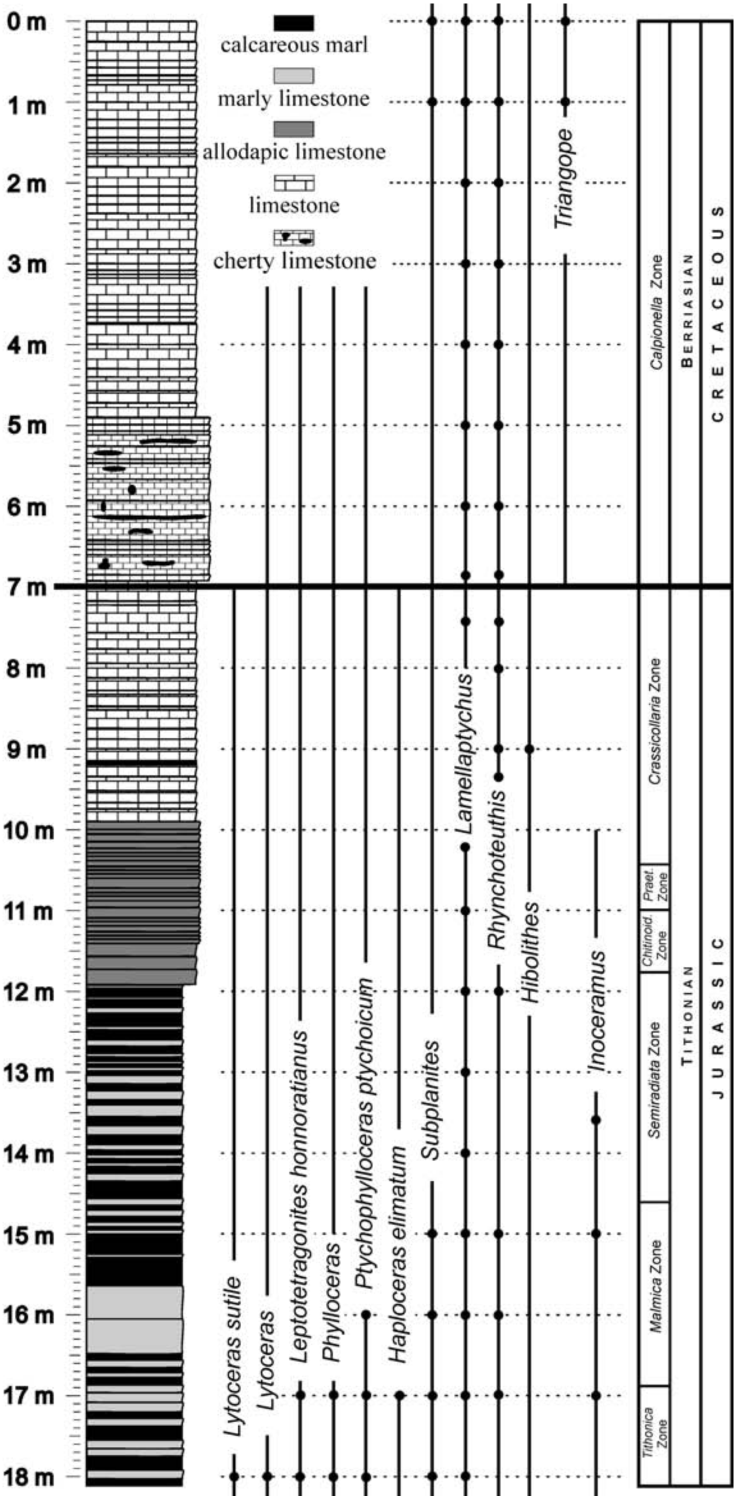

Fig. 3: Lithological log with macrofossil occurrence and range from the Nutzhof locality.

5. Palaeontology – The macrofauna

Conventions. The material examined is stored in the palaeontological collection of the Natural History Museum (NHMW), Vienna, Austria (Burgring 7, 1010 Vienna). All specimens in Plate 1, 2 and 3 were coated with ammonium chloride before photographing.

Ammonites

Lytoceras sutile Oppel, 1865, *Lytoceras* sp., *Leptotergaonites honnoratianus* (d'Orbigny, 1841), *Phylloceras* sp., *Ptychophylloceras ptychoicum* (Quenstedt, 1845), *Haploceras* (*Haploceras*) *elimatum* (Oppel, 1865), *Subplanites fasciculatiformis* sp. nov. (fig. 4). The similar, but only Berriasian species *Pseudosubplanites fasciculatus* was recently introduced by Bogdanova & Arkadiev (2005).

The ammonite fauna comprises 6 different genera. The occurrence at the Nutzhof section is dominated by ammonites of the perisphinctid-type (*Subplanites*). Accordingly, Ammonitina present the most frequent component (60 %; *Subplanites* and *Haploceras*), followed by the Phylloceratina (25 %; *Ptychophylloceras* and *Phylloceras*), and the Lytoceratina (15 %; represented by *Lytoceras* and *Leptotetragonites*) (fig. 4). Only Mediterranean cephalopod elements are present at Nutzhof.

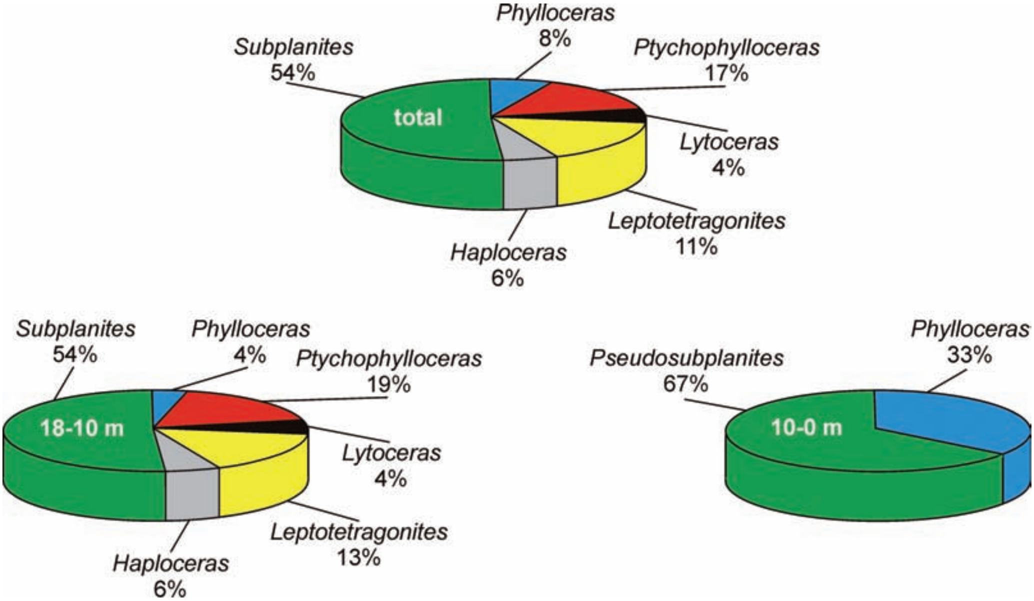

Fig. 4: Ammonite spectra from Nutzhof. On top, overall (total log) spectrum with indicated genera. Note the dominance of the perisphinctids and their abundant genus *Subplanites*. Below, splitted ammonite spectra of log ranges from 18-10 m (left) and 10-0 m (right).

Cephalopod beaks

Lamellaptychus sp.

Belemnites

Hibolithes (gr.) *semisulcatus* (MÜNSTER, 1830)

Brachiopods

Triangope sp.

Bivalves

Inoceramus sp.

Echinoderms

Phyllocrinus sp.**,** *Saccocoma* sp.

6. Discussion

Interpretation of the section

The biostratigraphic analysis (macro-, micro-, and nannofossils; see also KROH & LUKENEDER 2009; PRUNER et al. 2009; REHAKOVA et al. 2009; all this volume) proved that the lower part of the section, including the investigated lithostratigraphic boundary between the marly-limestone succession (18.0-10.00) and limestone succession (10.0-0.0), is continuous. No distinct stratigraphic discontinuity can be detected at the lithostratigraphic boundary at meter 10.0. Moreover, the biostratigraphy clearly demonstrates that the outcrop comprises a tectonically inverted block of about 18 m thickness.

The cephalopod assemblage from Nutzhof shows a typical Late Jurassic (Tithonian) to Early Cretaceous (Berriasian) composition. Additional findings of typical brachiopods (*Triangope*) fit into the picture of the Jurassic/Cretaceous boundary. The fauna is comparable to other Tithonian-Berriasian sections from the Waschbergzone (Ernstbrunner Kalk; ZEISS 2001), the Stramberger Schichten (Štramberk; BLASCHKE 1911) and similar assemblages from the Northern Calcareous Alps of Austria (Oberalmer Schichten; BOOROVÁ et al. 1999). Tithonian persiphinctid- and saccocomid-dominated successions pass into deeper aptychi- and calpionellid-dominated.Berriasian limestones.

The presented data (see also KROH & LUKENEDER 2009; PRUNER et al. 2009; REHAKOVA et al. 2009; all this volume) allow a more precise reconstruction of the paleogeographic setting of the studied section (LUKENEDER et al. in prep). Accordingly, the described specimens were deposited in habitats of the outer shelf situated on the southern edge of the European mainland at the Late Jurassic to Early Cretaceous.

7. Conclusions

The presented results are based on new macrofossil findings from the Gresten Klippenbelt at Nutzhof.

The macrofauna, as already stated, is represented especially by ammonites, belemnoids, aptychi and bivalves. The whole section yielded about 46 ammonite individuals. The sparse and selective occurrence of the ammonites within the section at Nutzhof and the lithologic character of the sediments makes the sampling difficult.

The stratigraphic investigation of the cephalopod, micro- and nanno-fauna revealed that the Nutzhof section comprises Tithonian to Berriassian sediments. The ammonoid fauna contains solely representatives of the Mediterranean Province. The described specimens of *Subplanites* are the first evidence of these ammonites within the Gresten Klippenbelt.

The new ammonite findings from the Lower Austrian locality of Nutzhof show the importance of correlating macrofaunas with the accompanying micro- and nannofossils. Restricting the stratigraphic evaluation to the Nutzhof ammonites would have indicated a time span and age from Tithonian to Early Berriasian.

The presented fauna is also a step forward in our understanding of ammonite faunas from a crucial area at and around the Jurassic/Cretaceous boundary: the Gresten Klippenbelt and the neighbouring Waschberg Zone. Both were located at the northern margin of the Penninic Ocean at this time.

Further investigations on magnetostratigraphy, geochemistry and isotopes will shed light on the environmental history of this little-known area at the Jurassic (Tithonian) – Cretaceous (Berriasian) transitional phase.

Sediment deposition at Nutzhof took place during conditions of relatively stable water masses and during relatively low sedimentation rates but unstable sedimentological conditions (allodapic limestones and microturbidites). This is shown by the change in lithology and the occurrence of numerous event layers with redeposited faunal elements (e.g. saccocomids etc.) from more shallow areas from the north. The depositional area was situated on the passive northern margin of the Penninic Ocean influenced and closely connected by the opening of this Ocean during the Upper Jurassic to Lower Cretaceous. The log shows a significant deepening at the late Tithonian (at 10.0 m) marked by a major lithological change from marly sediments to almost pure limestones.

The ammonites were apparently not redeposited from shallower shelf regions into a deeper shelf environment. The ammonite fauna of the Nutzhof section is interpreted as an assemblage comprising only “autochthonous” and parautochthonous pelagic elements from the open sea. The ammonite shells found their final resting place on the deeper shelf or upper slope of the European side of the Penninic Ocean.

Although the section is not very long, the presence of the Jurassic/Cretaceous boundary and the occurrence of a lithologic change make the section at Nutzhof suitable for the present investigation. Finally, different methods of biostratigraphic correlation based on macro-, micro- and nannofossils proved, also in the Gresten Klippenbelt, to be a powerful tool for stratigraphic dating of Late Jurassic – Early Cretaceous deep-water successions.

Acknowledgements

Thanks are due to the Austrian Science Fund (FWF) for financial support (project P20018-N10). I am particularly grateful to Miguel COMPANY (Granada), Federico OLORIZ (Granada), Jose Maria TAVERA (Granada) and Tamara BOGDANOVA (St. Petersburg) for important discussions on some of the ammonite specimens. The author is indebted to thank Michael WAGREICH (Wien) for a careful review of this paper. Sincere thanks go to Hans EGGER (Vienna) for showing us the outcrop. Photographs were taken by Alice SCHUMACHER (Natural History Museum, Vienna).

References

BLASCHKE, F. (1911): Zur Tithonfauna von Stramberg in Mähren. – Annalen des k.k. Naturhistorischen Hofmuseums, **25**: 143-222.

BOGDANOVA, T.N. & ARKADIEV, V.V. (2005): Revison of species of the ammonite genus *Pseudosubplanites* from the Berriasian of the Crimean mountains. – Cretaceous Research, **26**: 488-506.

BOOROVÁ, D., LOBITZER, H., SKUPIEN, P. & VAŠIČEK, Z. (1999): Biostratigraphy and facies of Upper Jurassic-Lower Cretaceous pelagic carbonate sediments (Oberalm-, Schrambach- and Roßfeld-Formation) in the Northern Calcareous Alps, South of Salzburg. – Abhandlungen der Geologischen Bundesanstalt, **56**/2: 273-318.

CŽJŽEK, J. (1852): Aptychenschiefer in Niederösterreich. – Jahrbuch der Geologischen Reichs-Anstalt, **3**/3: 1-7.

DECKER, K. (1990): Plate tectonics and pelagic facies: Late Jurassic to Early Cretaceous deep-sea sediments of the Ybbsitz ophiolite unit (Eastern Alps, Austria). – Sedimentary Geology, **67**: 85-99.

——— , & RÖGL, F. (1988): Early Cretaceous agglutinated foraminifera from limestone-marly rhythmites of the Gresten Klippen Belt (Eastern Alps Austria). – Abhandlungen der Geologischen Bundes-Anstalt, **41**: 41-59.

FAUPL, P. (2003): Historische Geologie: eine Einführung. Facultas, Wien, 271 pp.

——— , & WAGREICH, M. (2000): Late Jurassic to Eocene Palaeogeography and Geodynamic Evolution of the Eastern Alps. – Mitteilungen der Österreichischen Geologischen Gesellschaft, **92**: 79-94.

GOTTSCHLING, P. (1965): Zur Geologie der Hauptklippenzone und der Laaber Teildecke im Bereich von Glashütte bis Bernreith (Niederösterreich). – Mitteilungen der Geologischen Gesellschaft in Wien, **58**: 23-86.

KROH, A. & LUKENEDER, A. (2009): Crinoids from the Late Jurassic – Early Cretaceous of the Nutzhof section (Lower Austria, Pieniny Klippenbelt). – Annalen des Naturhistorischen Museum Wien, Serie A, **110**: 383-399.

KÜHN, O. (1962): Autriche. – Lexique Stratigraphique Internatinale, Europe, **8**: 646 pp.

KÜPPER, H. (1962): Beobachtungen in der Hauptklippenzone bei Stollberg, N.Ö. – Verhandlungen der Geologischen Bundesanstalt, **2**: 263-268.

MANDIC, O. & LUKENEDER, A. (2008): Dating the Penninic Ocean subduction: new data from planktonic foraminifera. – Cretaceous Research, **29**: 901-912.

PRUNER, P., SCHNABL, P. & LUKENEDER, A. (2009): Preliminary results of magnetostratigraphic investigations across the Jurassic/Cretaceous boundary strata in the Nutzhof, Austria. – Annalen des Naturhistorischen Museum Wien, Serie A, **110**: 331-344.

REHÁKOVÁ, D., HALÁSOVÁ, E. & LUKENEDER A. (2009): The Jurassic-Cretaceous boundary in the Austrian Klippen Belt (Nutzhof, Lower Austria): Implications on Micro- and Nannofacies analysis. – Annalen des Naturhistorischen Museum Wien, Serie A, **110**: 345-381.

SCOTESE, C.R. (2001): Atlas of Earth History, Paleomap project, Arlington, 52 pp., Texas,

STAMPFLI, G. & MOSAR, J. (1999): The making and becoming of Apulia. – Memorie di Sciénce Géologiche (University of Padova). – Special volume, 3rd Workshop on Alpine Geology, **51**/1: 141-154.

WAGREICH, M. (2003): A slope-apron succession filling a piggyback basin: the Tannheim and Losenstein Formations (Aptian – Cenomanian) of the eastern part of the Northern Calcareous Alps (Austria). – Mitteilungen der Österreichischen Geologischen Gesellschaft, **93** (2000): 31-54.

ZEISS, A. (2001): Die Ammonitenfauna der Tithonklippen von Ernstbrunn, Niederösterreich. – Neue Denkschriften des Naturhistorischen Museums in Wien, **6**: 1-117.

Plate 1

Fig. A: *Leptotetragonites honnoratianus* (D'ORBIGNY, 1841), Nutzhof section, 17.0 – x 1, NHMW 2008z0264/0001.

Fig. B: *Leptotetragonites honnoratianus* (D'ORBIGNY, 1841), Nutzhof section, 18.0 – x 1, NHMW 2008z0264/0002.

Fig. C: *Haploceras elimatum* (OPPEL, 1865), Nutzhof section, 13.0 – x 1, NHMW 2008z0264/0003.

Fig. D: *Lytoceras* sp., Nutzhof section, 180 – x 1, NHMW 2008z0264/0004.

Fig. E: *Lytoceras* sp., Nutzhof section, 17.0 – x 1, NHMW 2008z0264/0005.

Fig. F: *Ptychophylloceras ptychoicum* (QUENSTEDT, 1845), Nutzhof section, 18.0 – x 1, NHMW 2008z0264/0006.

Fig. G: *Ptychophylloceras ptychoicum* (QUENSTEDT, 1845), Nutzhof section, 17.0 – x 1, NHMW 2008z0264/0007.

Fig. H: *Ptychophylloceras ptychoicum* (QUENSTEDT, 1845), Nutzhof section, 18.0 – x 1, NHMW 2008z0264/0008.

Fig. I: *Leptotetragonites honnoratianus* (D'ORBIGNY, 1841), Nutzhof section, 18.0 – x 1, NHMW 2008z0264/0009.

Fig. J: *Haploceras elimatum* (OPPEL, 1865), Nutzhof section, 18.0 – x 1, NHMW 2008z0264/0010.

Fig. K: *Lytoceras sutile* OPPEL 1865, Nutzhof section, 18.0 – x 1, NHMW 2008z0264/0011

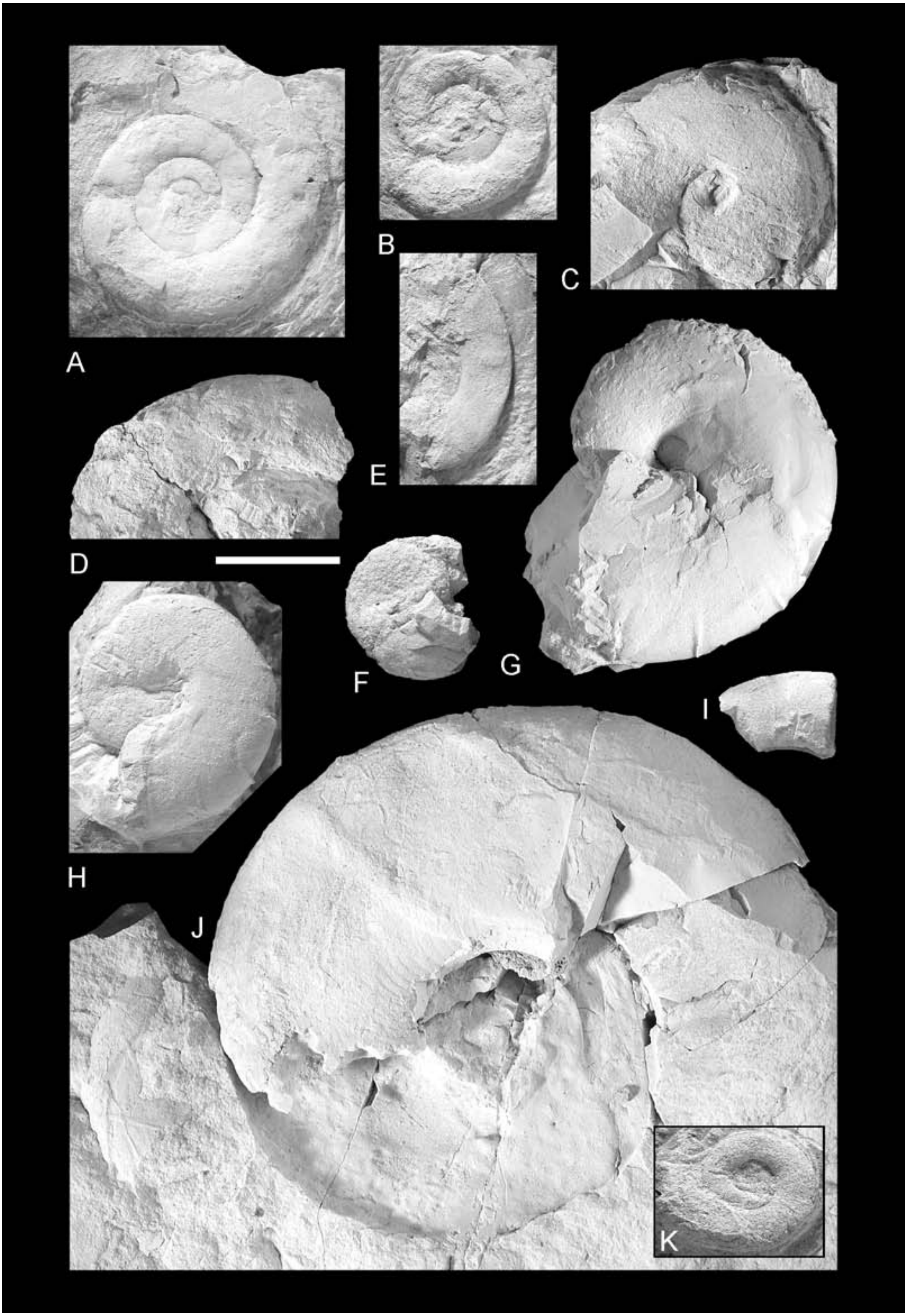
A
B
C
D
E
F
G
H
I
J
K

Plate 2

Fig. A: *Subplanites fasciculatiformis* sp. nov., Nutzhof section, 17.0 – x 1, NHMW 2008z0264/0012.

Fig. B: *Subplanites fasciculatiformis* sp. nov., Nutzhof section, 18.0 – x 1, NHMW 2008z0264/0013.

Fig. C: *Subplanites fasciculatiformis* sp. nov., Nutzhof section, 18.0 – x 1, NHMW 2008z0264/0014.

Fig. D: *Subplanites fasciculatiformis* sp. nov., Nutzhof section, 18.0 – x 1, NHMW 2008z0264/0015.

Fig. E: *Subplanites* sp., Nutzhof section, 0.0 – x 1, NHMW 2008z0264/0016.

Fig. F: *Subplanites* sp., Nutzhof section, 17.0 – x 0.75, NHMW 2008z0264/0017.

Fig. G: *Subplanites* sp., Nutzhof section, 17.0 – x 0.75, NHMW 2008z0264/0018.

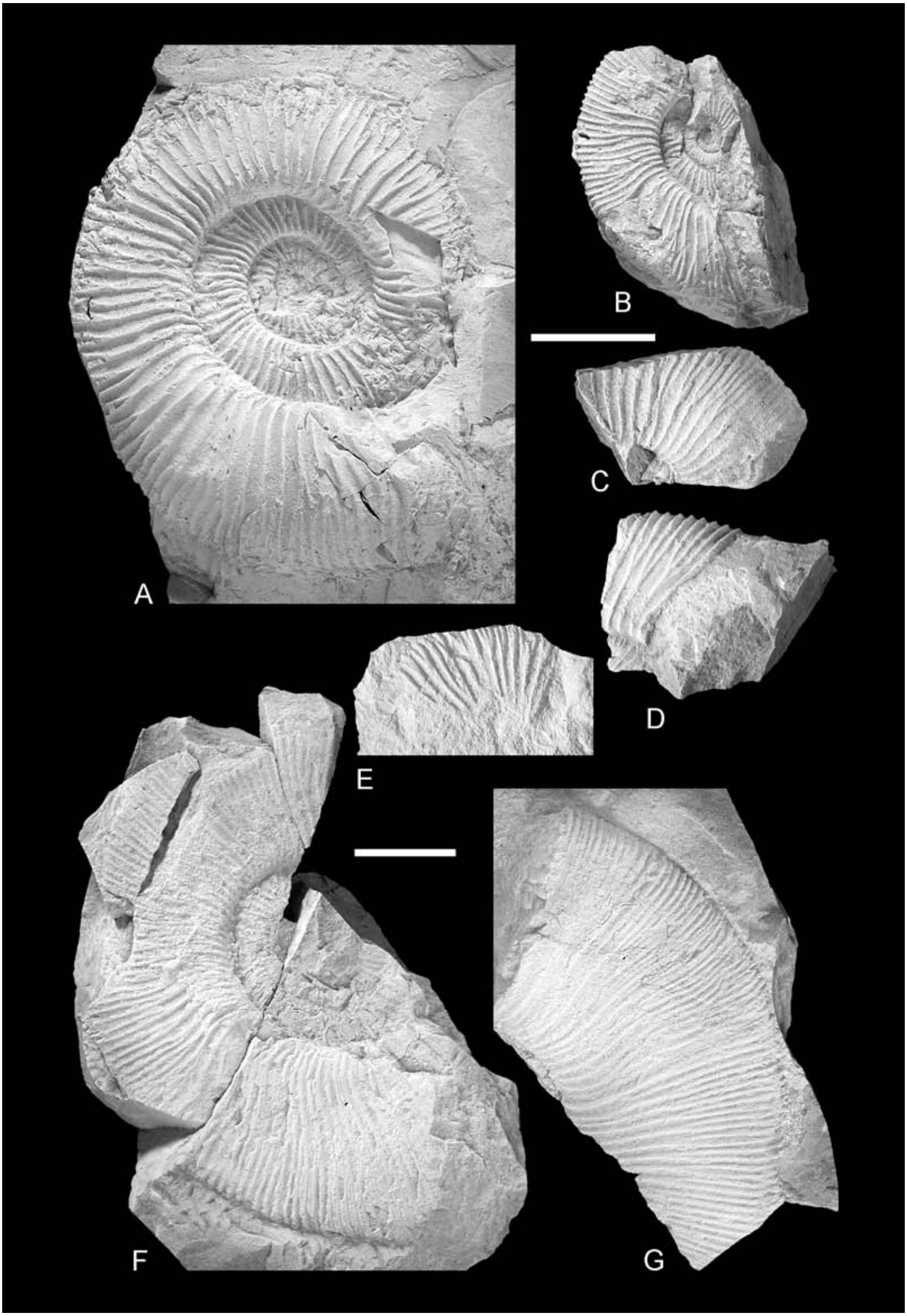
A
B
C
D
E
F
G

Plate 3

Fig. A: *Subplanites fasciculatiformis* sp. nov., Nutzhof section, 18.0 – x 1, NHMW 2008z0264/0019.

Fig. B: *Subplanites fasciculatiformis* sp. nov., Nutzhof section, 17.0 – x 0.5, NHMW 2008z0264/0020.

Fig. C: *Subplanites* sp., Nutzhof section, 17.0 – x 1, NHMW 2008z0264/0021.

Fig. D: *Lamellaptychus* sp., Nutzhof section, 13.8 – x 0.5, NHMW 2008z0264/0022.

Fig. E: *Lamellaptychus* sp., Nutzhof section, 13.9 – x 1, NHMW 2008z0264/0023.

Fig. F: *Lamellaptychus* sp., Nutzhof section, 18.0 – x 1, NHMW 2008z0264/0024.

Fig. G: *Hibolithes* (gr.) *semisulcatus* (MÜNSTER, 1830), Nutzhof section, 14.3 – x 1, NHMW 2008z0264/0025.

Fig. H: *Inoceramus* sp., Nutzhof section, 14.0 – x 0.75, NHMW 2008z0264/0026.

Fig. I: Brachiopod, front view, Nutzhof section, 2.0 – x 1, NHMW 2008z0264/0027.

Fig. J: Brachiopod, upper view, Nutzhof section, 2.0 – x 1, NHMW 2008z0264/0027.

Fig. K: *Triangope* sp., Nutzhof section, 1.0 – x 1, NHMW 2008z0264/0028.

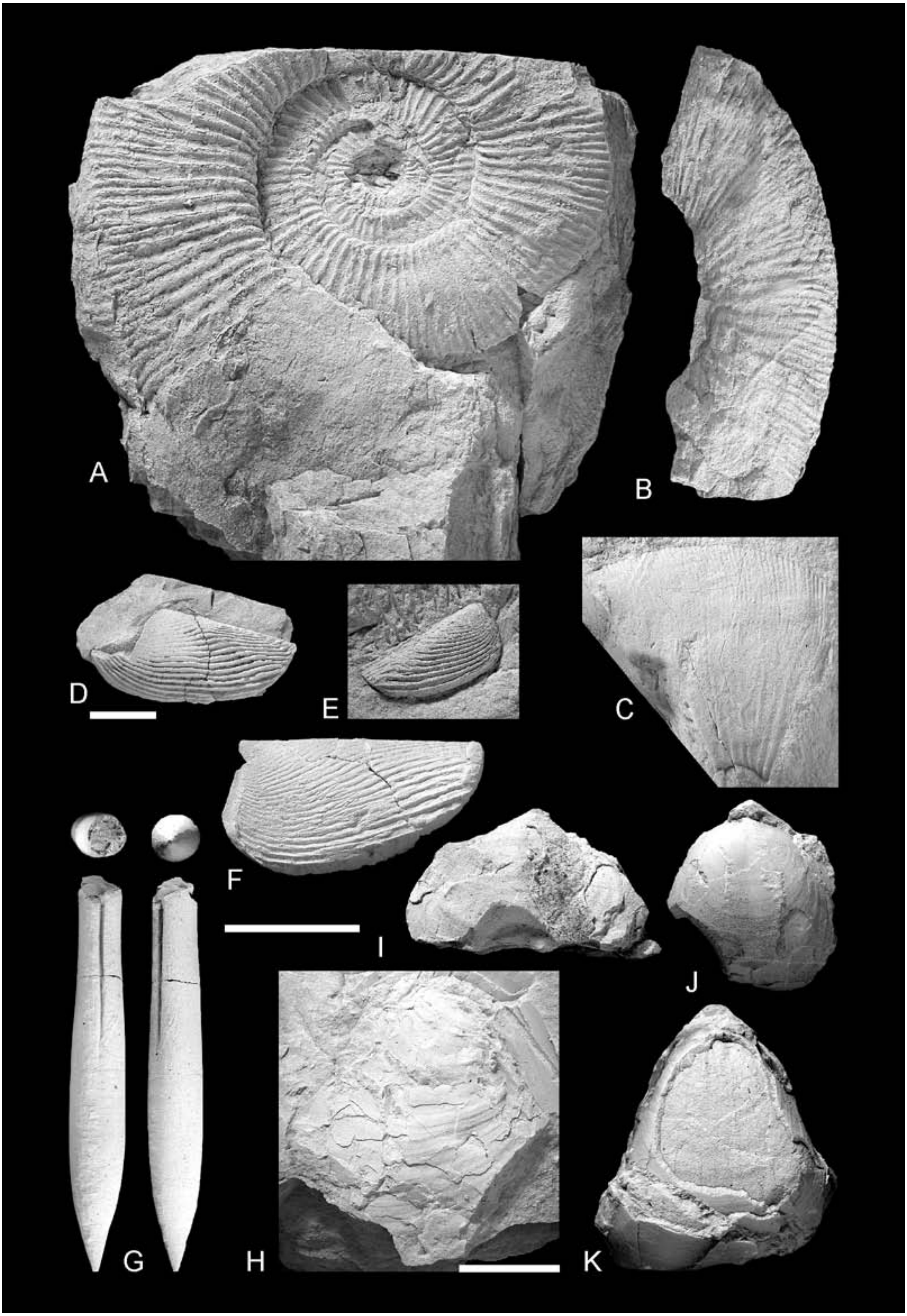
A
B
C
D
E
F
G
H
I
J
K

Appendix

Order Ammonoidea ZITTEL, 1884

Family Perisphinctidae STEINMANN, 1890

Subfamily Virgatosphinctinae SPATH, 1923

Genus *Subplanites* SPATH, 1925

Type species: *Virgatosphinctes* (*Perisphinctes*) *reisi* SCHNEID, 1914; Reisbergschichten, Unterstall bei Neuburg an der Donau, Kimmeridgian.

Diagnosis: Rather evolute shell with subquadrate whorl section. Steep umbilical wall, rounded in adults. Sharp, slightly prorsiradiate and straight, bifurcated ribbing on early whorls. Later intercalated with fasciculate ribbing on same whorl. Ribs start at bottom of umbilical wall and cross round venter at all stages. Ribbing rather distinct.

Subplanites fasciculatiformis LUKENEDER sp. nov.

Plate 2, Figs. A-D; Pl. 3, Figs. A-B

Derivation of name: After the morphology of its intercalated fasciculate ribbing (Latin, *fasciculatus* = bundle like).

Holotype: Natural History Museum, Vienna, NHMW 2008z0264/0012, steinkern, diameter 81 mm, whorl height 27 mm, whorl width 22 mm, umbilical width 32 mm, ribs per whorl 59 (Pl. 2, fig. A).

Paratypes: NHMW2008z0264/0013 (Pl. 2, Fig. B), NHMW2008z0264/0019 (Pl. 3, Fig. A).

Material: 24 specimens preserved as steinkerns, no shell is preserved, preservation in limestone, most of specimens are fragments, suture line is not visible.

Type locality and horizon: Nutzhof, Lower Austria, Gresten Klippenbelt, limestones of the Blassenstein Formation, log NU at N 48° 04’ 49’’ and E 15° 47’ 36’’, beds 13-18, Early-Middle Tithonian.

Description: Medium-sized, strongly ribbed steinkerns and negatives. Additional material as reproduced casts of the latter. Rather evolute and subrectangular, compressed whorls. Umbilicus wide and shallow. Flanks rather straight in early whorls and slightly convex in adults. Bifurcating ribs passing onto subrounded venter. Slightly prorsiradiate ribbing strong and prominent throughout. Ribs projected by approx. 5°-10° to aperture. Ribs straight, not curved. Bifurcated ribs start in the middle of lateral wall, whereas fasciculate ribbing starts on the inner half of whorl height. 59 primary ribs are counted per whorl on umbilical edge.

Remarks: As noted by BOGDANOVA & ARKADIEV (2005) similarities can be observed in *Subplanites* and *Pseudosubplanites*. The vertical umbilical wall, the straight ribbing and more compressed whorls distinguish *Subplanites* from *Pseudosubplanites*. *Pseudosubplanites* is noted by the latter authors to be only a Berriasian genus. Most morphological similarities are observed between the herein erected *Subplanites fasciculatiformis* sp. nov. and the Crimean Berriasian species *Pseudosubplanites fasciculatus* BOGDANOVA & ARKADIEV (2005). The main difference is the higher number (59) of umbilical ribs in *S. fasciculatiformis* sp. nov. (compared at same sizes) in addition to straighter ribbing. Both possess the typical fasciculated ribs. As noted by BOGDANOVA & ARKADIEV (2005) such forms are morphologically closely related to the genus *Fauriella* due to their fasciculate ribbing, but differ in absence of umbilical tubercles. All other species in *Subplanites* and *Pseudosubplanites* differ in the absence of the characteristic fasciculate ribbing.

Occurrence: The genus *Subplanites* is known all over Europe and additionally from Jurassic beds of Borneo, ?Greenland, India, Mexico, Russia and Somalia. The herein erected species *S. fasciculatiformis* sp. nov. occurs in section Nutzhof from beds 13-18 (Early-Middle Tithonian).

Ann. Naturhist. Mus. Wien	110 A	331–344	Wien, Jänner 2009

Preliminary results of magnetostratigraphic investigations across the Jurassic/Cretaceous boundary strata at Nutzhof, Austria

By Petr PRUNER[1], Petr SCHNABL[1], Alexander LUKENEDER[2]

(With 9 figures and 2 tables)

Manuscript submitted on September 8th 2008,
the revised manuscript on November 3rd 2008

Abstract

The principal aim of detailed magnetostratigraphic and micropalaeontological investigation on the Jurassic/Cretaceous (J/K) boundary is precisely determine the boundaries of magnetozones and narrow reverse subzones, and find global correlation across the J/K boundary. A high resolution study focusing on the detailed biostratigraphy of the limestone-, marly limestone- and marl succession at Nutzhof has been carried out at a new outcrop in the Gresten Klippenbelt of Lower Austria. Eleven magnetic polarity zones, six reverse (R) and five normal (N) polarity – are included in the whole interval (18 m) around J/K boundary of Nutzhof section. The J/K boundary (the Berriasian Stage base), located near *Calpionella* Zone base (REHÁKOVÁ et al. 2008; REHÁKOVÁ et al. this volume) roughly corresponds to magnetozone M19N a succession of M-zones correlative with M17N to M22R. Low-field magnetic susceptibility (k) ranges from -5.9 to 94.9×10^{-6} SI and the intensity of the natural remanent magnetization (NRM) varies between 31 and 615×10^{-6} A/m. The samples display a two- to three-component remanence. The average sampling density for the whole section was around two samples per 1 m of true thickness of limestone strata in these preliminary results. The next step of investigation will be to precisely determine the boundaries of magnetozones M19 and M20 including narrow reverse subzones with the high resolution sampling density for the whole section.

Keywords: Austria, Gresten Klippenbelt, Nutzhof, J/K magnetostratigraphy, magnetomineralogy.

Zusammenfassung

Das primäre Ziel detaillierter magnetostratigrafischer und mikropaläontologischer Untersuchungen der Jura/Kreide (J/K) Grenze ist die genaue Einstufung der Grenzen zwischen Magnetozonen und den engen, reversen Subzonen, sowie die Korrelation mit einer globalen Zonierung rund um die J/K Grenze. Eine hochauflösende Studie, fokusiert auf die detailierte Biostratigrafie der Kalk-, Mergelkalk- und Mergel-Abfolge am Nutzhof wurde an einem neu bearbeiteten Aufschluss in der Grestener Klippenzone in Niederösterreich durchgeführt. Elf magnetische Polritäts-Zonen – sechs reverse (R) und fünf normale (N) – sind im gesamten Intervall (18 m) um die J/K Grenze der Nutzhof Sektion vertreten. Die J/K Grenze (die Basis der Berriasium Stufe), lokalisiert an der Basis der *Calpionella* Zone (REHÁKOVÁ et al. 2008; REHÁKOVÁ et al. dieser Band), stimmt etwa mit der Magnetozone M19N überein, einer Abfolge von M-Zonen vergleichbar

---

[1] Institute of Geology, Academy of Sciences of the Czech Republic v.v.i., Rozvojová 269, 165 00, Praha 6 – Lysolaje, Czech Republic; e-mail: pruner@gli.cas.cz; schnabl@gli.cas.cz

[2] Natural History Museum, Geological-Palaeontological Department, Burgring 7, 1010 Vienna, Austria; e-mail: alexander.lukeneder@nhm-wien.ac.at

mit M17N bis M22R. Die schwach-Feld magnetische Suszeptibilität (k) reicht von -5.9 bis 94.9×10^{-6} SI und die Intensität der natürlichen Restmagnetisierung (NRM) variiert von 31 bis 615×10^{-6} A/m. Die Proben zeigen eine zwei- bis drei-Komponenten Remanenz. Die durchschnittliche Zahl der Probennahme des gesamten Abschnittes betrug zwei Proben pro 1 m echter Mächtigkeit der Kalke in diesen vorläufigen Ergebnissen. Der nächste Schritt in den Untersuchungen wird die genaue Fixierung der Magnetozonen M19 and M20 und die exakte Festlegung der reversen Subzonen, durch eine enge Probennahme im gesamten Abschnitt sein.

Schlüsselworte: Österreich, Grestener Klippenzone, Nutzhof, J/K Magnetostratigraphie, Magnetomineralogie

1. Introduction

This study is a continuation of a joint geophysical and palaeontological project focused on detailed magnetostratigraphic and palaeontological studies of the Jurassic/Cretaceous (J/K) boundary. The aims of this project are globally and objectively establish a correlation between biozones around J/K boundary in the Tethyan Realm using global palaeomagnetic events. During the last 30 years, several magnetostratigraphic investigations across the J/K boundary strata have been reported from the Tethyan Realm (e.g. CIRILLI et al. 1984 or OGG & LOWRIE 1986). The analyses of these sections are typically aimed at the formulation of synoptic charts of normal and reverse magnetozones however, there are not a detailed unity in determination of their boundaries in biostratigraphic terms or a precise definition of subzones close to the J/K boundary. The boundary is placed by different authors at various levels within the range of magnetozones M19–M17. A synoptic magnetostratigraphic profile for Upper Mesozoic rocks from Tunisia was published by NAIRN et al. (1981). LOWRIE & CHANNELL (1983) placed the boundary in the lowermost part of magnetozone M17 in a section through the Maiolica Fm of pelagic limestones in the Bosso Valley, Italy. After the correlation of magnetostratigraphic data with calpionellid zones, MÁRTON (1986) proposed placing the J/K boundary close to the base of M17, as LOWRIE & CHANNELL (1983) had done. The section at Brodno near Žilina, W Slovakia (HOUŠA et al. 1999), was the first section investigated with high-resolution magnetostratigraphy and micropalaeontology in the Carpathians. HOUŠA et al. (1999) detected magnetozones M20r–M17r in the Brodno section near Žilina and, on the basis of calpionellid zonation, placed the J/K boundary at approximately the middle of M19n, between M19r and reverse subzone M19n-1 (the Brodno Subzone). The magnetostratigraphic study was extended to other localities in the Tethyan realm, namely at the Bosso Valley in Umbria, Italy (HOUŠA et al. 2004), in the Tatra Mountains, Poland (Grabowski & Pszczółkowski 2006) and at Puerto Escaño, Spain (HOUŠA et al. 2000), where the magnetostratigraphy and biostratigraphy were well documented. This provided a precise record of polarity changes in the Earth's magnetic and determined their positions precisely relative to the biostratigraphic zonation.

The detailed biostratigraphy of the limestone-, marly limestone- and marl succession at Nutzhof has been studied at a new outcrop in the Gresten Klippenbelt of Lower Austria (Fig. 1). The cross-section at Nutzhof contains 18 m of overturned layers, which are 1 to 50 cm thick. At the 7th meter lies the Jurassic-Cretaceous boundary located near *Calpionella* Zone base (REHÁKOVÁ et al. 2008). The stratigraphic investigation of the micro- and nannofauna revealed that the Nutzhof section comprises sedimentary sequence of Early Tithonian to Middle Berriasian in age. The ammonites from the lower

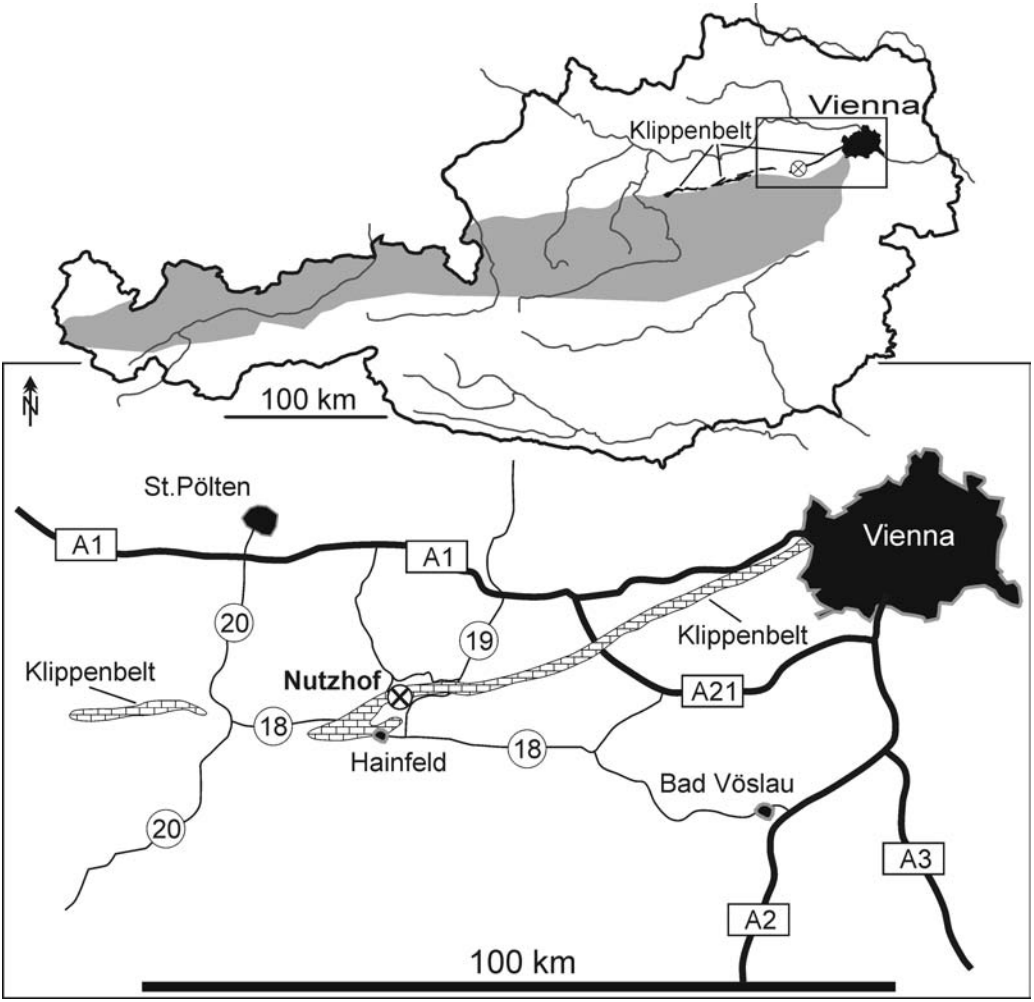

Fig. 1: Location map of the Nutzhof area (Lower Austria) from LUKENEDER (this volume).

part strengthen these results. The upper part shows aptychi but is barren of ammonites. The fact that the Jurassic-Cretaceous boundary is detected in this outcrop by detailed biostratigraphy makes magnetostratigraphic study reasonable.

2. Geographical and geological setting

The assembled outcrop is located about 20 km south of Böheimkirchen and 5 km north of Hainfeld. The surrounding area is called Kleindurlas and the locality itself Nutzhof. The Gresten Klippenbelt is in this area a small band of Upper Jurassic to Lower Cretaceous sediments from 200-500 m breadth. It is surrounded by sediments of the Rhenodanubian Flysch Zone. Tectonically, the outcrop is situated only 5 km north of the main border between the Rhenodanubian Flysch Zone and Northern Calcareous Alps. Lithological, sedimentological and palaeoecological studies of the succession uncovered rich spectra of Tithonian to Berriasian macro- and microfaunal elements. The evaluation of the thin sections and washed samples indicates a change from a saccocomid facies to a calpionellid facies within the succession.

3. Rockmagnetic investigation

Isothermal remanent magnetization (IRM) to saturation was measured to identify coercivity spectra of the magnetically active minerals. The whole rock samples were magnetized on the Pulse Magnetizer MMPM 10, demagnetized on LDA-3 AF Demagnetizer and measured on JR6 a magnetometer. The used field range was 10 to 2900 mT. IRM curves demonstrated in Fig. 2 show two different magnetic minerals. Graph a) demonstrates magnetically soft magnetite and graph b) shows samples with magnetically hard goethite and negligible amount of magnetite.

4. Methods

Oriented hand samples (38) from the Nutzhof section were cut to 111 laboratory specimens. Remanent magnetization (RM) of the rocks was easily measured using JR-5A spinner magnetometer or Liquid helium-free Superconducting Rock Magnetometer, type 755 4K SRM and the magnetic susceptibility of the samples was measured using a KLY-4 Kappabridge (Jelínek 1966, 1973). Mean values of the modulus of natural RM

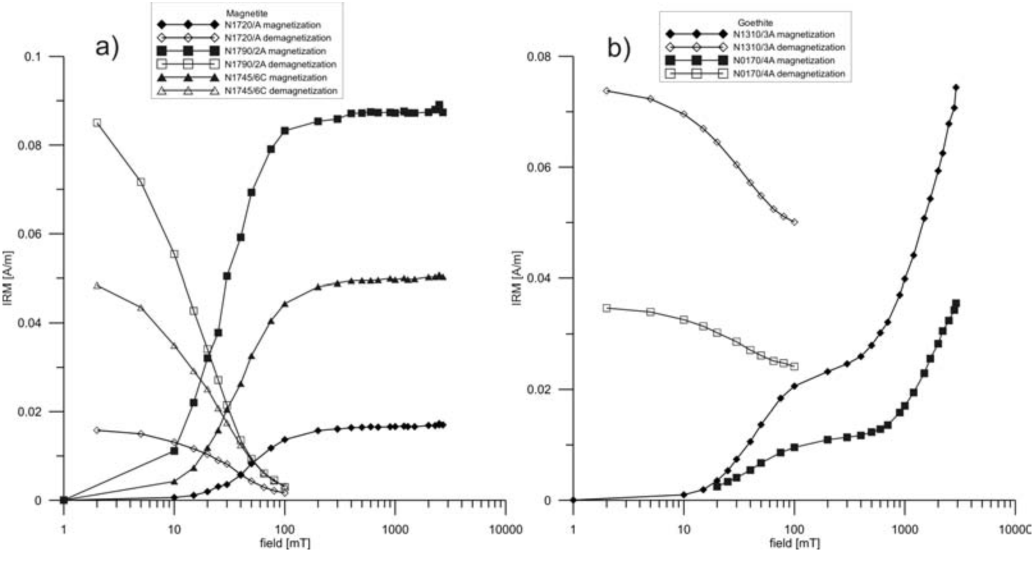

Fig. 2: Examples of IRM acquisition and AF demagnetization curves, limestone samples: a) samples with magnetically soft magnetite and b) samples with magnetically hard goethite and negligible amount of magnetite.

(Jn) and of volume magnetic susceptibility (kn) for 111 samples of upper Tithonian and lower Berriasian limestones are shown in Table 1. These data given in the magnetostratigraphic profile indicate a significant jump of remanent magnetization and magnetic susceptibility, in the meter 10. The reason of this jump is change in lithology, from meter 0 to 10 prevailing limestones and from meter 10 started siltstones. Several pilot samples were experimentally subjected to alternating field (AF) demagnetization using a LDA -3A demagnetizer. The method of progressive thermal demagnetization (TD) using the MAVACS demagnetizer (PŘÍHODA et al. 1989) gave considerably better results. Each of the 86 samples studied was subjected to TD or AF demagnetization in 11–12 temperatures or fields. As a result, the individual components could be precisely established in the vast majority of samples using the multicomponent analysis of remanence (KIRSCHVINK 1980). Zijderveld diagrams and diagrams of Mt/Mn values vs. laboratory thermal demagnetizing field t (°C) were constructed for all samples.

Table 1: Basic magnetic parameters and statistical properties of the physical quantities in the basic groups of samples from the Nutzhof.

Age	Magnetozone	Number of samples	Modulus of natural remanent magnetization M [10^{-6} A/m]		Volume magnetic susceptibility k [10^{-6} SI]	
			Mean value	Standard deviation	Mean value	Standard deviation
Early Berriasian	N+R	19	108	42	3.2	2.4
Late Tithonian	N+R	92	224	112	58	12

Limestone beds at the Nutzhof display uniform overturned bedding-plane orientation, with the mean strike of 151°±30° and the mean dip angle of 44°±22°. From paleomagnetic point of view the mean strike is 331°±30° and the mean dip angle is 136°±22°. The uniform bedding plane orientation is also responsible for the equal dispersions of the mean directions of remanence components in situ (not corrected for tectonic dip) and those corrected for tectonic dip. According these values we used tilt test, the fold test was not possible to apply in this case.

5. Analysis of magnetic and palaeomagnetic properties

Results of AF and TD demagnetization procedures are displayed in Figures 3–4. They refer to two limestone samples with normal palaeomagnetic directions (sample N 0720-1 from M19N of the magnetostratigraphic profile and sample N 1720-3B from M22N) and two limestone samples with reverse palaeomagnetic directions (sample N 0430i1 from M17R of the magnetostratigraphic profile and sample N 1280-3 from M20R). Analogous results were obtained for most samples from the whole Nutzhof section. The remanent magnetization directions shown in the projections are corrected for the dip of strata. Results of the multi-component analysis of remanence show that the rock samples from Nutzhof display a three-component remanent magnetization. The A-component is undoubtedly of viscous origin and is demagnetizable in the temperature range of 20–

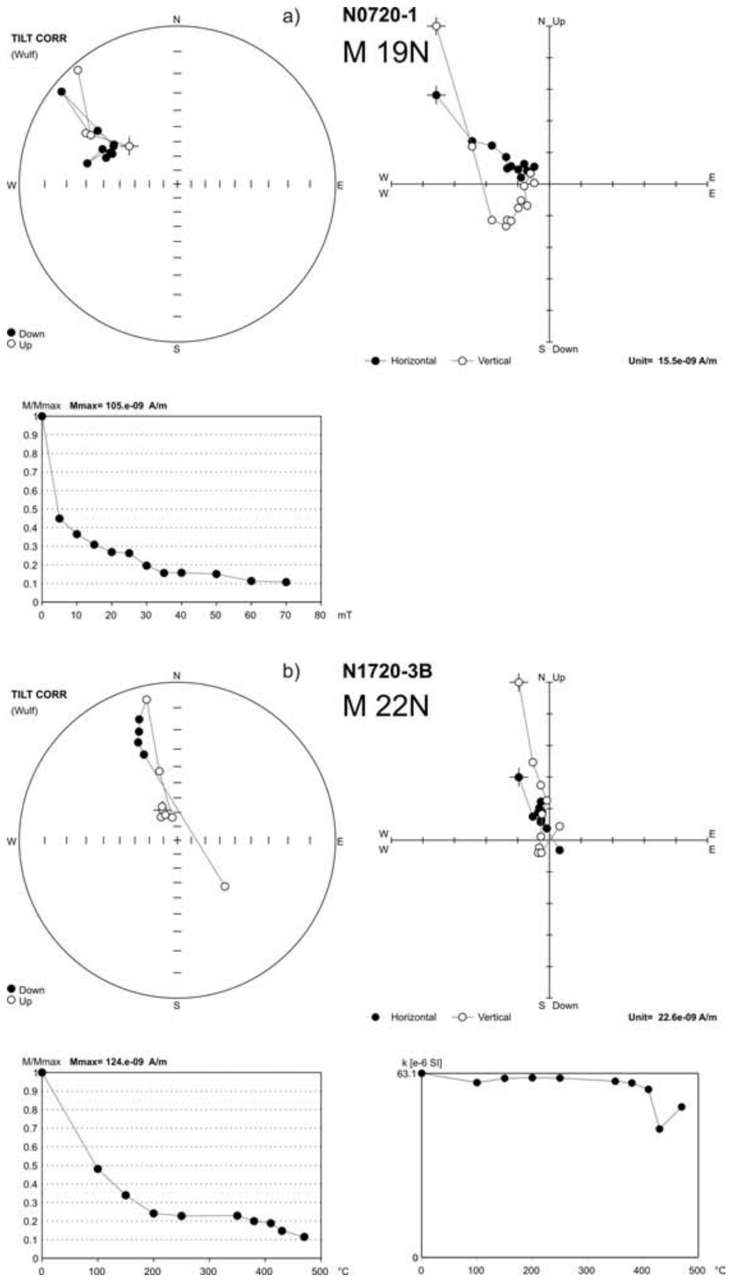

Fig. 3: Results of AF and TD demagnetization of two limestone samples (a – N0720-1; b – N1720-3B) with normal palaeomagnetic polarity. Top left: Stereographic projection of NRM vector variations during AF (a) and TD (b) demagnetization, solid and open circles denote projections of NRM vectors on the lower and upper hemispheres, respectively. Top right: Zijderveld diagram, solid circles represent projection on the horizontal plane (XY), open circles represent projections on the north–south vertical plane (XZ). NRM module (M) as dependent on AF intensity (a) and TD field (b). A graph of volume magnetic susceptibility as dependent on TD field (b).

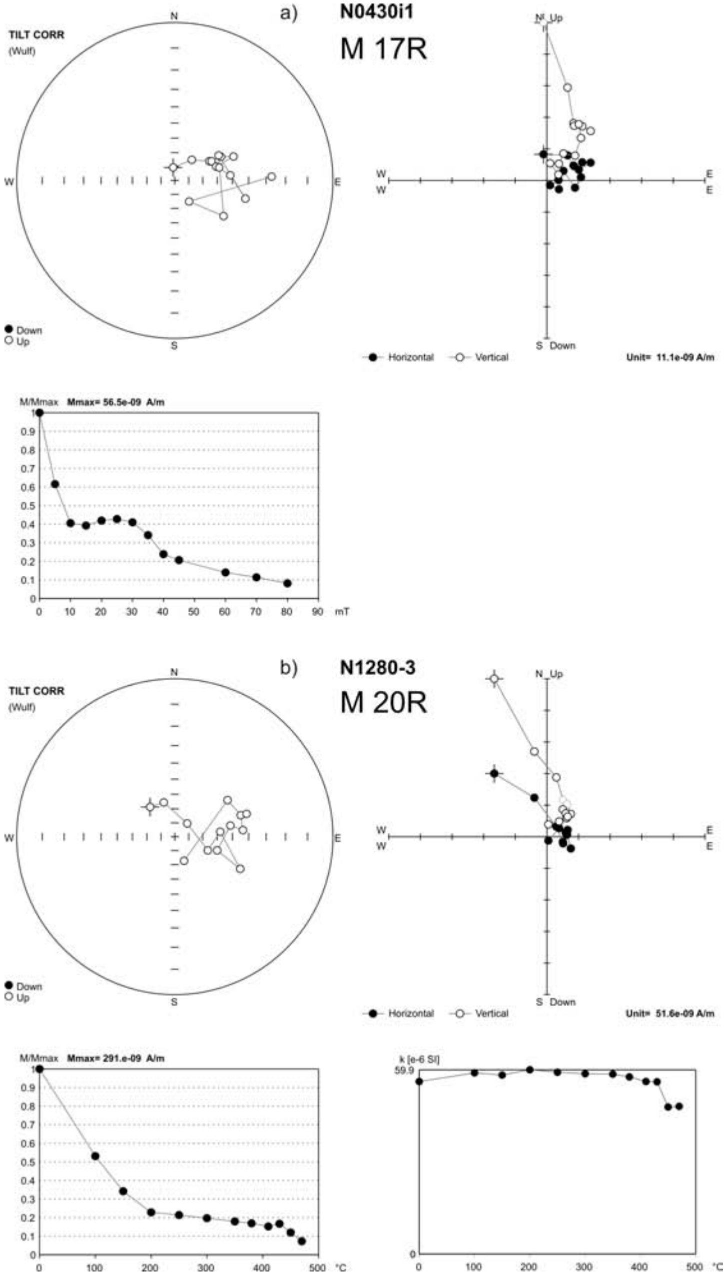

Fig. 4: Results of AF and TD demagnetization of two limestone samples (a – N0430i1; b – N1280-3) with reverse palaeomagnetic polarity. See caption for Fig. 3.

100 °C (or AF 0-5 mT); the B-component is also of secondary origin but shows harder magnetic properties being demagnetizable in temperature range of 100–200 °C (or AF 5-20 mT); the C-component is the most stable, being demagnetizable in temperature-range of *c*. 350–500 °C (or AF 30-100 mT). The origin of the B-component was studied by statistical processing of a larger set of data and is discussed below (section 6). The mean directions and dispersions of components were calculated using Fisher's statistics (FISHER 1953) and were displayed on Wulf stereographic projection. They are marked either by full or empty crossed circles with a confidence circle circumscribed around the mean direction at the 95 % probability level. Low-field magnetic susceptibility (k) ranges from -5.9 to 94.9×10^{-6} SI and the intensity of the natural remanent magnetization (NRM) varies between 31 and 615×10^{-6} A/m.

6. Discussion of the main results

The paleomagnetic data given in the magnetostratigraphic profile indicate a significant jump of remanent magnetization and magnetic susceptibility, in the meter 10. The reason of this change is lithology, from meter 0 to 10 prevailing limestones and from meter 10 started siltstones. The mean B-component directions of the sets of rocks, upper Tithonian and lower Berriasian display a somewhat higher dispersion, see Table 2. Inclination of the field of theoretical co-axial geocentric magnetic dipole for the Nutzhof is 64.2°; the mean inclination of B-component (secondary or "present day" component) calculated from our data set is higher (73°), the B-component is considered without correction for the dip of strata (in situ directions), see Fig 5. These components were undoubtedly imprinted in the near past during normal polarity of the Earth's magnetic field, most probably in the Neogene, after Alpine folding. Both magnetic polarities are present in C-component directions, but the directions are highly scattered (Table 2). Consequently, the mean direction for samples with normal polarity is D=314.7°, I=32.0°, α_{95}=12.5° (Fig 6).

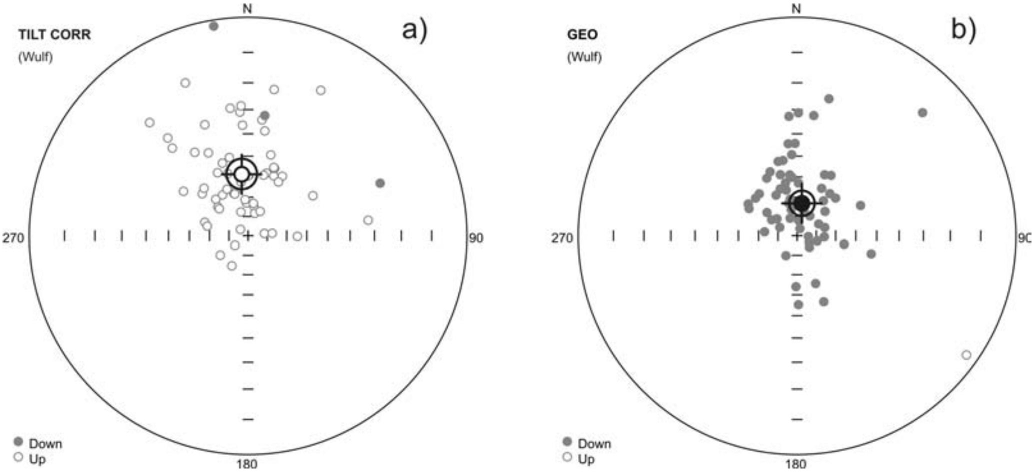

Fig. 5: J/K limestones and marls, directions of B-components of RM corrected (a) and not corrected (b) for dip of strata. Stereographic projection, full (open) small circles represent projection onto the lower (upper) hemisphere.

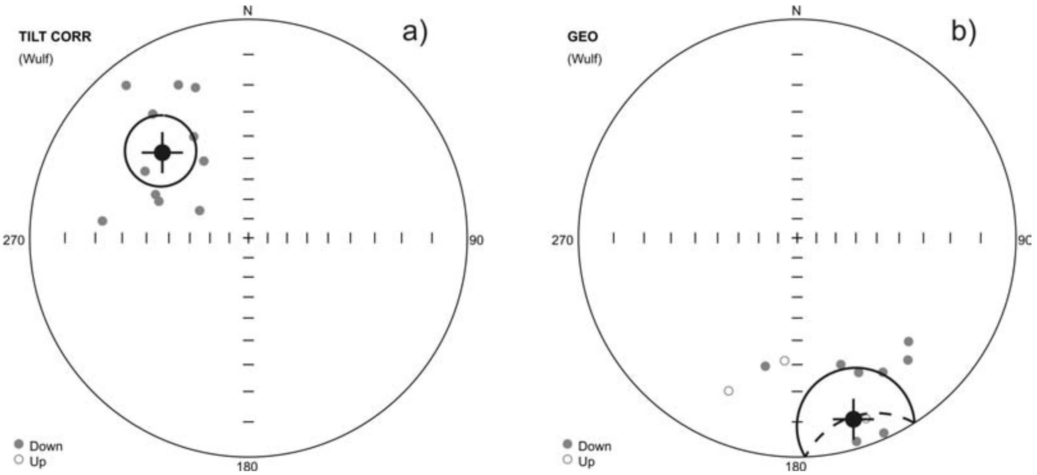

Fig. 6: J/K limestones and marls, directions (N polarity) of C-components of RM corrected (a) and not corrected (b) for dip of strata. See caption for Fig. 5.

For reverse polarity we obtained two groups, the first (R1) is D=76.1°, I=-39.3°, α_{95} =8.4° and the second (R2) is D=192.8°, I=-45.2°, α_{95} =14.5° (Figs 7 and 8). This normal polarity direction is in agreement with the magnetic field for the J/K, but the reverse polarity presents high difference of declination. Table 2 shows that the dispersions of C-componet directions are always wider for rocks in situ (not corrected for dip of strata) than dispersions of directions corrected for dip of strata. The mean values of C-component of normal polarity directions are anomalous, having been affected by counterclockwise paleotectonic rotation. An analogous palaeotectonic rotation has been reported for Cretaceous and

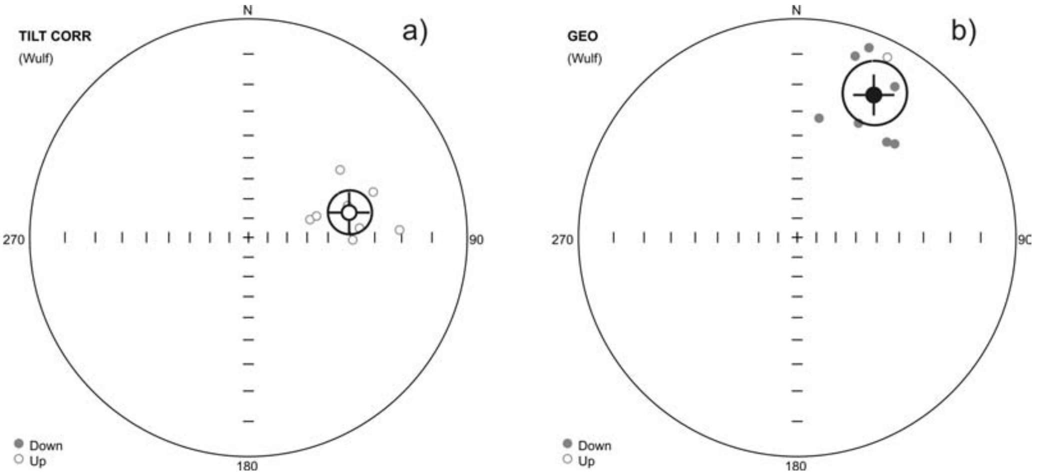

Fig. 7: J/K limestones and marls, directions (R1 polarity) of C-components of RM corrected (a) and not corrected (b) for dip of strata. See caption for Fig. 5.

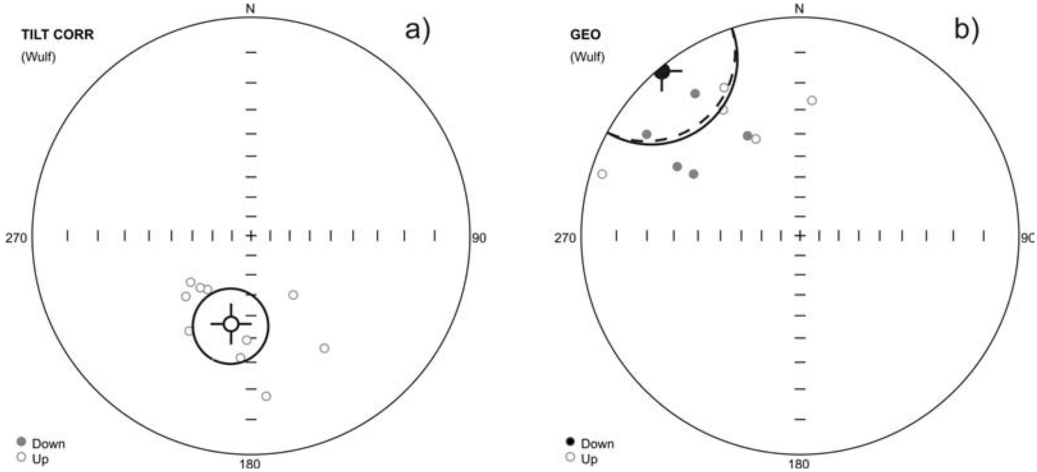

Fig. 8: J/K limestones and marls, directions (R2 polarity) of C-components of RM corrected (a) and not corrected (b) for dip of strata.See caption for Fig. 5.

Jurassic rocks in a broader region of the Eastern Alps. The nearest profiles that had been palaeomagneticaly studied are in Eastern Alps intramontane basins filled with Miocene sediments; it shows counter-clockwise rotations from 27° to 59° (Márton et al. 2000). On the contrary the second closest sets of profiles, the Gossau sediments (upper Cretaceous), shows clockwise rotations from 26° to 59° (Mauritsch & Becke 1987).

Table 2: Mean directions of B (LFC or LTD) and C-components (HFC or HTD) corrected and not corrected for structural tilt.

Age of rocks	Component of remanence	Polarity	Structural tilt correction				No structural tilt correction (in-situ directions)				n	See Figure
			Mean directions		α_{95} [°]	k	Mean directions		α_{95} [°]	k		
			Decl. [°]	Incl. [°]			Decl. [°]	Incl. [°]				
L. Tith.+ E.Berr.	B	R	354.1	-58.4	6.8	6.9	8.5	73.0	6.0	8.7	62	5
L. Tith.+ E.Berr.	C	N	314.7	32.0	12.5	11.4	162.7	8.2	17.2	8.0	11	6
L. Tith.+ E.Berr.	C	R1	76.1	-39.3	8.4	31.1	28.3	17.0	9.6	23.7	9	7
L. Tith.+ E.Berr.	C	R2	192.8	-45.2	14.5	9.3	320.0	0.9	18.3	5.9	10	8

N, R, normal, reverse polarity

7. Magnetostratigraphic profile

The section at Nutzhof complies with our aims in three fundamental criteria: (a) continuous sedimentation not interrupted by marked diastems; (b) rich fossil associations (calpionellids, amonites) allowing a detailed biostratigraphic division; and (c) rocks with magnetic properties that are favourable for reliable determination of palaeomagnetic polarity. The calpionellid associations are very well preserved and highly diversified (REHÁKOVÁ et al. 2008). The log at Nutzhof contains 18 m of inverse, cm to dm beds showing at meter 7 the Jurassic-Cretaceous boundary (REHÁKOVÁ et al. this volume).

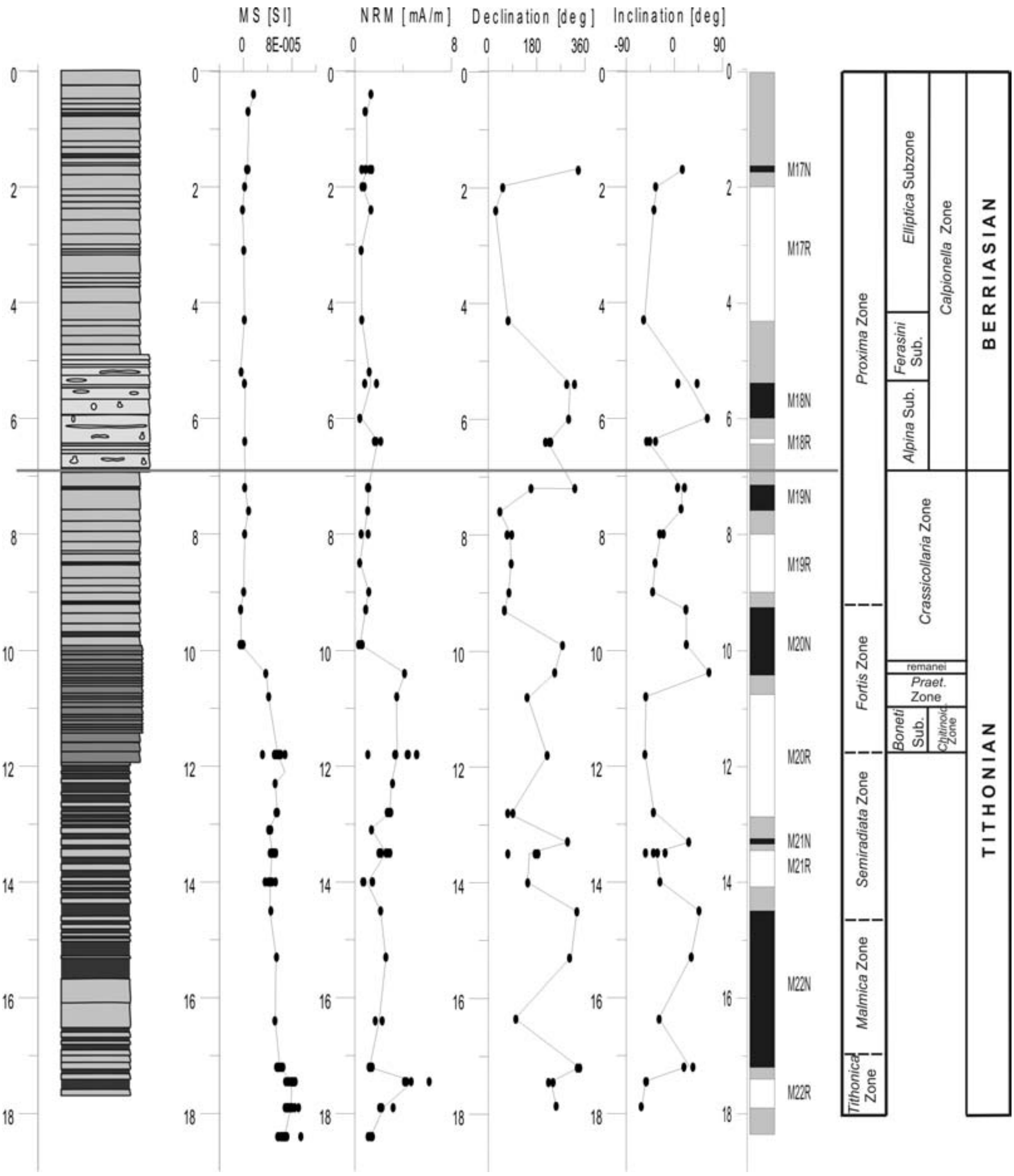

Fig. 9: Magnetostratigraphic profile across the Nutzhof J/K boundary strata, preliminary results of magnetic, palaeomagnetic and lithostratigraphic data. M – NRM in the natural state; k – value of volume magnetic susceptibility in the natural state; D – declination; I – inclination. Normal magnetozones are denoted in black, reverse in white and unknown in grey. Calpionellid biostratigraphy from REHÁKOVÁ et al. (this volume).

Our study concentrated on the investigation of the basal 18-m thick portion of the section, on the limestone strata around the J/K boundary, to preliminarily determine the boundaries of magnetozones M17N to M22R (six reverse and six normal zones), see Fig. 9. In order to identify the detected polarity zones against the M-sequence of polarity intervals given by the GPTS (GRADSTEIN et al. 2004).

The localities in the Tethyan realm include the J/K sections at Brodno near Žilina (Western Carpathians, W Slovakia), the Tatra Mountains (central Western Carpathians, Poland), the Bosso Valley (Umbria, central Italy) and at Puerto Escaño (Province of Cordóba, S Spain). These localities provided very detailed to high-resolution magnetostratigraphic data across the J/K boundary. The reverse subzones were precisely localized in all the sections in analogous relative positions in magnetozones M20N (Kysuca Subzone) and M19N (Brodno Subzone), respectively. Identification of the magnetozones enables a rough estimation of sedimentation rates for these studied sections. The average sedimentation rate in our section (Nutzhof) is around 2.5 m/Ma. The average sampling density of the whole section was around two samples per 1 m of true thickness of limestone strata. The value of sedimentation rate for the Nutzhof section corresponds to an average sedimentation rate of 2.27 m/Ma in Brodno and 2.88 m/Ma in Puerto Escaño. Relatively low value (1 m/Ma) are recorded in Bosso Valley, but mostly higher values (3-20 m/Ma) are given by GRABOWSKI & PSZCZÓŁKOWSKI (2006) for sections in the Tatra Mountains.

8. Conclusions

The magnetostratigraphic study concentrated on the investigation of the basal 18 m thick portion of the Nutzhof section, on the limestone strata around the J/K boundary, to preliminarily determine the boundaries of magnetozones M17N to M22R (according correlation with GPTS), it means six reverse and six normal zones. The directions of B-component (LFC and LTC) are most probably secondary origin (the Neogene), after the rocks had been folded. Both magnetic polarities are present of C-component (HFC and HTC) directions, but the directions are highly scattered. This normal polarity direction is in agreement with the magnetic field for the J/K, but the reverse polarity presents two groups with difference in declination. The next step of magnetostratigraphic investigation will be to determine the boundaries of magnetozones M19 and M20, the average sampling density for the whole section must be around 5 to 8 samples per 1 m and 20 and more samples per 1 m in critical portions of the section.

Acknowledgements

We thank Daniela REHÁKOVÁ (Department of Geology and Palaeontology, Faculty of Natural Sciences, Comenius University, Bratislava) and Emö MARTON (Eötvös Lorand Geophysical Institute, Paleomagnetic Laboratory, Budapest) for constructive comments. We acknowledge field assistance by Stanislav ŠLECHTA. Paleomagnetic analyses were performed by Daniela VENHODOVÁ, Jana DRAHOTOVÁ, and Jiří PETRÁČEK (Institute of Geology ASCR v.v.i., Paleomagnetic laboratory, Prague). Software for evaluation of palaeomagnetic measurements was prepared by Otakar MAN and Martin CHADIMA (Institute of Geology ASCR v.v.i., Paleomagnetic laboratory, Prague). We also gratefully acknowledge the Grant Agency of the Czech Republic for financial support (Grant No. GACR 205-07-1365) and Research Plan of the IG AS CR No.

CEZ AV0Z30130516 and the Austrian Science Fund (FWF) for the financial support of the project P20018-N10. Critical reviews of the manuscript by Jacek GRABOWSKI (Polish Geological Institute, Warszawa) and Robert SCHOLGER (University Leoben) are gratefully acknowledged.

References

CIRILLI, S., MÁRTON, P. & Vigli, L. (1984): Implications of a combined biostratigraphic and palaeomagnetic study of the Umbrian Maiolica Formation. – Earth Planetary Science Letter, **69**: 203-214.

FISHER, R. (1953): Dispersion on a sphere. – Proceedings of the Royal Society, Series A, **217**: 295-305.

FISHER, N. I., LEWIS, T. & EMBLETON, B. J. J. (1987): Statistical analysis of spherical data, 329 pp., Cambridge (Cambridge University Press).

GRABOWSKI, J & PSZCZÓŁKOWSKI, A. (2006): Magneto- and biostratigraphy of the Tithonian-Berriasian pelagic sediments in the Tatra Mountains (central Western Carpathians, Poland): sedimentary and rock magnetic changes at the Jurassic/Cretaceous boundary. – Cretaceous Research, **27**: 398-417.

GRADSTEIN, F.M., OGG, J.G. & SMITH, A.G. (Eds) (2004): A gelogic Time Scale 2004. – 589 p., Cambridge, U.K. (Cambridge University Press).

HOUŠA, V., KRS, M., KRSOVÁ, M., MAN, O., PRUNER, P. & VENHODOVÁ, D. (1999): High-resolution magnetostratigraphy and micropaleontology across the J/K boundary strata at Brodno near Žilina, western Slovakia: summary results. – Cretaceous Research, **20**: 699-717.

——— , KRS, M., MAN, O., PRUNER, P.,VENHODOVÁ, D., CECCA, F., NARDI, G. & PISCITELLO, M. (2004): Combined magnetostratigraphic, paleomagnetic and calpionellid investigations across Jurassic/Cretaceous boundary strata in the Bosso Valley, Umbria, central Italy. – Cretaceous Research, **25**: 771-785.

——— , KRS, M., MAN, O., PRUNER, P., VENHODOVÁ, D., OLÓRIZ, F. & TAVERA, J.M. (2000): Detailed magnetostratigraphy and micropalaeontology across the J/K boundary strata at Puerto Escaño, S. Spain. – Geophysical Research Abstracts (GRA), **2**: 71.

JELÍNEK, V. (1966): A high sensitivity spinner magnetometer. – Studia Geophysica at Geodaetica, **10**: 58-78.

——— (1973): Precision A.C. bridge set for measuring magnetic susceptibility and its anisotropy. – Studia Geophysica at Geodaetica, **17**: 36-48.

KIRSCHVINK, J. L. (1980): The least-squares line and plane and the analysis of palaeomagnetic data. – Geophysical Journal of the Royal Astronomical Society, **62**: 699-718.

LOWRIE, W. & CHANNELL, J. E. T. (1983): Magnetostratigraphy of the Jurassic-Cretaceous boundary in the Maiolica limestone (Umbria, Italy). – Geology, **12**: 44-47.

MÁRTON, E. (1986): The problems of correlation between magnetozones and calpionellid zones in Late Jurassic–Early Cretaceous sections. – Acta Geologica Hungarica, **29**: 125-131.

——— , KUHLEMANN, J., FRISCH, W. & DUNKL, I. (2000): Miocene rotations in the Eastern Alps – palaeomagnetic results from intramontane basin sediments. – Tectonophysics, **323**/3-4: 163-182.

MAURITSCH, H. J. & BECKE, M. (1987): Paleomagnetic investigations in the Eastern Alps and Southern Border Zone. – In: FLÜGEL, H.W. & FAUPL, P. (eds.): Geodynamics of the Eastern Alps. – pp. 282-309, Vienna.

LOWRIE, W. & CHANNELL, J. E. T. (1983): Magnetostratigraphy of the Jurassic–Cretaceous boundary in the Maiolica Limestone (Umbria, Italy). – Geology, **12**: 44-47.

NAIRN, A. E. M., SCHMITT, T. J. & SMITHWICK, M. E. (1981): A palaeomagnetic study of the upper Mesozoic succesion in northern Tunisia. – Geophysical Journal of the Royal Astronomical Society, **65**: 1-18.

OGG, J. G. & LOWRIE, W. (1986): Magnetostratigraphy of the Jurassic/Cretaceous boundary. – Geology, **14**: 547-550.

PŘÍHODA, K., KRS, M., PEŠINA, B. & BLÁHA, J. (1989): MAVACS – a new system creating a nonmagnetic environment for palaeomagnetic studies. – In: BANDA, E. (ed.): Paleomagnetismo – palaeomagnetism, Cuadernos de Geologia Iberica pp. 223-250 (CSIC, Madrid, 1988–1989).

REHAKOVA, D., HALASOVA, E. & LUKENEDER, A. (2008): The Jurassic/Cretaceous boundary in the Austrian Klippen belt (Nutzhof, Lower Austria): Implications on micro- and nannofacies analysis. – Berichte der Geologischen Bundesanstalt, **74**: 95-97.

Ann. Naturhist. Mus. Wien	110 A	345–381	Wien, Jänner 2009

The Jurassic-Cretaceous boundary in the Gresten Klippenbelt (Nutzhof, Lower Austria): Implications for Micro- and Nannofacies analysis

Daniela REHÁKOVÁ[1], Eva HALÁSOVÁ[1], Alexander LUKENEDER[2]

(With 6 plates and 4 figures)

Manuscript submitted on September 11th 2008,
the revised manuscript on November 3rd 2008.

Abstract

The paper discusses the results of an integrated study of three microplankton groups (calpionellids, calcareous dinoflagellates and nannofossils) and macrofauna (ammonites, belemnites and aptychi) in the Nutzhof section. The stratigraphic investigation of the microfauna revealed that Nutzhof comprises a sedimentary sequence of Early Tithonian to Middle Berriasian age. Based on the distribution of the stratigraphically important planktonic organisms, several coeval calpionellid, dinocyst and nannofossil bioevents were recorded along the Jurassic-Cretaceous boundary beds.

Keywords: Calcareous microfossils, Nannofossils, Pelagic carbonates, J/K boundary, Gresten Klippenbelt.

Zusammenfassung

Der Artikel diskutiert die Ergebnisse einer ganzheitlichen Studie von drei Mikroplankton Gruppen (Calpionellen, kalkigen Dinoflagellaten und Nannofossilien) und der Makrofauna (Ammoniten, Belemniten und Aptychen) an der Sektion Nutzhof. Die stratigrafischen Untersuchungen der Mikrofauna erbrachten für die sedimentäre Sequenz von Nutzhof ein Alter von unterem Tithonium bis mittlerem Berriasium. Basierend auf der Verbreitung von stratigrafisch wichtigen planktonischen Organismen, konnten einige gleichaltrige Calpionellen-, Dinozysten- und Nannofossil-Events um die Jura-Kreide Grenz Schichten nachgewiesen werden.

Schlüsselworte: Kalkige Mikrofossilien, Nannofossilien, Pelagische Karbonate, J/K Grenze, Grestener Klippenzone.

1. Introduction to the geology and lithology of the Nutzhof section

This study presents the results of a joint geophysical and palaeontological project focused on detailed palaeontological studies around the Jurassic-Cretaceous (J/K) boundary. The Nutzhof section is situated in the Gresten Klippenbelt at Nutzhof (Lower Austria) (Fig.

---

[1] Department of Geology and Palaeontology, Faculty of Natural Sciences, Comenius University, Mlynská dolina G-1, 842 15 Bratislava, Slovakia; e-mail: rehakova@fns.uniba.sk; halasova@fns.uniba.sk

[2] Natural History Museum Vienna, Geological-Palaeontological Department, Burgring 7, 1010 Vienna, Austria; e-mail: alexander.lukeneder@nhm-wien.ac.at

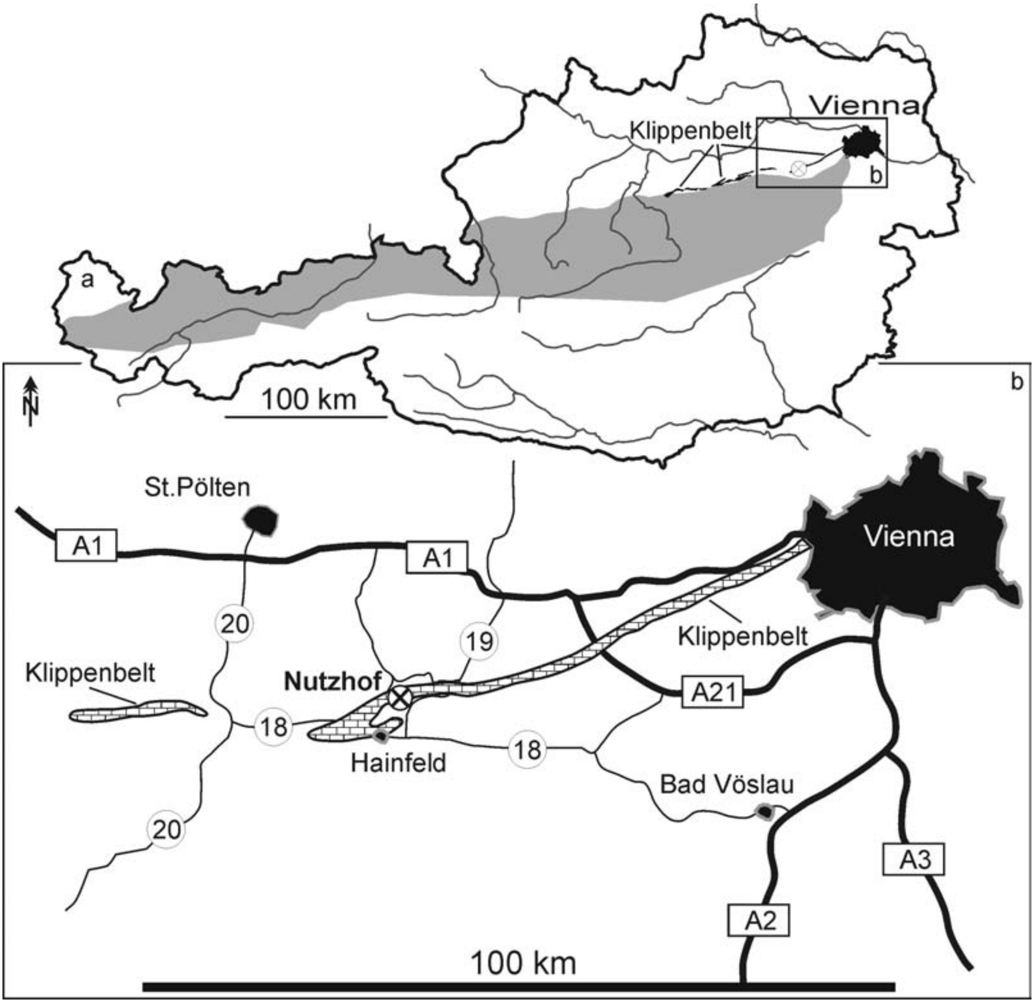

Fig. 1: Geological situation and localization of the Nutzhof section in Lower Austria from LUKENEDER (2009; this volume).

1). It yields a record of pelagic marine sedimentation in the Austrian Gresten Klippenbelt, located in the southern Flysch Zone. The first study of the lithology and stratigraphy of this area was provided by CŽIŽEK (1852), followed later by KÜPPER (1962). For a more detailed description of the Nutzhof section see LUKENEDER (this volume).

The preliminary results of micro- and nannofacies analysis and magnetostratigraphic investigations of the limestone sequence in the Nutzhof section were published by REHÁKOVÁ et al. (2009) and PRUNER et al. (2009). The data presented in this paper show that the Jurassic-Cretaceous pelagic limestone sequence of the Nutzhof section offers the possibility to clearly document the J/K boundary interval in the Austrian Gresten Klippenbelt based solely on the good calpionellid, dinoflagellate and nannofossil stratigraphic record.

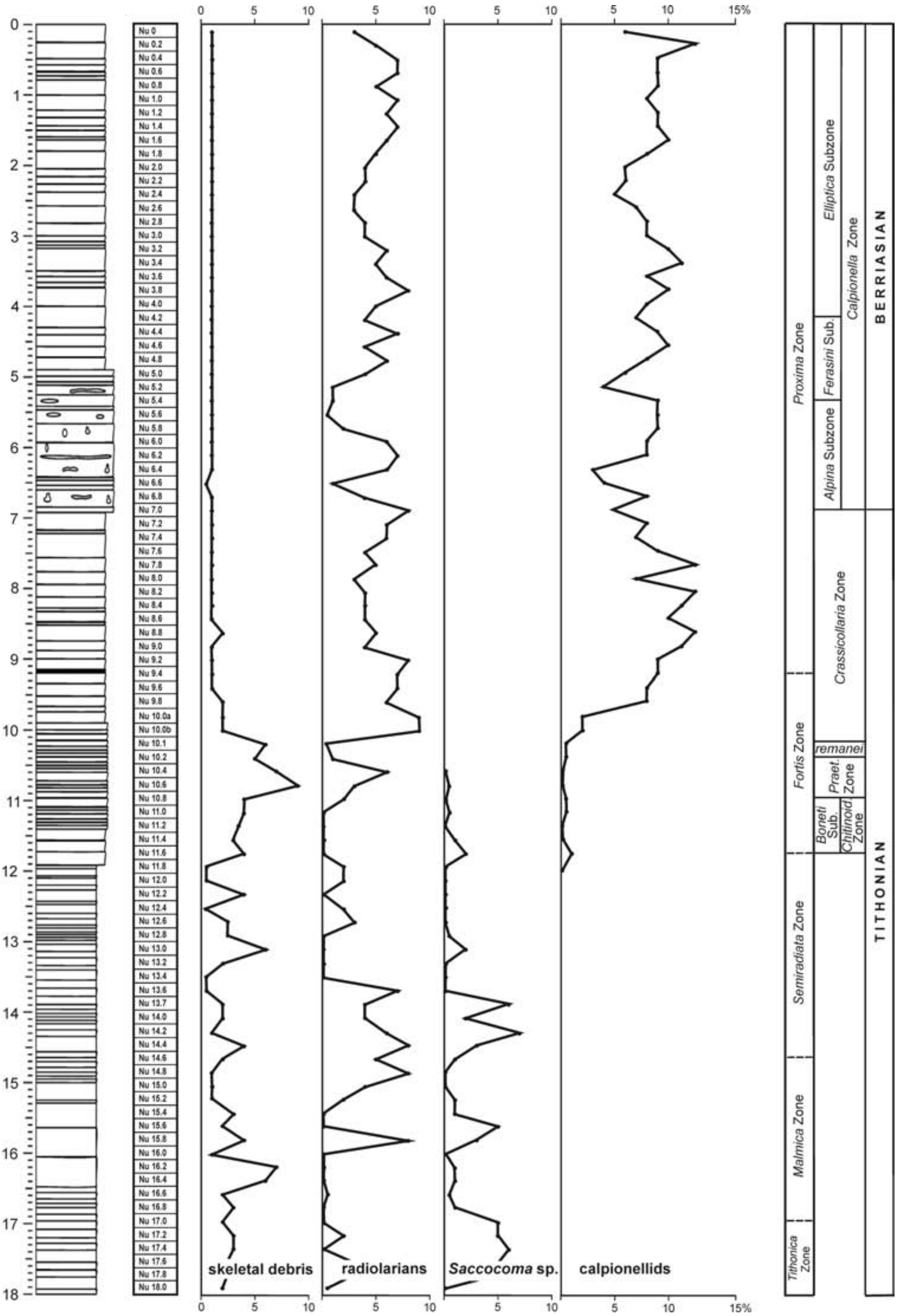

Fig. 2: Age, lithology and quantitative abundance of selected groups of organisms of the Nutzhof section.

2. Material and methods

The Jurassic-Cretaceous boundary sequence of the Nutzhof section was studied using an integrated biostratigraphy approach on the detailed rock section sampled. A quantitative microfacies analysis involved a thin sections study (fig. 2). Sample numbers, for example Nu 10.0, correspond to the sample interval at 10.0 meter within the log (for all numbers and figures, Nu Nutzhof). The calpionellids and calcareous dinoflagellates were studied under a light microscope LEICA DM 2500 P in 93 thin sections and they were documented by camera LEICA DFC 290 HD in Bratislava. Thin sections are deposited in the archive of the Natural History Museum in Wien (NHMW 2008z0271/0001-0036). Changes in the distribution of these organism remnants (fig. 3) in the microfacies were studied in detail in order to correlate them with the changes in nannoplankton associations (fig. 4).

Calcareous nannofossils were analyzed semiquantitatively in 19 smear slides prepared from all lithologies by standard techniques. The study was carried out using a light polarizing microscope at 1250x magnification. In order to obtain relative abundances, at least 200 specimens were counted in each slide. Their vertical distributions were recorded (fig. 4). Nannofossil preservation can be characterized as moderately to heavily etched by dissolution. Our study follows the zonal scheme proposed by BRALOWER et al. (1989).

A total of 46 ammonite specimens and 238 lamellaptychi were examined (LUKENEDER this volume). Four brachiopods and 3 inoceramids, along with single belemnite specimen, were collected. Ammonites are preserved (moderately well) as steinkerns. No shell is present. The phramocones are mostly flattened, whereas the body chambers are better preserved because of their history of early sediment infilling. The fragmentation is due to preburial-transport, sediment compaction and considerable tectonic deformation. This complicates the precise determination of most cephalopods with chambered hardparts (e.g. ammonites and belemnites). Most of the ammonite specimens were collected using hammers. The specimens required preparation with vibration tools after having been washed.

3. Results

3.1. Microfacies analysis – calpionellid and dinoflagellate biostratigraphy

The studied limestones are wackestones, packstones or mudstones. The observed fine-grained micrite with pelagic microfossils (calpionellids, calcareous dinoflagellates, radiolarians and calcareous nannofossils) is common in open-marine environments. The rare skeletal debris derived from fragmented and disintegrated shells of invertebrates (benthic foraminifers, echinoderms, molluscs) come from shallower environments. The studied microfacies are typical for basinal settings, which could also be situated in tectonically influenced, subsiding shelf areas.

The distribution, abundance and diversity of calcareous dinoflagellate cysts are important from both the stratigraphic and palaeoenvironmental points of view. We followed the calcareous dinoflagellate cyst zonation sensu REHÁKOVÁ (2000b). The preservation of the calpionellids is generally good. Their quantitative representation is variable, from

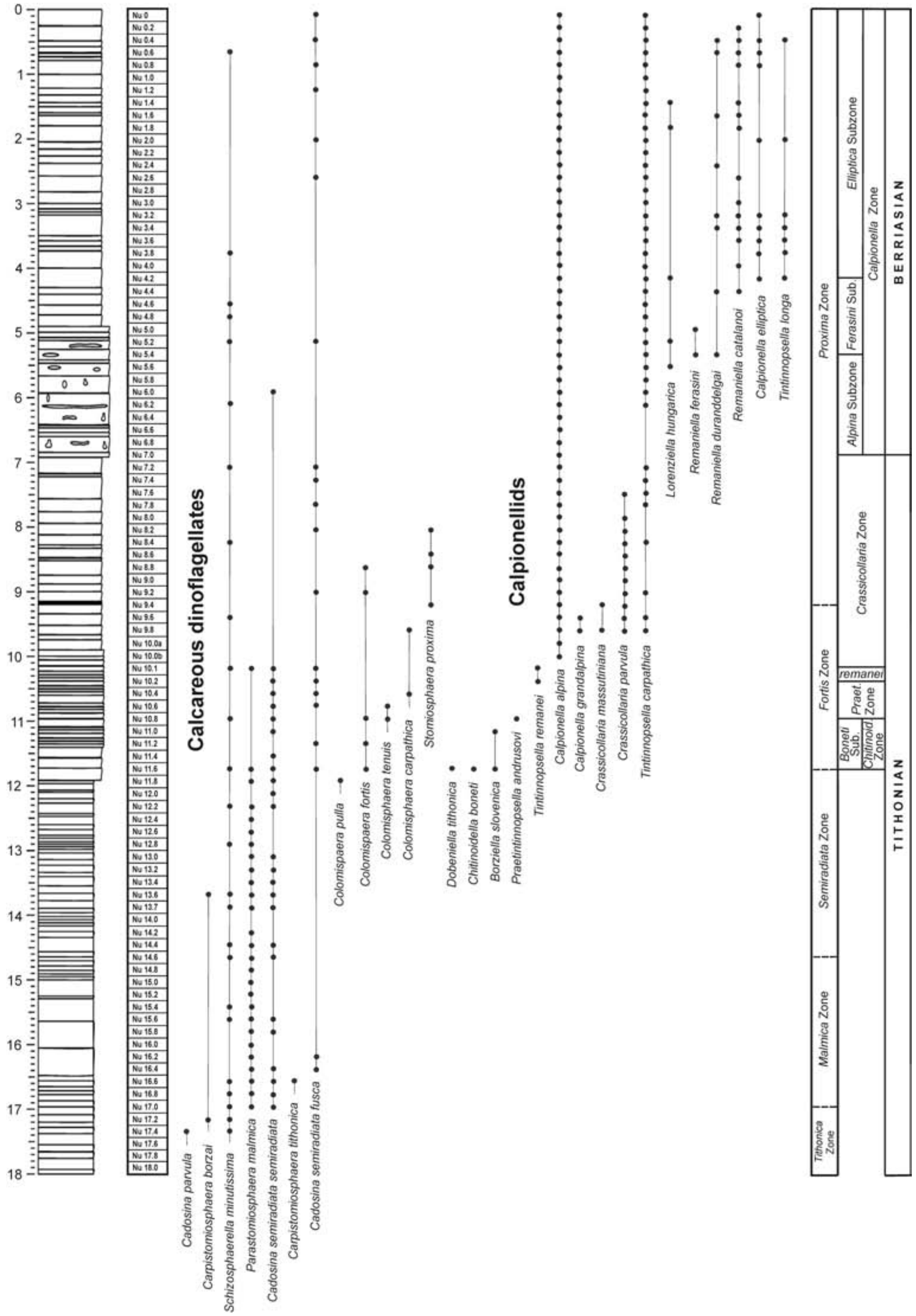

Fig. 3: Age, lithology, calpionellid and calcareous dinoflagellate biostratigraphy and vertical distribution of the recorded calpionellid and dinoflagellate species of the Nutzhof section.

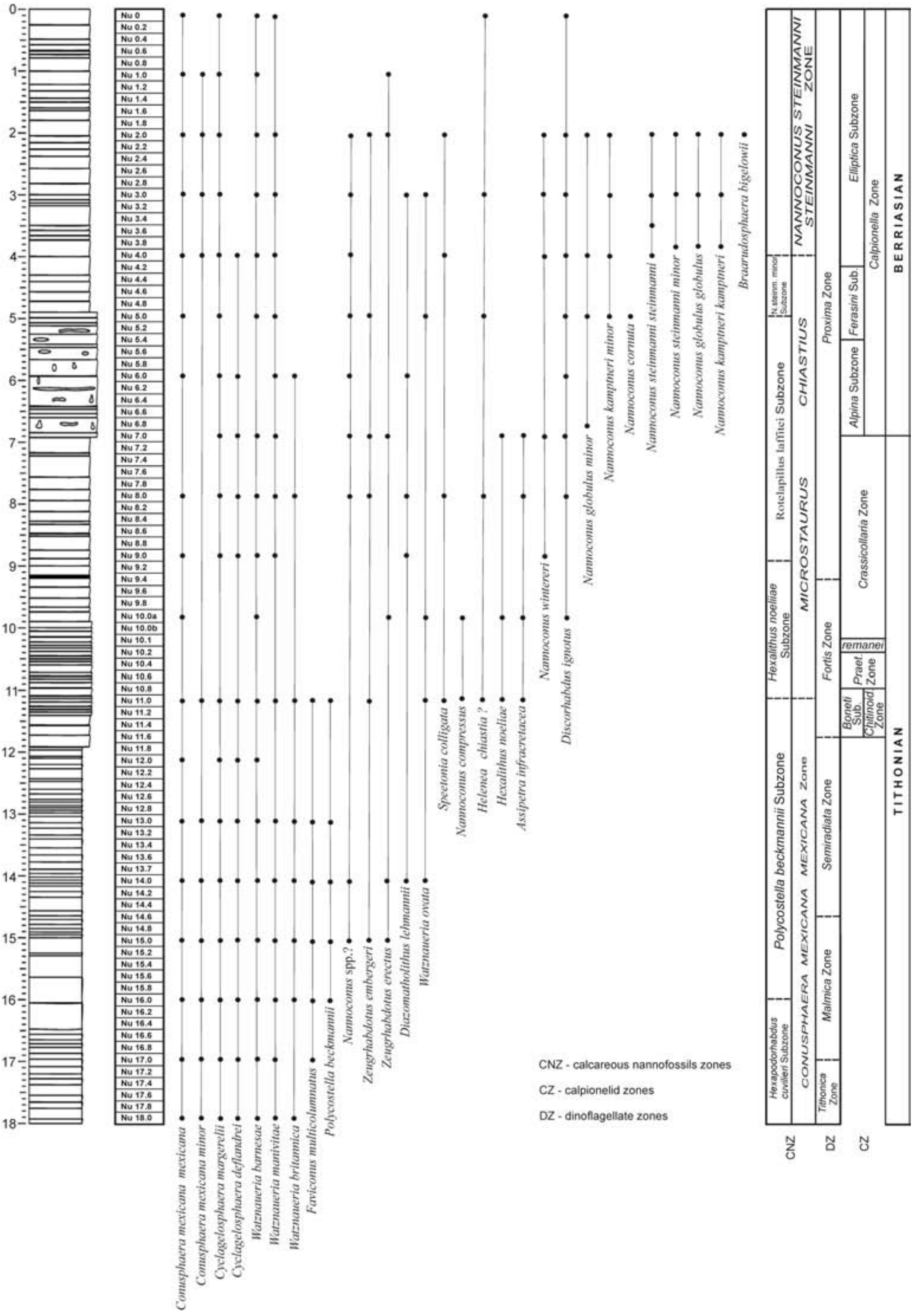

Fig. 4: Age, lithology, nannofossil biostratigraphy and vertical distribution of nannofossil species of the Nutzhof section.

less frequent in the case of chitinoidellids to more abundant in the hyaline forms of calpionellids. Although the chitinoidellids are not perfectly preserved, they enabled the application of POP´s (1997) and REHÁKOVÁ´s (2002) taxonomy. This study allows the *Boneti* Subzone to be recognized in the frame of the *Chitinoidella* Zone. The standard calpionellid zones and subzones, as proposed by REHÁKOVÁ (1995) and REHÁKOVÁ & MICHALÍK (1997), were adopted.

The following dinoflagellate and calpionellid associations and zones were recognized in the Nutzhof section (fig. 3).

***Tithonica* Zone** (the interval limited by samples 18.0 – 17.2)

It is represented by bioturbated biomicrite limestones (mudstones) with variable abundance of skeletal debris. Limestones contain calcified radiolarians (locally pyritized), sponge spicules, aptychi, ostracod and crinoid fragments, rare *Saccocoma* sp., *Cadosina parvula* NAGY, *Schizosphaerella minutissima* (COLOM), *Carpistomiosphaera borzai* (NAGY; pl. 1, fig.1) and *Carpistomiosphaera tithonica* NOWAK. Skeletal fragments are concentrated in nests and irregular fine-grained laminae or in tiny layers often rich in Fe-hydroxides. The matrix is stylolitized; locally, many composed stylolites and also thin calcite veins penetrate the biomicrite mudstones. Silty glauconite is also visible. **Early Tithonian.**

***Malmica* Zone** (the interval limited by samples 17.0 – 14.8)

The layers are built by bioturbated mudstones with rare biofragments dispersed in the matrix (pl. III. figs. 1, 2): bivalves, ostracods, ophiurid and ryncholite fragments (pl. 4, fig. 1), calcified radiolarians, sponge spicules, *Dentalina* sp., *Spirilina* sp., *Saccocoma* sp., *Parastomiosphaera malmica* (BORZA; pl. 1, fig. 2), *Cadosina semiradiata semiradiata* WANNER (pl. 1, fig. 3), *Cadosina semiradiata fusca* (WANNER), *Carpistomiosphaera tithonica* NOWAK and *Schizosphaerella minutissima* (COLOM). The matrix is penetrated by thin calcite veins. Thin laminae composed of fine-grained silt with muscovite and clay minerals and matrix rich in stylolites, framboidal pyrite and glauconite are documented in several thin sections. Pyrite is usually concentrated into the nests (pl. 3, fig. 3). Locally, the marly matrix has a pelitic structure. In this case the content of biofragments is very low – (thin sections contain very rare *Parastomiosphaera malmica* (BORZA) and silty glauconite). The last sample of this interval shows a distinct gradation of biodetritus. **Early Tithonian.**

***Semiradiata* Zone** (samples 14.6 – 11.8)

Marly limestones – biomicrite mudstones often bioturbated, containing aptychi, ostracods, crinoids, juvenile ammonite, bivalves, sponge spicules, calcified radiolarians concentrated in nests, *Saccocoma* sp., dinocysts: *Parastomiosphaera malmica* (BORZA), *Colomisphaera pulla* (BORZA; pl. 1, fig. 4), *Cadosina semiradiata semiradiata* WANNER and *Schizosphaerella minutissima* (COLOM). Biofragments are impregnated by Fe oxides/hydroxides (pl. 3, fig. 4). Locally, the matrix is penetrated by abundant calcite veins; it also contains framboidal pyrite and silty glauconite. The matrix in sample 13.4 reveals the marks of synsedimentary deformation (pl. 4, fig. 2), sample 13.2 contains thin layers (or laminae) rich in biodetritus. The matrix has a micropelitic structure locally. **Early Tithonian–Middle Tithonian**.

***Chitinoidella* Zone** (samples 11.6 – 11.0)

Biomicrite limestones – mudstones with input of skeletal debris concentrated in thin laminae (pl. III. fig. 5). They contain aptychi, bivalves, ostracods (locally also with ornamented shells), crinoids, ophiurids, sponge spicules, *Saccocoma* sp., *Colomisphaera fortis* Řehánek (pl. 1, figs. 5-6), *Parastomiosphaera malmica* (Borza), *Schizosphaerella minutissima* (Colom), *Cadosina semiradiata semiradiata* Wanner. The calpionellid assemblage is characterized by: *Borziella slovenica* (Borza; pl. 2, fig. 1), *Dobeniella tithonica* (Borza) and *Chitinoidella boneti* Doben (pl. 2, fig. 2). Part of the thin section (sample 11.6) rich in biodetritus is limited by the thin clay laminae and slowly passes to micrite limestone, which is penetrated by abundant calcite veins. Besides a fine clay admixture, the samples also contain glauconite, locally accumulations of pyrite cubes or framboidal pyrite (pl. 3, fig. 6). **Middle Tithonian.**

***Praetintinnopsella* Zone** (samples 10.8 – 10.4)

Bioturbated mudstones with laminae of fine detritus (pl. 4, figs. 3, 4). The studied samples contain radiolarians, ostracods, crinoids, sponge spicules, bivalves, foraminifers, *Cadosina semiradiata semiradiata* Wanner, *Schizosphaerella minutissima* (Colom), *Colomisphaera fortis* Řehánek, *Colomisphaera carpathica* (Borza), *Colomisphaera tenuis* (Nagy; pl. 1, fig. 7), and *Praetintinnopsella andrusovi* Borza. They also contain a small portion of glauconite and pyrite (locally nests of framboidal pyrite). The matrix in some samples is penetrated by thin calcite veins. Locally, mudstone passes to radiolarian-sponge wackestone with rich accumulation of radiolarians and sponge spicules. **Earliest Late Tithonian**.

***Crassicollaria* Zone, *Remanei* Subzone** (samples 10.2 – 10.1)

Bioturbated mudstone with laminae of fine biodetritus rich in calcareous cysts. It contains radiolarians, sponge spicules, ostracods, *Tintinnopsella remanei* Borza (pl. 2, fig. 3), *Cadosina semiradiata semiradiata* Wanner, *Schizosphaerella minutissima* (Colom) and *Parastomiosphaera malmica* (Borza). The matrix is penetrated by abundant, thin calcite veins. **Late Tithonian**.

***Crassicollaria* Zone**, ***Intermedia* Subzone** (samples 10.0 – 7.2)

Radiolarian-calpionellid or calpionellid-radiolarian wackestones (pl. 4, fig. 5). Wackestones pass locally to radiolarian packstone (mainly in small chert accumulations). The matrix contains aptychi, foraminifers, radiolarians, bivalves, sponge spicules, *Calpionella alpina* Lorenz (loricas are locally coated by dark, microgranular calcite), *Calpionella grandalpina* Nagy (pl. 2, fig. 4), *Crassicollaria massutiniana* (Colom), *Crassicollaria parvula* Remane (pl. 2, fig. 5), *Tintinnopsella carpathica* (Murgeanu & Filipescu), *Colomisphaera carpathica* (Borza), *Schizosphaerella minutissima* (Colom), *Stomiosphaerina proxima* Řehánek (pl. 1, fig. 8), *Cadosina semiradiata fusca* (Wanner) and *Colomisphaera fortis* Řehánek. The matrix of several samples is penetrated by rich calcite veins of different orientation. They are filled by blocky and fibrous calcite crystals. **Late Tithonian.**

***Calpionella* Zone, *Alpina* Subzone** (samples 7.0 – 5.6)

Calpionellid-radiolarian, radiolarian-calpionellid wackestones, locally calpionellid mudstones or mudstones penetrated by calcite veins (pl. 4, fig. 6). They contain aptychi, bivalves, crinoids, sponges, and radiolarians. In the lower part of the studied interval, a monospecific calpionellid association consisting of *Calpionella alpina* LORENZ is present, being accompanied in the overlying beds by *Tintinnopsella carpathica* (MURGEANU & FILIPESCU), *Lorenziella hungarica* KNAUER, *Stomiosphaerina proxima* ŘEHÁNEK (pl. 1, fig. 9) and *Schizosphaerella minutissima* (COLOM). **Lower Berriasian-J/K boundary**.

***Calpionella* Zone, *Ferasini* Subzone** (samples 5.4 – 4.4)

Radiolarian-calpionellid, calpionellid-radiolarian, locally calpionellid wackestones with calcified radiolarians, crinoids, aptychi, bivalves, ostracods, *Schizosphaerella minutissima*, *Cadosina semiradiata fusca*, *Calpionella alpina* LORENZ, *Tintinnopsella carpathica* (MURGEANU & FILIPESCU), *Remaniella ferasini* (CATALANO), *Remaniella duranddelgai* POP (pl. 2, fig. 6), *Remaniella catalanoi* POP and *Lorenziella hungarica* KNAUER. The matrix is locally penetrated by calcite veins. **Lower Berriasian**.

***Calpionella* Zone, *Elliptica* Subzone** (samples 4.2 – 0.0)

Predominantly radiolarian-calpionellid wackestones with radiolarians, sponge spicules, aptychi, *Punctaptychus*, crinoids, ostracods, bivalves, foraminifers, *Lenticulina* sp., *Schizosphaerella minutissima* (COLOM), *Cadosina semiradiata fusca* (WANNER), *Calpionella alpina* LORENZ, *Tintinnopsella carpathica* (MURGEANU & FILIPESCU), *Tintinnopsella longa* (COLOM; pl. 2, fig. 7), *Remaniella catalanoi* POP (pl. 2, fig. 8), *Remaniella duranddelgai* POP, *Calpionella elliptica* CADISCH (pl. 2, fig. 9) and *Lorenziella hungarica* KNAUER (part of loricas have dark coats). Locally, the matrix contains dispersed pyrite; moreover, part of the organic fragments is impregnated by Fe oxides. Abundant calcite veins oriented in several different directions are visible in some thin sections. **Middle Berriasian.**

3.2. Calcareous nannofossil biostratigraphy

A selected set of rock samples from the Nutzhof section were analysed for their calcareous nannofossil content. The succession of the nannofossil species identified in this study is represented in fig. 4. The semiquantitative study reveals that only the taxa *Nannoconus* spp., *Conusphaera* spp., *Polycostella* spp., *Cyclagelosphaera margerelii* NOËL, *Watznaueria barnesae* (BLACK) PERCH-NIELSEN, and *W. manivitae* BUKRY display significant abundances; nannofossils indicative of eutrophic environments such as *Zeugrhabdotus erectus* (DEFLANDRE) Reinhardt, *Diazomatholithus lehmannii* NOËL, and *Discorhabdus ignotus* (GÓRKA) PERCH-NIELSEN occur sporadically.

The calcareous nannofossil assemblage from the basal part of the Nutzhof section (samples 17, 18, *Tithonica* dinoflagellate Zone) contains the dissolution-resistant nannofossil species *Conusphaera mexicana* TREJO subsp. *mexicana* BRALOWER et al., (pl. 5, fig. 16), *Conusphaera mexicana* TREJO subsp. *minor* BOWN & COOPER (pl. 5, figs. 19-20), *Cyclagelosphaera margerelii* (pl. 5, fig. 11), *Cyclagelosphaera deflandrei*

(Manivit) Roth (pl. 5, figs. 13), *Watznaueria barnesae* (pl. 5, fig. 7), *Watznaueria britannica* (Stradner) Reinhardt (pl. 5, fig. 9), and *Watznaueria manivitae*. The FAD (first appearance datum) of *Faviconus multicolumnatus* Bralower (pl. 5, fig. 22) was recorded. The absence of the nannolith *Polycostella beckmannii* Thierstein allowed us to distinguish the *Conusphaera mexicana mexicana* NJ 20 Zone; *Hexapodorhabdus cuvillieri* Subzone NJ 20-A (Roth et al. 1983; emended Bralower et al. 1989) of the Early Tithonian in age.

The calcareous nannofossil assemblages from the samples 16 to 12 show dominance of the groups *Watznaueria* and *Conusphaera*. The FADs of *Zeugrhabdotus embergeri* (Noël) Perch-Nielsen (pl. 5, fig. 1), *Zeugrhabdotus erectus* (pl. 5, fig. 2), and *Diazomatholithus lehmannii* were observed. The FAD of the nannolith *Polycostella beckmannii* (pl. 6, figs. 21-26) is the most significant marker indicating the base of the *Polycostella beckmannii* Subzone NJ 20-B of the *Conusphaera mexicana mexicana* Zone, NJ-20 (Roth et al. 1983, emended Bralower et al. 1989). The age of this Subzone is Middle Tithonian. The range of the *Polycostella beckmannii* Subzone NJ 20-B fits with dinoflagellate *Malmica* and *Semiradiata* Zones and the lower part of the *Chitinoidella* Zone.

The calcareous nannofossils investigated in sample 11 reflect a rather distinct change. The FAD of *Helenea chiastia* Worsley (pl. 5, fig. 4), *Hexalithus noeliae* Loeblich & Tappan (pl. 6, fig. 30) and the nannolith species *Nannoconus compressus* Bralower et al. (pl. 5, figs. 23-24) are evidence for the base of the *Microstaurus chiastius* Zone NJK Bralower et al., 1989 and its *Hexalithus noeliae* Subzone NJK-A, which is thought to present the Late Tithonian interval. The Subzone coincides with the upper part of the *Chitinoidella* Zone.

The calcareous nannofossil assemblage selected from samples 9.0 to 6.0 contain the dissolution-resistant nannofossil genera *Conusphaera*, *Cyclagelosphaera*, *Watznaueria*, *Diazomatholithus* and *Assipetra*. The FAD of *Nannoconus wintereri* Bralower & Thierstein (pl. 5, figs. 25-26) was observed (sample 9.0). Many remains of dissolution-susceptible coccoliths are present. In the upper part of the studied interval, the abundance of *Conusphaera* drops. This interval was correlated with the *Microstaurus chiastius* Zone NJK, Subzone *Rotelapillus laffitei* NJK-C, determining the J/K boundary interval. It shows good correlation with the upper part of the Late Tithonian *Crassicollaria* Zone and the *Calpionella* Zone (*Alpina* Subzone), which represent the J/K boundary interval.

The interval bearing the calpionellid species of the Lower Berriasian *Calpionella* Zone (*Ferasini* Subzone) (sample 5.0) shows a distinctive change in the calcareous nannofossil assemblage – the onset of nannoconids (*Nannoconus globulus minor* Bralower (pl. 5, figs. 27-28), *Nannoconus steinmanni minor* Deres & Achéritéquy (pl. 6, fig. 1), *Nannoconus kamptneri minor* Bralower, *Nannoconus cornuta* Deres & Achéritéquy (pl. 5, figs. 29). This nannofossil event indicates the base of the *Nannoconus steinmannii minor* Subzone NJK-D (*Microstaurus chiastius* Zone NJK) Bralower et al., which is lowermost Berriasian in age.

The calcareous nannofossils studied from the sample interval 4.2 – 0.0 (correlating with the calpionellid *Calpionella* Zone, *Elliptica* Subzone) reveal the diversification of nannoconids. The FAD of *Nannoconus steinmanni steinmanni* Kamptner (pl. 5, fig. 30; pl. 6, figs. 4, 8,9) was registered. It could reflect the explosion in nannoconid abundance (sensu Bralower et al. 1989: p. 188). *Nannoconus globulus minor* (pl. 6, figs. 7, 11), *Nannoconus kamptneri minor* (pl. VI. figs. 2, 3), *Nannoconus wintereri*, *Nannoconus globulus* Brönnimann subsp. *globulus* Deres & Achéritéquy (pl. 6, fig. 5), *Nannoconus steinmanni minor* Deres & Achéritéquy (pl. 6, figs. 1, 13, 16-18), *Nannoconus steinmanni steinmanni* (pl. 6, figs. 19-20), and *Nannoconus kamptneri kamptneri* Brönnimann (pl. 6, figs. 2-3, 6, 15), *Nannoconus* spp. (pl. 6, figs. 12), indicated the *Nannoconus steinmannii steinmannii* Zone NK-1, Bralower et al., 1989, which is Middle Berriasian in age.

Based on the calcareous nannofossil distribution, the interval between the FO of *Nannoconus wintereri* co-occurring with small nannoconids (sample 9.0) and the FO of *Nannoconus steinmanni minor* in sample 5.0 (FAD after Hardenbol et al. 1998 – 143.92 Ma) can be interpreted in the Nutzhof section as the Tithonian-Berriasian boundary interval.

3.3. Cephalopod fauna

The cephalopod fauna from the Blassenstein Formation, correlated with micro- and nannofossil data from the marl-limestone succession, indicates Early Tithonian to Middle Berriasian age (*Hybonoticeras hybonotum* Zone up to the *Subthurmannia occitanica* Zone). According to the correlation of the fossil and magnetostratigraphic data, the entire log of the Nutzhof section embraces a duration of approx. 7 million years (approx. 150 – 143 mya). Six different genera were recorded, each apparently represented by a single species. The occurrence at the Nutzhof section is dominated by ammonites of the perisphinctid-type. Ammonitina are the most frequent component (60 %; *Subplanites* and *Haploceras*), followed by the Phylloceratina (25 %; *Ptychophylloceras* and *Phylloceras*), and the Lytoceratina (15; represented by *Lytoceras* and *Leptotetragonites*). The cephalopod fauna consists solely of Mediterranean elements (for more details see Lukeneder 2009; this volume).

4. Discussion

The high-resolution quantitative analysis of selected organic groups (radiolarians, saccocomids, calpionellids) indicates major variations in their abundance and composition (fig. 2). While the Upper Jurassic settings of the Nutzhof section were more or less influenced by the periodic input of biodetritus from surrounding shallow marine palaeoenvironments, the Berriasian settings were more equalized: the pelagic sediments were predominantly composed of remnants of planktonic microorganisms (radiolarians, calpionellids, dinoflagellates and nannofossils).

The calcareous dinoflagellates predominate in the Lower and Upper Tithonian sequence (Fig. 3), being represented by *Cadosina parvula* Nagy, *Carpistomiosphaera borzai* (Nagy), *Schizosphaerella minutissima* (Colom), *Parastomiosphaera malmica* (Borza), *Cadosina semiradiata semiradiata* Wanner, *Cadosina semiradiata fusca* (Wanner), *Carpistomiosphaera tithonica* Nowak, *Colomisphaera fortis* Řehánek, *Colomisphaera tenuis* (Nagy), *Colomisphaera carpathica* (Borza), and *Stomiosphaerina proxima* Řehánek. Several dinoflagellate zones were recognizable: *Tithonica*, *Malmica* and *Semiradiata* Zones. For the first time the appearance of *Colomisphaera fortis* Řehánek precedes the appearance of *Colomisphaera tenuis* (NAGY), preventing the determination of the *Tenuis* and *Fortis* dinoflagellate Zones sensu ŘEHÁNEK (1992).

The stratigraphic and palaeoecological potential of calcareous dinoflagellates has been discussed by REHÁKOVÁ (2000a, b). In the Nutzhof section, the Lower Tithonian record of these microorganisms shows a distinct change in abundance and composition. Orthopithonellid forms dominated in the *Tithonica* and *Malmica* Zones, but were replaced by obliquipithonellid species dominated by *Cadosina semiradiata semiradiata* WANNER in the *Semiradiata* Zone. According to MICHALÍK et al. (in print), coinciding acme peaks of *Cadosina semiradiata semiradiata* WANNER and *Conusphaera* spp. probably indicate warmer surface waters.

Based on the vertical calpionellid distribution, the J/K boundary interval can be characterized by several calpionellid events – the onset, diversification, and extinction of chitinoidellids (Middle Tithonian); the onset, burst of diversification, and extinction of crassicollarians (Late Tithonian); and the onset of the monospecific *Calpionella alpina* association just at the J/K boundary (REHÁKOVÁ in MICHALÍK et al., in print).

Chitinoidellids in the Nutzhof section (fig. 3) are very rare, being represented by *Borziella slovenica* (BORZA), *Dobeniella tithonica* (BORZA) and *Chitinoidella boneti* DOBEN, species typical for the *Boneti* Subzone of the *Chitinoidella* Zone. The appearance of first hyaline calpionellid loricas represented by *Praetintinnopsella andrusovi* BORZA and *Tintinnopsella remanei* BORZA precede the crassicolarian radiation. *Crassicollaria parvula* REMANE and *Calpionella alpina* LORENZ dominate over *Crassicollaria massutiniana* (COLOM), *Calpionella grandalpina* NAGY and *Tintinnopsella carpathica* (MURGEANU & FILIPESCU) in the *Remanei* Subzone of the *Crassicollaria* Zone. The interval with the monospecific calpionellid association consisting predominantly of *Calpionella alpina* LORENZ was also identified in the section. A similar interpretation of calpionellid evolution and the biostratigraphy of the Jurassic-Cretaceous boundary interval was given by REMANE (1986), POP (1994), REHÁKOVÁ (1995), OLÓRIZ et al. (1995), GRÜN & BLAU (1997), and ANDREINI et al. (2007).

Despite the inconvenient lithology, the calcareous nannofossil distribution in the Nutzhof section showed its potential for a stratigraphy of the deposits of the J/K boundary interval.

The major role of the coccoliths of the family Watznaueriaceae and three nannolithic genera (*Conusphaera*, *Nannoconus*, and *Polycostella*) was evident in the assemblage composition, which is in agreement with the results of nannofossil studies in other locations at low latitudes across the J/K boundary (THIERSTEIN 1971, 1973, 1975; ERBA 1989; GARDIN & MANIVIT 1993; ÖZKAN 1993; TAVERA et al. 1994; BORNEMANN et al. 2003; PSZCZÓŁKOWSKI & MYCZYŃSKI 2004; TREMOLADA et al. 2006; HALÁSOVÁ in MICHALÍK et al. in print.).

The first occurrences of nannofossils are perhaps somewhat unreliable due to the bad conditions of preservation, but we tentatively determined the boundaries of zones and subzones based on certain stratigraphic markers (*Polycostella beckmannii*, *Helenea chiastia*, *Hexalithus noeliae*, *Nannoconus wintereri*, *Nannoconus globulus minor*, *Nannoconus steinmanni minor*, *Nannoconus kamptneri minor*, *Nannoconus steinmanni steinmanni*, *Nannoconus kamptneri kamptneri*, *Nannoconus globulus globulus*).

TREMOLADA et al. (2006) detected that *Conusphaera* dominates the nannolith assemblage in the late Middle Tithonian (“*Conusphaera* world”). This agrees with data obtained in the Nutzhof section. The acme peak of the genus *Polycostella* in samples 13.0 and 14.0 coincides with the Middle Tithonian *Semiradiata* Subzone (REHÁKOVÁ 2000b). If compared with the Brodno section (MICHALÍK et al. 2007 and MICHALÍK et al. in print), the dominance of the Brodno nannoliths represented by *Polycostella beckmannii* was somewhat higher in the *Chitinoidella* Zone. The first appearance of *Helenea chiastia* also shows a similar diachroneity: it was identified in the Brodno section close to the onset of the calpionellid *Crassicolaria* Zone, whereas in the Nutzhof section its first appearance was recorded in the uppermost part of the *Chitinoidella* Zone.

The most distinct nannofossil event was observed in the lowermost Berriasian (in the interval of calpionellid *Calpionella* Zone, *Ferasini* Subzone of the Lower Berriasian age), the onset of nannoconids. This indicates the change in the palaeooceanographic regime and, from the biostratigraphic point of view, the upper J/K boundary datum based on the nannofossils (BORNEMANN et al., 2003).

Most of the ammonite specimens were apparently not redeposited from shallower shelf regions into a deeper shelf environment. The ammonite fauna of the Nutzhof section is interpreted as an assemblage comprising only “autochthonous” and parautochthonous pelagic elements from the open sea. The ammonite shells found their final resting place on the deeper shelf or upper slope of the European side of the Penninic Ocean.

5. Conclusions

The biostratigraphic study based on the distribution of calpionellids allowed us to distinguish the *Boneti* Subzone of the *Chitinoidella* Zone in the Nutzhof section. The J/K boundary in this section is situated between the *Crassicollaria* and *Calpionella* Zone (interval limited by samples 7.0 – 5.6). This base is defined by the morphological change of *Calpionella alpina* tests. The base of the *Crassicollaria* Zone approximately coincides with the onset of *Tintinnopsella remanei* BORZA and the base of the standard *Calpionella* Zone, with the monospecific calpionellid association being dominated by *Calpionella alpina* LORENZ. Two further Subzones (*Ferasini* and *Elliptica*) of the standard *Calpionella* Zone were recognized in radiolarian-calpionellid and calpionellid-radiolarian wackestones in the overlying topmost part of the investigated sequence.

Calcareous nannofossils from the Nutzhof section belong to low poorly diversified, because of the lithology. Nonetheless, the appearance of several important genera was determined, allowing the studied deposits to be attributed to the Early, Middle and Late Tithonian, the approximation of the Tithonian-Berriasian boundary, and the definition of the Early Berriasian nannofossil zones. The results show the major role of the coccoliths of the family Watznaueriaceae and nannoliths of the genera *Conusphaera, Nannoconus* and *Polycostella* in the assemblage composition. The interval between the FAD of *Nannoconus wintereri* co-occurring with small nannoconids in sample No 9 (the uppermost Tithonian) and the FAD of *Nannoconus kamptneri minor* in sample No 5 (lowermost Berriasian; 143.92 Ma after HARDENBOL et al. 1998) is interpreted as the Tithonian-Berriasian boundary interval. The nannoconid dominance (“*Nannoconus* world", Tremolada et al. 2006) starts, also in Nutzhof profile, in the lowermost Berriasian.

The macrofauna is represented especially by ammonoids, belemnoids, aptychi and bivalves. The whole section yielded about 46 ammonites. The sparse and selective occurrence of the ammonites within the Nutzhof log and the lithologic character of the Formation made sampling difficult.

The stratigraphic investigation of the cephalopods, microfauna and nannofauna revealed that the Nutzhof section comprises Tithonian to Berriassian sediments. The ammonoid fauna solely contains descendants of the Mediterranean Province. The ammonite fauna comprises 6 different genera, dominated by the perisphinctid-type. Ammonitina are the most frequent component (60 %; *Subplanites* and *Haploceras*), followed by the Phylloceratina (25 %; *Ptychophylloceras* and *Phylloceras*), and the Lytoceratina (15 %; represented by *Lytoceras* and *Leptotetragonites*). The cephalopod fauna consists solely of Mediterranean elements. The described descendants of *Subplanites* display the first evidence of these ammonoids within the Gresten Klippenbelt.

The cephalopod fauna from the Nutzhof section correlated with micro- and nannofossil data from the marl-limestone succession, indicating Early Tithonian to Middle Berriasian age (*Hybonoticeras hybonotum* Zone up to the *Subthurmannia occitanica* Zone). According to the correlation of the fossil and magnetostratigraphic data, the entire log of the Nutzhof section embraces a duration of approx. 7 million years (approx. 150 – 143 mya).

Acknowledgments

The authors thank to Sevinç Özkan-Altiner (Ankara), Gloria Andreini (Perugia) and Andreas Kroh (Vienna) for their valuable remarks and comments. Sincere thanks go to Hans Egger (Vienna) for showing us the outcrop. This research was supported by the Grant Agency for Sciences in Slovakia APVV (projects APVV-0280-07, APVV-0248-07, APVV-0465-06 and APVV-51-011305). We also gratefully acknowledge the Austrian Science Fund (FWF) for the financial support of project P20018-N10. Photographic work was done by Alice Schumacher (Natural History Museum, Vienna).

References

Andreini, G., Caracuel J. E. & Parisi, G. (2007): Calpionellid biostratigraphy of the Upper Tithonian – Upper Valanginian interval in Western Sicily (Italy). – Swiss Journal of Geosciences, **100**: 179-198.

Bornemann, A., Aschwer, U. & Mutterlose, J. (2003): The impact of calcareous nannofossils on the pelagic carbonate accumulation across the Jurassic–Cretaceous boundary interval. – Palaeogeography, Palaeoclimatology, Palaeoecology, **199**: 187-228.

Bralower, T. J., Monechi, S. & Thierstein, H. R. (1989): Calcareous nannofossil zonation of the Jurassic-Cretaceous boundary interval and correlation with the geomagnetic polarity timescale. – Marine Micropaleontology, **14**: 153-235.

Cžjžek, J. (1852): Aptychenschiefer in Niederösterreich. – Jahrbuch der Kaiserlich-Königlich Geologischen Reichs-Anstalt, **3**: 1-7.

Erba, E. (1989): Calcareous nannofossil zonation of the Jurassic-Cretaceous boundary interval and correlation with the geomagnetic polarity timescale. – Marine Micropaleontology, **14**: 153-235.

Gardin, S. & Manivit, H. (1993): Upper Tithonian and Berriasian calcareous nannofossils from the Vocontian Trough (SE France): Biostratigraphy and sequence stratigraphy. – Bulletin des Centres de Recherches Exploration – Production Elf-Aquitaine, **17**/1: 277-289.

Grün, B., & Blau, J. (1997): New aspects of calpionellid biochronology: proposal for a revised calpionellid zonal and subzonal division. – Revue de Paléobiologie, **16**: 197-214.

Hardenbol, J., Thierry, J., Farley, M. B., Jacquin, T., de Graciansky, P. C. & Vail, P. R. (1998): Mesozoic and Cenozoic sequence stratigraphy of European basins. – SEMP, Special Publications, **60**, 1998. Tulsa.

Küpper, H. (1962): Beobachtungen in der Hauptklippenzone bei Stollberg, N.Ö. – Verhandlungen der Geologischen Bundesanstalt, **2**: 263-268.

Michalík , J., Reháková, D., Halásová, E. & Lintnerová, O. (2007): Integrated stratigraphy of the Jurassic/Cretaceous boundary at the Brodno section (the Kysuca Unit, Pieniny Klippen Belt, Western Carpathians). – Abstract book, International geological correlation programme 506 – Jurassic marine: non-marine correlation, University of Bristol, p. 3.

——— , Reháková, D., Halásová, E. & Lintnerová, O. (in print): A possible West Carpathian regional stratotype of the Jurassic/Cretaceous boundary (the Brodno section near Žilina). – Geologica Carpathica.

Olóriz, F., Caracuel, J. E., Marques, B. & Rodríguez-Tovar, F. J. (1995): Asociaciones de Tintinnoides en facies Ammonitico Rosso de la Sierra Norte (Mallorca). – Revista Españolade Paleontología, No. Homenaje al Dr. G. Colom, 77-93.

Özkan, S. (1993): Calcareous nannofossils from the Late Jurassic-Early Cretaceous of Northwest Anatolia, Turkey. – Geological Journal, **28**/3-4: 295-307.

Pop, G. (1994): Calpionellid evolutive events and their use in biostratigraphy. – Romanian Journal of Stratigraphy **76**: 7-24.

——— (1997) : Révision systématique des chitinoidelles tithoniennes des carpathes méridionales (Roumanie). – Compte Rendus de l´Académie des Sciences, Paris, Série II a, **342**: 931-938.

Pszczółkowski, A. & Myczyński, R. (2004): Ammonite-supported microfossil and nannoconid stratigraphy of the Tithonian-Hauterivian limestones in selected sections of the Branisko Succession, Pieniny Klippen Belt (Poland). – Studia Geologica Polonica, **123**: 133-197.

Pruner, P., Schnabl, P., & Lukeneder, A. (2009): Preliminary results of magnetostratigraphic investigations across the Jurassic/Cretaceous boundary strata in the Nutzhof, Austria. – Berichte der Geologischen Bundesanstalt, **74**: 83-84.

Reháková, D. (1995): New data on calpionellid distribution in the Upper Jurassic/Lower Cretaceous formations (Western Carpathians). – Mineralia Slovaca, **27**: 308-318. [In Slovak].

——— & Michalík, J. (1997): Evolution and distribution of calpionellids – the most characteristic constituents of Lower Cretaceous tethyan microplankton. – Cretaceous Research **18**: 493-504.

——— (1998): Calpionellid genus *Remaniella* Catalano 1956 in Lower Cretaceous pelagic deposits of Western Carpathians. – Mineralia Slovaca, **30**: 443-452.

——— (2000a): Evolution and distribution of the Late Jurassic and Early Cretaceous calcareous dinoflagellates recorded in the Western Carpathian pelagic carbonate facies. – Mineralia Slovaca, **32**: 79-88.

——— (2000b): Calcareous dinoflagellate and calpinellid bioevents versus sea-level fluctuations recorded in the West-Carpathian (Late Jurassic/ Early Cretaceous) pelagic environments. – Geologica Carpathica, **51**/4: 229-243.

——— (2002): Chitinoidella Trejo, 1975 in Middle Tithonian carbonate pelagic sequences of the West Carpathian tethyan area. – Geologica Carpathica, **55**/6: 369-379.

——— , Halásová, E. & Lukeneder, A. (2009): The Jurassic-Cretaceous boundary in the Austrian Klippen Belt (Nutzhof, Lower Austria): Implications on micro- and nannofacies analysis. – Berichte der Geologischen Bundesanstalt, **74**: 95-95.

Řehánek, J. (1992): Valuable species of cadosinids and stomiosphaerids for determination of the Jurassic-Cretaceous boundary (vertical distribution, biozonation). – Scripta, **22**: 117-122.

Remane, J. (1986): Calpionellids and the Jurassic-Cretaceous boundary. – Acta Geologica Hungarica, **29**: 15-26.

Roth, P. H., Medd, A. W. & Watkins D,. K. (1983): Jurassic calcareous nannofossil zonation, an overview with new evidence from Deep Sea Drilling Project Site 534A. In Sheridan R.E., Gradstein F.M. et al., Initial Reports DSDP **76**: 573-579.

Tavera J. M., Aguado R., Company M. & Olóriz F. (1994): Integrated biostratigraphy of the. Durangites and Jacobi Zones (J/K boundary) at the Puerto Escaño section in Southern Spain (province of Cordoba). – Geobios, M.S., **17**: 469-476.

Thierstein, H. (1971). Tentantive Lower Cretaceous Calcareous Nanoplankton Zonation. – Eclogae Geologicae Helvetiae, **64**, 3: 437-652.

——— (1973). Lower Cretaceous Calcareous Nannoplankton Biostratigraphy. – Abhandlungen der Geologischen Bundesanstalt, **29**: 3-52.

——— (1975): Calcareous nannoplankton biostratigraphy at the Jurassic-Cretaceous boundary. Colloque sur la Limite Jurassique-Crétacé. – Bureau de Recherches Géologique et Minières, Mémoires, **86**: 84-94.

Tremolada F., Bornemann A., Bralower T., Koeberl C., van de Schootbrugge B. (2006): Paleoceanographic changes across the Jurassic/Cretaceous Boundary: the calcareous phytoplankton response. Earth and Planetary Science Letters **241**: 361-371.

Appendix

Nutzhof section – microfacies analysis of thin sections studied

No. 18.0
Bioturbated mudstone – rare radiolarians, sponge spicules, aptychy and ostracod fragments. Matrix penetrated by thin calcite veins.

No. 17.8
Bioturbated mudstone – rare *Saccocoma* sp., calcified radiolarians and sponge spicules, aptychy and ostracod fragments. Biodetritus are concentrated in nests and irregular fine grained layers which are rich in Fe-hydroxides.

No. 17.6
Bioturbated mudstone – rare *Saccocoma* sp., calcified radiolarians. Biodetritus is concentrated in nests which are rich in Fe- oxydes/hydroxides. Matrix is stylolitized; there are many composed stylolites and also thin calcite veins penetrating biomicrite mudstone.

No. 17.4
Bioturbated mudstone. Biodetrit increases in abundance. There are sponge spicules, rare *Saccocoma* sp., aptychy, crinoid fragments, *Cadosina parvula* and *Schizosphaerella minutissima* observed in thin section. Silty glauconit is also visible.

No. 17.4
Bioturbated mudstone – *Saccocoma* sp., aptychy, crinoids, sponge spicules, (without radiolarians), also *Cadosina parvula* and *Schizosphaerella minutissima*, glauconite of silt size.

No. 17.2
Bioturbated mudstone. *Carpistomiosphaera borzai*, *Schizosphaerella minutissima*, *Saccocoma* sp., aptychy, crinoids, sponge spicules, radiolarians (many of them are pyritized), ostracods. Matrix is stylolitized. ***Tithonica*** **Zone**

No 17.0
Bioturbated mudstone with rare organic fragments – *Saccocoma* sp., *Cadosina semiradiata semiradiata*, *Parastomiosphaera malmica*, *Schizosphaerella minutissima*, ostracods. Matrix penetrated by thin calcite veins. ***Malmica*** **Zone**.

No. 16.8
Mudstone with rare biofragments. It contains *Saccocoma* sp., *Cadosina semiradiata semiradiata*, *Parastomiosphaera malmica*, *Schizosphaerella minutissima*, *Dentalina* sp., bivalves, ostracods, framboidal pyrit and glauconit. Thin laminae composed of fine frained silt with muscovite and clay minerals are documented in the thin section.

No. 16.6
Bioturbated mudstone with rare skeletal fragments – ostracods, calcified radiolarians, *Saccocoma* sp., *Cadosina semiradiata semiradiata*, *Parastomiosphaera malmica*, *Schizosphaerella minutissima*, *Carpistomiosphaera tithonica*, Matrix is rich in stylolites.

No. 16.4
Marly limestone – mudstone with fine grained biofragments dispersed in matrix. It contains *Parastomiosphaera malmica*, *Cadosina semiradiata fusca*, *Cadosina semiradiata semiradiata*, *Saccocoma* sp., ostracods, silty glauconit and abundant pyrit.

No. 16.2
Bioturbated mudstone with *Saccocoma* sp., *Parastomiosphaera malmica*, *Cadosina semiradiata fusca* and ostracods. Pyrit is concentrated into the nests, there are several layers rich in silted admixure with glauconite and muscovite.

No. 16,0
Mudstone. Marly matrix with peletic structure (content of bio fragments is very low). It contains *Parastomiosphaera malmica* (one cyst in thin section) and glauconite.

No. 15.8
Bioturbated mudstone with nests rich in pyrite accumulations. It contains sponge spicules, radiolarians, bivalves, *Cadosina semiradiata semiradiata*, *Parastomiosphaera malmica*, *Spirilina* sp., *Saccocoma* sp.

No. 15.6
Marly biomicrite limestone with laminae of parallel oriented biodetrite – *Saccocoma* sp., *Parastomiosphaera malmica*, *Schizosphaerella minutissima*, *Cadosina semiradiata semiradiata*, ophiurid fragment, ryncholite, bivalves and ostracods.

No. 15.6
Marly biomicrite limestone with laminas of oriented biodetrite – *Saccocoma* sp., *Parastomiosphaera malmica*, *Schizosphaerella minutissima*, *Cadosina semiradiata semiradiata*, ophiuroid fragment, rhyncholit, sponge spicules, bivalves and ostracods, glauconite and pyrite.

No. 15.4
Bioturbated marly biomicrite limestone with laminas of oriented biodetrite – *Saccocoma* sp., *Parastomiosphaera malmica*, *Schizosphaerella minutissima*, *Dentalina* sp., ostracods and foraminifers. Matrix is stylolitized.

No. 15.2
Bioturbated mudstone – radiolarians, ostracods, foraminifers, *Saccocoma* sp., *Parastomiosphaera malmica*. Matrix is penetrated by thin calcite veins and stylolites impregnated by Fe-minerals.

No. 15.0
Bioturbated biomicrite limestone to mudstone. It contains *Parastomiosphaera malmica*. Pyrite is accumulated in nests.

No. 14.8
Bioturbated mudstone with distinct gradation. Radiolarians increase in abundance. It contains also aptychy fragments.

No. 14.6
Biomicrite limestone – mudstone with *Saccocoma* sp., ostracods, crinoids, *Parastomiosphaera malmica*, *Cadosina semiradiata semiradiata*, *Schizosphaerella minutissima*, juvenile ammonite.
***Semiradiata* Zone**

No. 14.4
Bioturbated mudstone with the nests riched in radiolarians, aptychy, ostracods, *Saccocoma* sp., *Parastomiosphaera malmica*, *Cadosina semiradiata semiradiata* and *Schizosphaerella minutissima*.

No. 14.2
Bioturbated mudstone with ostracods, *Saccocoma* sp., radiolarians, sponge spicules, frequent *Parastomiosphaera malmica*. Biofragments are impregnated by pyrit. Matrix contains also silty glauconit.

No. 14.0
Bioturbated mudstone penetrated by abundant calcite veins. It contains calcified radiolarians, ostracods, *Saccocoma* sp. Fe-minerals impregnate biodetrite fragments and stylolites.

No. 13.7
Bioturbated mudstone with tiny layers rich in silty admixure. It contains ostracods, radiolarians, crinoids, bivalves, *Saccocoma* sp., *Parastomiosphaera malmica*, *Cadosina semiradiata semiradiata*, *Schizosphaerella minutissima*, framboidal pyrite and glauconit.

No. 13.6
Mudstone – aptychy, bivalve, radiolarians impregnated by Fe-oxydes, abundant *Parastomiosphaera malmica*, *Carpistomiosphaera borzai*, *Schizosphaerella minutissima*.

No. 13.4
Marly limestone – mudstone – *Parastomiosphaera malmica*, *Cadosina semiradiata semiradiata*, pyrite and glauconite. Matrix brings the marks of synsedimentary deformation.

No. 13.2
Mudstone with thin layers rich in biodetrite. It contains foraminifers, ostracods, *Parastomiosphaera malmica* and *Cadosina semiradiata semiradiata*.

No. 13.0
Bioturbated mudstone with *Saccocoma* sp., foraminifers, *Parastomiosphaera malmica, Cadosina semiradiata semiradiata*, aptychy, crinoids and nests of pyrite. Matrix is fine grained, composed mainly of nannofossils. It is localy micropeletic.

No. 12.8
Mudstone – small fragments of biodetrite are localy concentated into fine laminae. Limestone contains *Saccocoma* sp., *Schizosphaerella minutissima*, *Parastomiosphaera malmica*, foraminifers, crinoids, aptychy, ostracods, glauconite and pyrite.

No. 12.6
Mudstone with *Parastomiosphaera malmica*, *Saccocoma* sp., aptychy, crinoids, radiolarians, bivalves. Matrix is stylolitised and it contains nests of pyrite and calcite veins of several generation (also raster types of calcite veins are present). Fe oxydes/hydroxides impregnate biofragments.

No. 12.4
Mudstone – *Parastomiosphaera malmica*, radiolarians, sponge spicules, ostracods, foraminifers, bivalves. Silty glauconite, nests of pyrite, stylolites, calcite veins.

No. 12.2
Mudstone – there are marks of synsedimentary deformation visible in the lower part of the thin section. *Parastomiosphaera malmica*, *Schizosphaerella minutissima*, *Cadosina semiradiata semiradiata* and silty glauconite are present.

No. 12.0
Mudstone – radiolarians, sponge spicules, *Cadosina semiradiata semiradiata*. nests of pyrite, stylolites, calcite veins.

No. 11.8
Mudstone – with frequent biodetrite concentrated in its lower part. Radiolarians, sponge spicules, abundant *Cadosina semiradiata semiradiata*, *Colomisphaera pulla*, *Parastomiosphaera malmica*. Matrix build predominantly by nannofossils.

No. 11.6
Biomicrite limestone – mudstone with input of skeletal debris concentrated in thin laminae. *Saccocoma* sp., *Colomisphaera fortis*, *Parastomiosphaera malmica*, *Schizosphaerella minutissima*, *Cadosina semiradiata semiradiata*, *Cadosina semiradiata fusca*, *Borziella slovenica*, *Dobeniella tithonica*, *Chitinoidella boneti*, aptychy, bivalves, ostracods, glauconite, pyrite. Part of thin section rich in biodetritus is limited by the thin clay laminae and slowly pass to micrite limestone which is penetrated by abundant calcite veins. ***Chitinoidella* Zone**.

No. 11.4
Micrite mudstone – *Saccocoma* sp., *Cadosina semiradiata semiradiata*, ostracods, crinoids, glauconite. Locally accumulations of pyrite cubes.

No. 11.2
Mudstone – with thin laminae rich in biodetrite – small fragments of crinoids, ostracods, aptychy, *Cadosina semiradiata semiradiata*, *Schizosphaerella minutissima*, *Colomisphaera fortis*. Fine clay admixture, pyrite, glauconite.

No. 11.0
Mudstone – small fragments of ostracods (partly with ornamented shells), crinoids, foraminifers, ophiurids, sponge spicules, aptychy, *Saccocoma* sp., *Cadosina semiradiata semiradiata*, *Borziella slovenica*, stylolites, glauconite, pyrite.

No. 10.8
Bioturbated mudstone penetrated by thin calcite veins. Radiolarians, ostracods, crinoids, sponge spicules, bivalves, foraminifers, *Cadosina semiradiata semiradiata*, *Schizosphaerella minutissima*, *Colomisphaera fortis*, *Colomisphaera tenuis*, *Praetintinnopsella andrusovi*, glauconite, pyrite. ***Praetintinnopsella* Zone**.

No. 10.6
Bioturbated mudstone with laminae of fine detrite. *Saccocoma* sp., *Cadosina semiradiata semiradiata*, radiolarians, crinoids, glauconite, pyrite, sponge spicules, bivalves. Nests of framboidal pyrite.

No. 10.4
Bioturbated mudstone passing to radiolarian–sponge wackestone with radiolarians, sponge spicules, ostracods, *Cadosina semiradiata semiradiata*, *Colomisphaera carpathica*.

No. 10.2
Bioturbated mudstone with laminae of fine biodetrite rich in calcareous cysts – *Cadosina semiradiata semiradiata*. It contains also *Tintinnopsella remanei* – the index species of ***Remanei* Subzone** of ***Crassicollaria* Zone**.

No. 10.1
Mudstone with laminae of fine detrite accumulation. It contains radiolarians, sponge spicules, ostracods, *Tintinnopsella remanei*, *Cadosina semiradiata semiradiata*, *Cadosina semiradiata fusca*, *Schizosphaerella minutissima*, *Parastomiosphaera malmica*. Matrix penetrated by abundant thin calcite veins.

No. 10.0
Radiolarian-calpionella wackestone passing to radiolarian packstone (in small chert accumulation). *Calpionella alpina* (loricas are coated by microgranular calcite dark in colour).

No. 9.8
Radiolarian-calpionella wackestone – *Calpionella alpina*, *Calpionella grandalpina*, *Crassicollaria parvula*, *Crassicollaria massutiniana*, *Tintinnopsella carpathica*, *Colomisphaera carpathica*, aptychy, foraminifers, radiolarians and bivalves.

No. 9.6
Radiolarian-calpionella wackestone with *Calpionella grandalpina*, *Calpionella alpina*, *Crassicollaria parvula*, *Tintinnopsella carpathica*, *Schizosphaerella minutissima*, aptychy, bivalves, sponge spicules. Nests of pyrite and calcite veins of different orientation.

No. 9.4
Radiolarian-calpionella wackestone. *Calpionella alpina*, *Crassicollaria massutiniana*, *Crassicollaria parvula*, *Stomiosphaerina proxima*, radiolarians, crinoids, bivalves, aptychy. Matrix is penetrated by rich calcite veins of different orientation, filled by blocky and fibrous calcite crystals.

No. 9.2
Calpionella-radiolarian wackestone – *Crassicollaria parvula*, *Calpionella alpina*, *Cadosina semiradiata fusca*, *Colomisphaera fortis*, aptychy, bivalves, sponge spicules, radiolarians, pyrite, foraminifers and abundant calcite veins.

No. 9.0
Radiolarian-calpionella wackestone. Radiolarians, sponge spicules, crinoids, *Calpionella alpina*, *Crassicollria parvula*.

No. 8.8
Radiolarian-calpionella wackestone. Crinoids, sponge spicules, bivalves, aptychy, *Calpionella alpina*, *Crassicollaria parvula*.

No. 8.6
Radiolarian-calpionella wackestone. Crinoids, sponge spicules, bivalves, *Crassicollaria parvula*, *Calpionella alpina*, *Stomiosphaerina proxima*.

No. 8.4
Radiolarian-calpionella wackestone. Sponges, crinoids, *Colomisphaera fortis*, *Schizosphaerella minutissima*, *Calpionella alpina*, *Crassicollaria parvula*, *Tintinnopsella carpathica*.

No. 8.2
Radiolarian-calpionella wackestone. Frequent *Cadosina semiradiata fusca*, radiolarians, sponges, bivalves, *Calpionella alpina*, *Tintinnopsella carpathic* and *Crassicollaria parvula*.

No. 8.0
Radiolarian-calpionella wackestone. Radiolarians decrease in abundance. *Calpionella alpina*, *Crassicollaria parvula*, aptychy, bivalves, crinoids, ostracods. Matrix penetrated by thin calcite veins.

No. 7.8
Radiolarian-calpionella wackestone. Radiolarians, foraminifers, bivalves, ostracods, aptychy, *Calpionella alpina*, *Tintinnopsella carpathica*, *Cadosina semiradiata fusca* and veins filled by calcite.

No. 7.6
Radiolarian-calpionella wackestone. Radiolarians, aptychy, bivalves, ostracods, *Calpionella alpina*, *Tintinnopsella carpathica* and *Crassicollaria parvula*.

No. 7.4
Radiolarian-calpionella wackestone. Radiolarians, sponges, crinoids, aptychy, bivalves, ostracods, foraminifers, *Calpionella alpina*, *Tintinnopsella carpathica*, *Crassicollaria parvula*, *Cadosina semiradiata fusca* and calcite veins.

No. 7.2
Radiolarian-calpionella wackestone. Radiolarians, bivalves, crinoids, foraminifers, *Calpionella alpina*, *Tintinnopsella carpathica*, *Crassicollaria parvula*, *Stomiosphaerina proxima*, *Schizosphaerella minutissima*, *Cadosina semiradiata fusca* and calcite veins.

No. 7.0
Calpionella-radiolarian wackestone – radiolarians dominated over *Calpionella alpina* (monospecific association of *Calpionella alpina*), aptychy, bivalves, sponges – **J/K boundary** – ***Alpina* Subzone** of ***Calpionella* Zone**.

No. 6.8
Calpionella mudstone – *Calpionella alpina*, aptychy, in lower part of the thin section radiolarians are also present.

No. 6.6
Mudstone penetrated by calcite veins. Biodetrite is not frequent. Radiolarians, *Calpionella alpina*, aptychy, bivalves and crinoids.

No. 6.4
Mudstone penetrated by rich thin calcite veins of different orientation. Radiolarians, *Calpionella alpina*, ostracods, bivalves and crinoids.

No. 6.2
Radiolarian-calpionella wackestone. *Calpionella alpina*, *Tintinnopsella carpathica*, radiolarians, *Schizosphaerella minutissima*, bivalves and crinoids.

No. 6.0
Calpionella-radiolarian wackestone. Crinoids, radiolarians, aptychy, bivalves, *Calpionella alpina* (typical Early Berriasian forms), *Tintinnopsella carpathica* and *Stomiosphaerina proxima*.

No. 5.8
Radiolarian-calpionella wackestone. Radiolarians, aptychy, bivalves, crinoids, ostracods, foraminifers, *Calpionella alpina*, *Tintinnopsella carpathica*. Calcite veins.

No. 5,6
Radiolarian-calpionella wackestone. Crinoids, aptychy (in average 1 or 2 pieces in thin section) radiolarians, *Calpionella alpina*, *Tintinnopsella carpathica* and *Lorenziella hungarica*.

No. 5.4
Radiolarian-calpionella wackestone. Radiolarians, crinoids, aptychy, *Calpionella alpina*, *Tintinnopsella carpathica*, *Remaniella ferasini*, *Remaniella duranddelgai*. Matrix is penetrated by calcite veins. ***Ferasini* Subzone** of the ***Calpionella* Zone**.

No. 5.2
Calpionella wackestone. Less radiolarians, aptychy, bivalves, crinoids, *Calpionella alpina*, *Tintinnopsella carpathica*, *Lorenziella hungarica*, *Cadosina semiradiata fusca* and *Schizosphaerella minutissima*.

No. 5.0
Radiolarian-calpionella wackestone. Radiolarians, aptychy, bivalves, *Calpionella alpina*, *Tintinnopsella carpathica* and *Remaniella ferasini*.

No. 4.8
Radiolarian-calpionella wackestone. Radiolarians, *Calpionella alpina*, *Tintinnopsella carpathica*, *Schizosphaerella minutissima* and bivalves.

No. 4.6
Radiolarian-calpionella wackestone. Radiolarians, bivalves, aptychy, crinoids, *Calpionella alpina*, *Tintinnopsella carpathica* and *Schizosphaerella minutissima*.

No. 4.4
Calpionella-radiolarian wackestone. Radiolarians, aptychy, bivalves, ostracods, *Remaniella catalanoi*, *Remaniella duranddelgai*, *Calpionella alpina* and *Tintinnopsella carpathica*.

No. 4.2
Radiolarian-calpionella wackestone. *Calpionella alpina*, *Calpionella elliptica*, *Tintinnopsella carpathica*, *Tintinnopsella longa*, *Lorenziella hungarica*, aptychy, bivalves, ostracods. Matrix contains dispersed pyrite, also part of the organic fragments is impregnated by Fe oxides. ***Elliptica* Subzone** of the ***Calpionella* Zone**.

No. 4.0
Radiolarian-calpionella wackestone, radiolarians, aptychy, bivalves, *Calpionella alpina*, *Tintinnopsella carpathica* and *Remaniella catalanoi*.

No. 3.8
Radiolarian-calpionella wackestone. Radiolarians, *Calpionella alpina*, *Calpionella elliptica*, *Tintinnopsella carpathica*, *Tintinnopsella longa*, *Schizosphaerella minutissima*, bivalves, aptychy and crinoids.

No. 3.6
Radiolarian-calpionella wackestone. Radiolarians, *Calpionella alpina*, *Calpionella elliptica*, *Tintinnopsella carpathica*, *Tintinnopsella longa*, *Remaniella catalanoi*, bivalves, aptychy and ostracods.

No. 3.4
Radiolarian-calpionella wackestone. Radiolarians, *Calpionella alpina*, *Calpionella elliptica*, *Tintinnopsella carpathica*, *Tintinnopsella longa*, *Remaniella catalanoi*, *Remaniella duranddelga* (part of loricas have dark coats), aptychy, bivalves and crinoids.

No. 3.2
Radiolarian-calpionella wackestone. Radiolarians, *Calpionella alpina*, *Calpionella elliptica*, *Tintinnopsella carpathica*, *Tintinnopsella longa*, *Remaniella duranddelgai*, *Remaniella catalanoi*. Abundant calcite veins oriented in several different directions.

No. 3.0
Radiolarian-calpionella wackestone. Fractures of several orientation filled by calcite. Radiolarians, bivalves, *Calpionella alpina*, *Tintinnopsella carpathica* and *Remaniella catalanoi*.

No. 2.8
Radiolarian-calpionella wackestone. Radiolarians, aptychy, bivalves, crinoids, *Calpionella alpina*, *Tintinnopsella carpathica* and calcite veins.

No. 2.8
Radiolarian-calpionella wackestone. Radiolarians, aptychy, bivalves, crinoids, *Calpionella alpina*, *Tintinnopsella carpathica* and calcite veins.

No. 2.6
Radiolarian-calpionella wackestone. Radiolarians, sponges, ostracods, *Calpionella alpina*, *Tintinnopsella carpathica*, *Remaniella catalanoi* and *Cadosina semiradiata fusca*.

No. 2.4
Radiolarian-calpionella wackestone. Radiolarians, ostracods, *Calpionella alpina*, *Tintinnopsella carpathica*, *Remaniella duranddelgai*. Calcite veins.

No. 2.2
Radiolarian-calpionella wackestone passing to mudstone. Aptychy, *Punctaptychus*, ostracods, (2 % of thin shells), radiolarians, bivalves, *Calpionella alpina*, *Tintinnopsella carpathica* and *Lorenziella hungarica*

No. 2.0
Radiolarian-calpionella wackestone passing to mudstone. Radiolarians, *Calpionella alpina*, *Calpionella elliptica*, *Tintinnopsella carpathica*, *Tintinnopsella longa*, *Cadosina semiradiata fusca*, bivalves and ostracods.

No. 1.8
Radiolarian-calpionella wackestone. Radiolarians, aptychy, bivalves, ostracods, *Calpionella alpina*, *Tintinnopsella carpathica*, *Remaniella catalanoi* and *Lorenziella hungarica*.

No. 1.6
Radiolarian-calpionella wackestone. Radiolarians, aptychy, bivalves, ostracods, *Calpionella alpina*, *Tintinnopsella carpathica*, *Remaniella duranddelgai*, *Remaniella catalanoi*.

No. 1.4
Radiolarian-calpionella wackestone. Radiolarians, aptychy, bivalves, ostracods, *Calpionella alpina*, *Tintinnopsella carpathica*, *Remaniella catalanoi* and *Lorenziella hungarica*.

No. 1.2
Radiolarian-calpionella wackestone. Radiolarians, aptychy, bivalves, ostracods, *Lenticulina* sp., *Calpionella alpina*, *Tintinnopsella carpathica* and *Cadosina semiradiata fusca*.

No. 1.0
Radiolarian-calpionella wackestone. Radiolarians, sponge spicules, aptychy, foraminifers, bivalves, *Calpionella alpina* and *Tintinnopsella carpathica*.

No. 0.8
Radiolarian-calpionella wackestone. Radiolarians, aptychy, bivalves, foraminifers, *Calpionella alpina*, *Calpionella elliptica*, *Tintinnopsella carpathica*, *Remaniella catalanoi* and *Cadosina semiradiata fusca*.

No. 0.6
Radiolarian-calpionella wackestone. Radiolarians, Aptychy, bivalves, *Calpionella alpina*, *Calpionella elliptica*, *Tintinnopsella carpathica*, *Remaniella duranddelgai*, *Remaniella catalanoi*, *Cadosina semiradiata fusca* and *Schizosphaerella minutissima*.

No. 0.4
Radiolarian-calpionella wackestone. Radiolarians, aptychy, bivalves, *Calpionella alpina*, *Calpionella elliptica*, *Tintinnopsella carpathica*, *Tintinnopsella longa*, *Remaniella catalanoi*, *Remaniella duranddelgai* and *Cadosina semiradiata fusca*.

No. 0.2
Radiolarian-calpionella wackestone – radiolarians, aptychy, bivalves, *Calpionella alpina*, *Remaniella catalanoi* and *Tintinnopsella carpathica*.

No. 0.0
Radiolarian-calpionella wackestone – radiolarians, *Calpionella alpina*, *Calpionella elliptica*, *Tintinnopsella carpathica* and *Cadosina semiradiata fusca*.

Plate 1

Fig. 1: *Carpistomiosphaera borzai* (NAGY) in bioturbated mudstone. Sample No. 17.2 (NHMW 2008z0271/0001).

Fig. 2: *Parastomiosphaera malmica* (BORZA) in bioturbated mudstone with rare skeletal debris. Sample No.13.0 (NHMW 2008z0271/0002).

Fig. 3: *Cadosina semiradiata semiradiata* WANNER in bioturbated mudstone with rare skeletal debris. Sample No. 17.0 (NHMW 2008z0271/0003).

Fig. 4: *Colomisphaera pulla* (BORZA) in biomicrite mudstone. Frequent skeletal fragments are concentrated in thin laminae. Sample No. 11.8 (NHMW 2008z0271/0004).

Figs 5-6: *Colomisphaera fortis* ŘEHÁNEK in bioturbated mudstone with rare skeletal debris dispersed in the micrite matrix. Sample No.10.8 (NHMW 2008z0271/0005).

Fig. 7: *Colomisphaera tenuis* (NAGY) in bioturbated mudstone containing rare skeletal debris dispersed in the micrite matrix. Sample No. 10.8 (NHMW 2008z0271/0005).

Figs 8-9: *Stomiosphaerina proxima* ŘEHÁNEK in radiolarian-calpionellid wackestone. Samples No. 9.4 (NHMW 2008z0271/0006) and No. 6.0 (NHMW 2008z0271/0007).

Scale bars equal 50 µm.

1
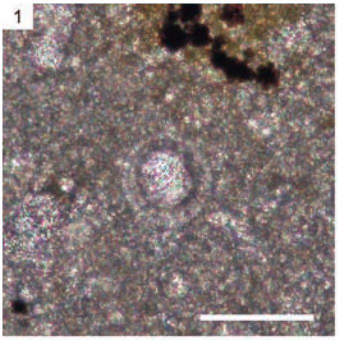

2
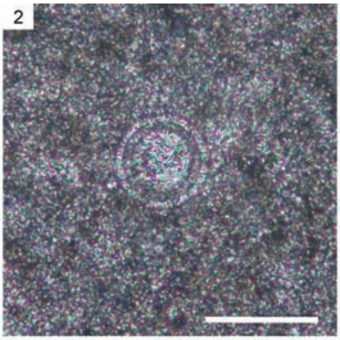

3
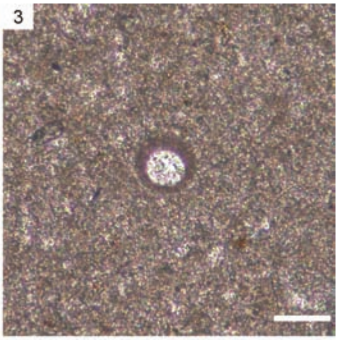

4
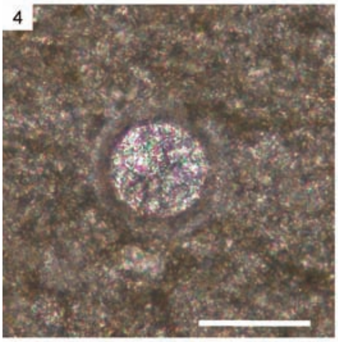

5
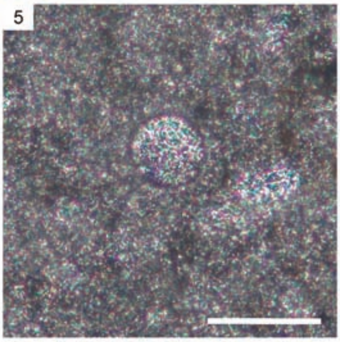

6
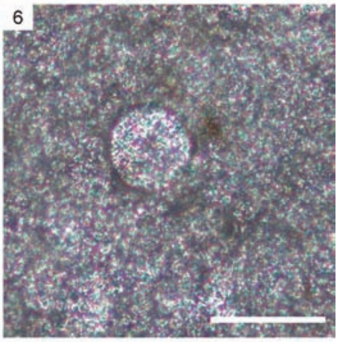

7
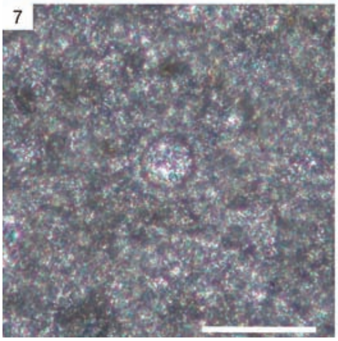

8
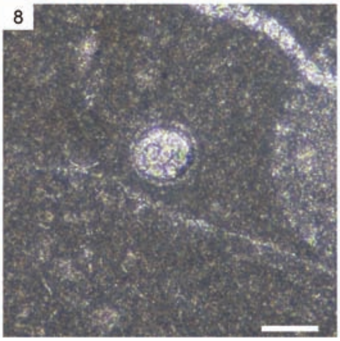

9
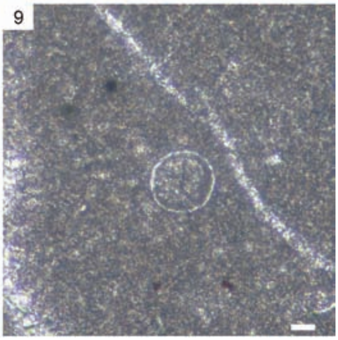

Plate 2

Fig. 1: *Borziella slovenica* (Borza) in mudstone containing rare skeletal debris dispersed in the micrite matrix. Sample No. 11.0 (NHMW 2008z0271/0008).

Fig. 2: *Chitinoidella boneti* Doben in biomicrite limestone – mudstone with skeletal debris concentrated in thin laminae. Sample No. 11.6 (NHMW 2008z0271/0009).

Fig. 3: *Tintinnopsella remanei* Borza in mudstone containing laminae of fine skeletal debris. Sample No. 10.1 (NHMW 2008z0271/0010).

Fig. 4: *Calpionella alpina* Lorenz and *Calpionella grandalpina* Nagy in radiolarian-calpionellid wackestone. Sample No. 9.8 (NHMW 2008z0271/0011).

Fig. 5: *Crassicollaria parvula* Remane and *Calpionella grandalpina* Nagy in radiolarian-calpionellid wackestone. Sample No. 9.6 (NHMW 2008z0271/0012).

Fig. 6: *Remaniella duranddelgai* Pop in calpionellid-radiolarian wackestone. Sample No. 4.4 (NHMW 2008z0271/0013).

Fig. 7: *Tintinnopsella longa* (Colom) in radiolarian-calpionellid wackestone. Sample No. 3.4 (NHMW 2008z0271/0014).

Fig. 8: *Remaniella catalanoi* Pop in radiolarian-calpionellid wackestone. Sample No. 3.4 (NHMW 2008z0271/0014).

Fig. 9: *Calpionella elliptica* Cadisch in radiolarian-calpionellid wackestone. Sample No. 3.2 (NHMW 2008z0271/0015).

Scale bars equal 50 µm.

1
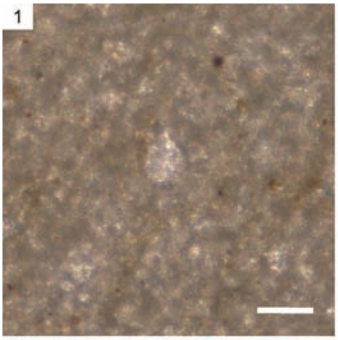

2
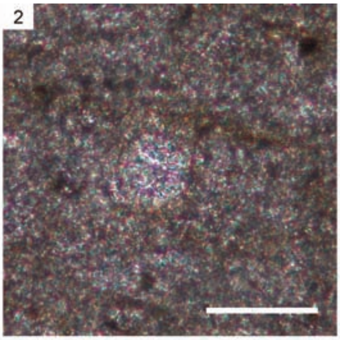

3
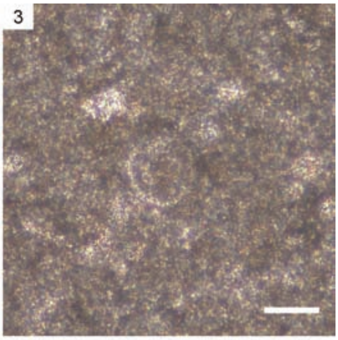

4
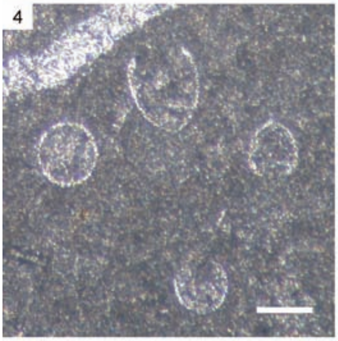

5
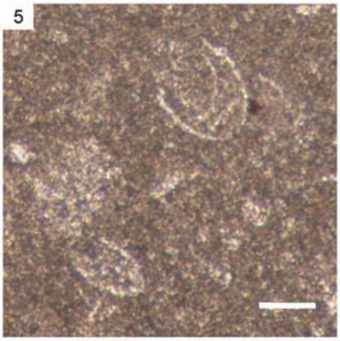

6
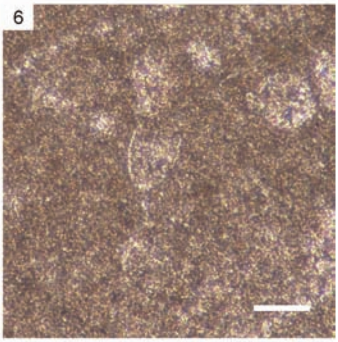

7
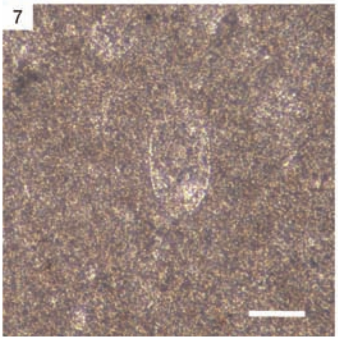

8
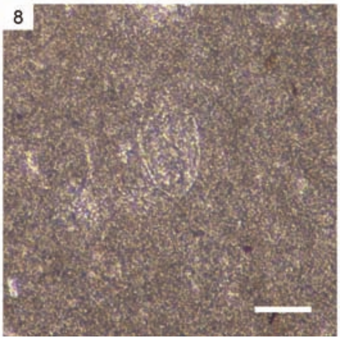

9
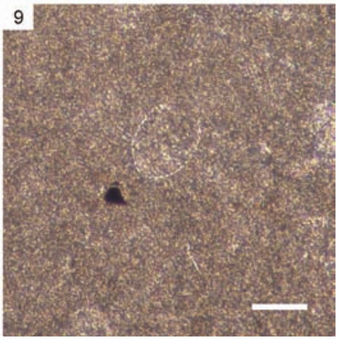

Plate 3

Fig. 1: Bioturbated biomicrite mudstone. Fine skeletal debris accumulated in circular swirl. Sample No. 15.8 (NHMW 2008z0271/0016).

Fig. 2: Fine skeletal fragments impregnated by Fe hydroxides concentrated in burrow filling. The absence of compaction indicates firmground substrate consistency.
Sample No. 15.8 (NHMW 2008z0271/0016).

Fig. 3: Fine skeletal fragments and nests rich in Fe hydroxide accumulations. Sample No. 15.8 (NHMW 2008z0271/0016).

Fig. 4: Pyritized radiolarian tests in biomicrite mudstone. Sample No. 13.6 (NHMW 2008z0271/0017).

Fig. 5: Lamination due to parallel oriented fragments of *Saccocoma* sp. Sample No. 11.6 (NHMW 2008z0271/0009).

Fig. 6: Accumulation of pyrite cubes in biomicrite mudstone. Sample No. 11.4 (NHMW 2008z0271/0018).

Scale bars equal 100 µm.

1

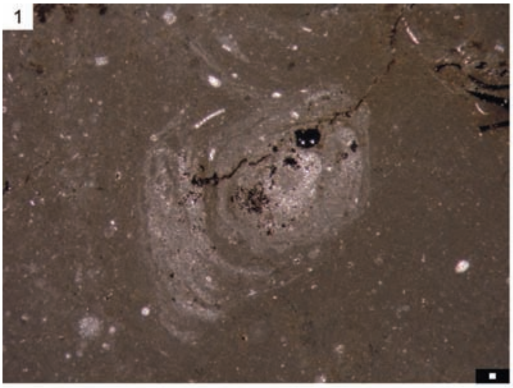

2

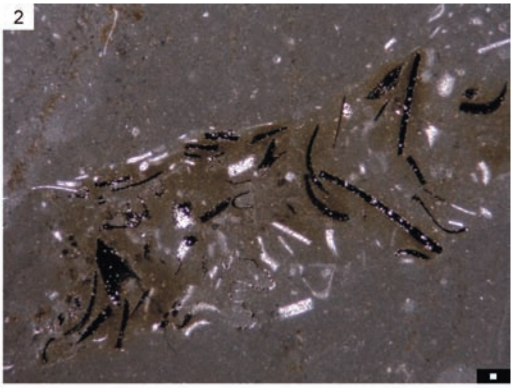

3

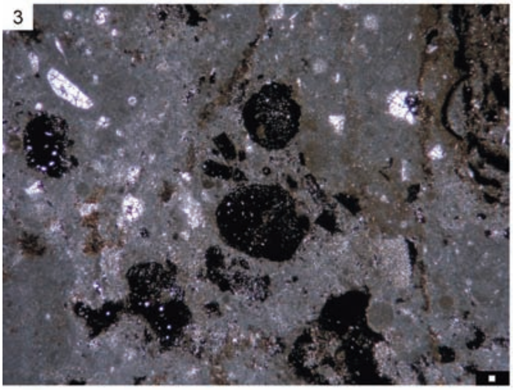

4

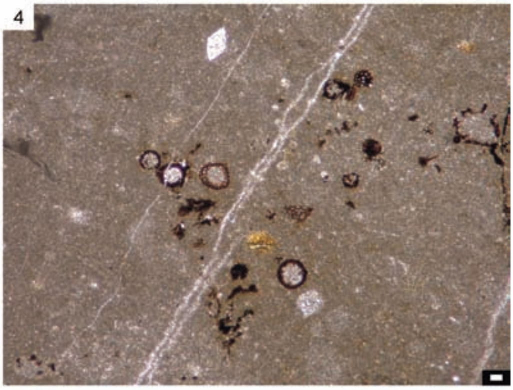

5

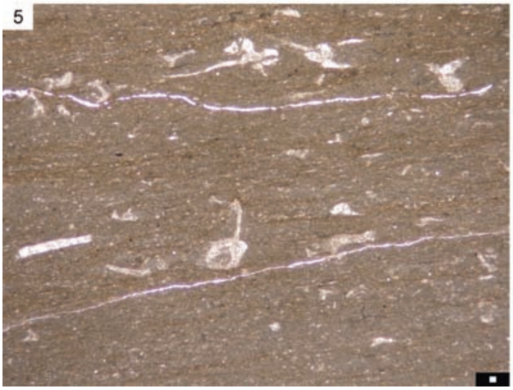

6

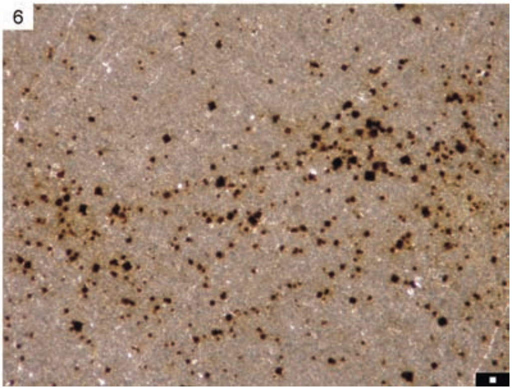

Plate 4

Fig. 1: Rhyncholite in biomicrite mudstone in marly biomicrite mudstone. Sample No.15.6 (NHMW 2008z0271/0019).

Fig. 2: Marks of synsedimentary deformation on the base of sample No. 12.2 (NHMW 2008z0271/0020).

Figs 3-4: Microsparitic laminae with peloids and *Cadosina semiradiata semiradiata* Wanner in biomicrite limestone – mudstone. Variously shaped micritic grains – mud peloids, commonly without internal structures. Grains originated from the reworking of weakly lithified carbonate mud; they were transported in suspension.
Sample No. 10.6 (NHMW 2008z0271/0021).

Fig. 5: Radiolarian-calpionellid wackestone penetrated by thin calcite veins. Sample No. 9.8 (NHMW 2008z0271/0011).

Fig. 6: Biomicrite mudstone with *Calpionella alpina* Lorenz penetrated by calcite veins of various size and orientation. Sample No. 6.4 (NHMW 2008z0271/0022).

Scale bars equal 100 µm.


1

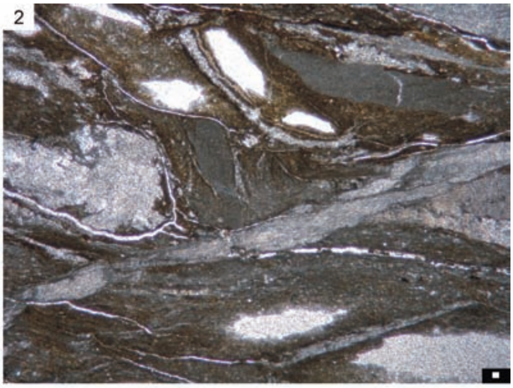
2

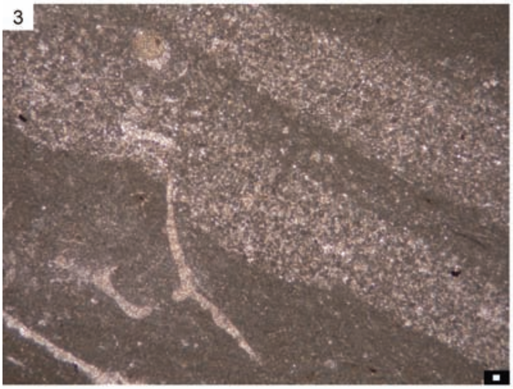
3

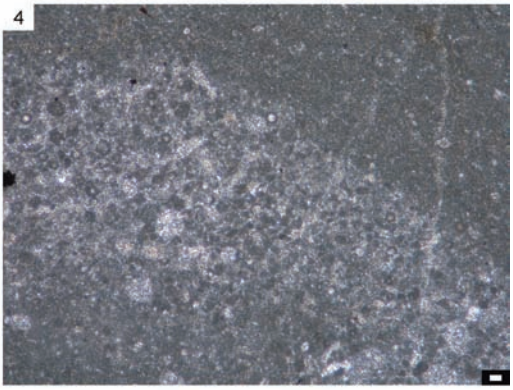
4

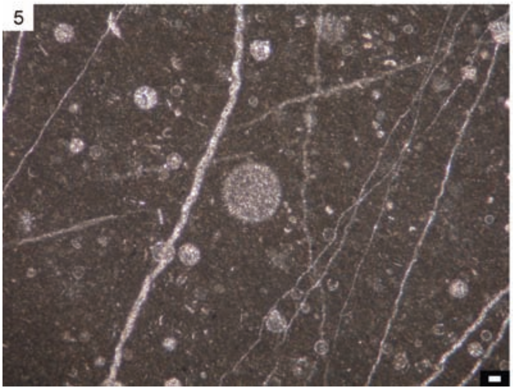
5

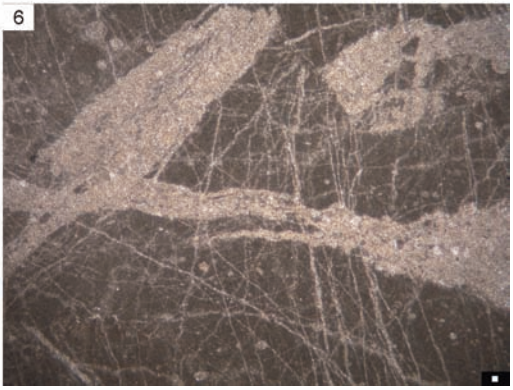
6

Plate 5

Fig. 1: *Zeugrhabdotus embergeri* (Noël) Perch-Nielsen; Sample No. 15.0 (NHMW 2008z0271/0023).

Fig. 2: *Zeugrhabdotus erectus* (Deflandre) Reinhardt; Sample No. 10.0 (NHMW 2008z0271/0024).

Fig. 3: *Discorhabdus ignotus* (Górka) Perch-Nielsen; Sample No. 9.0 (NHMW 2008z0271/0025).

Fig. 4: *Helenea chiastia* Worsley*;* Sample No. 11.0 (NHMW 2008z0271/0008).

Fig. 5: *Speetonia colligata* Black; Sample No. 8.0 (NHMW 2008z0271/0026).

Figs 6-8: *Watznaueria barnesae* (Black) Perch-Nielsen; Samples No. 9.0 (NHMW 2008z0271/0025), 17.0 (NHMW 2008z0271/0003), 9.0 (NHMW 2008z0271/0025).

Fig. 9: *Watznaueria britannica* (Stradner) Reinhardt; Sample No. 18.0 (NHMW 2008z0271/0028).

Fig. 10: *Watznaueria ovata* Bukry; Sample No. 9.0 (NHMW 2008z0271/0025).

Figs 11-12: *Cyclagelosphaera margerelii* Noël; Samples No. 18.0 (NHMW 2008z0271/0028), 15.0 (NHMW 2008z0271/0023).

Fig. 13: *Cyclagelosphaera deflandrei* (Manivit) Roth; Sample No. 17.0 (NHMW 2008z0271/0003).

Fig. 14: *Diazomatholithus lehmannii* Noël; Sample No. 3.0 (NHMW 2008z0271/0029).

Figs 15-18: *Conusphaera mexicana* Trejo subsp. *mexicana* Bralower et al.; Samples No. 11.0 (NHMW 2008z0271/0008), 15.0 (NHMW 2008z0271/0023), 17.0 (NHMW 2008z0271/0003).

Figs 19-20: *Conusphaera mexicana* Trejo subsp. *minor* Bown & Cooper; Sample No. 18.0 (NHMW 2008z0271/0028).

Figs 21-22: *Faviconus multicolumnatus* Bralower in Bralower et al.; Samples No. 14.0 (NHMW 2008z0271/0030), 17.0 (NHMW 2008z0271/0003).

Figs 23-24: *Nannoconus compressus* Bralower & Thierstein in Bralower et al.; Sample No. 11.0 (NHMW 2008z0271/0008).

Figs 25-26: ?*Nannoconus wintereri* Bralower & Thierstein in Bralower et al.; Sample No. 9.0 (NHMW 2008z0271/0025).

Figs 27-28: *Nannoconus globulus* Brönnimann ssp. *minor* Bralower in Bralower et al.; Samples No. 7.0 (NHMW 2008z0271/0032), 5.0 (NHMW 2008z0271/0033).

Fig. 29: *Nannoconus cornuta* Deres & Achéritéquy; Sample No. 5.0 (NHMW 2008z0271/0033).

Fig. 30: *Nannoconus steinmanni steinmanni* Kamptner; Sample No. 4.0 (NHMW 2008z0271/0034).

Light micrographs using an Olympus CAMEDIA digital camera C-4000 Zoom.
Scale bars equal 1 µm

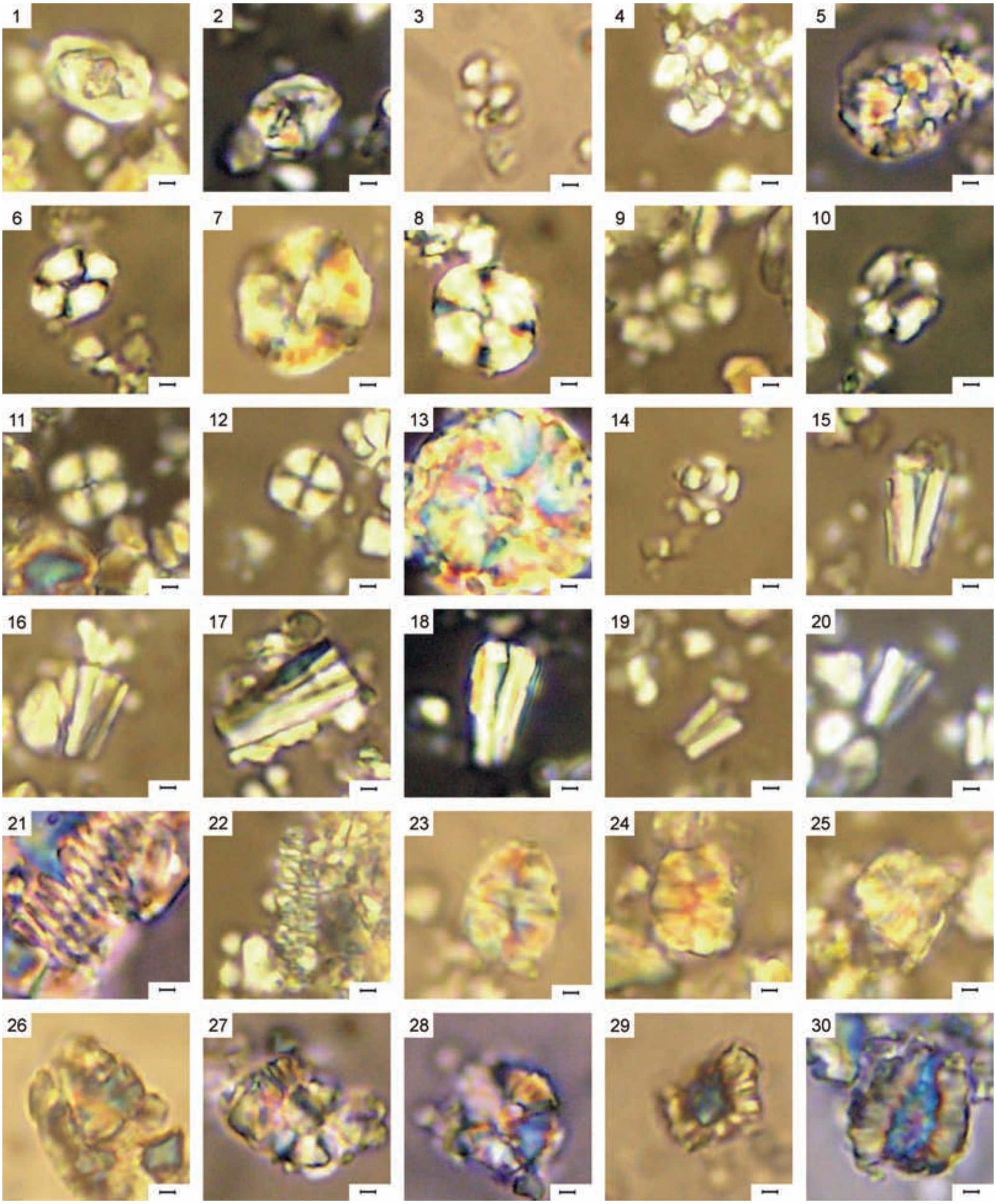
1
2
3
4
5
6
7
8
9
10
11
12
13
14
15
16
17
18
19
20
21
22
23
24
25
26
27
28
29
30

Plate 6

Fig. 1: *Nannoconus steinmanni minor* Deres & Achéritéquy; Sample No. 4.0 (NHMW 2008z0271/0034).

Figs 2-3: *Nannoconus kamptneri kamptneri* Brönnimann; Sample No. 4.0 (NHMW 2008z0271/0034).

Figs 4, 8, 9: *Nannoconus steinmanni steinmanni* Kamptner; figs show the same specimen, Sample No. 3.0 (NHMW 2008z0271/0029).

Fig. 5: *Nannoconus globulus globulus* Brönnimann; Sample No. 3.0 (NHMW 2008z0271/0029).

Fig. 6: *Nannoconus kamptneri kamptneri* Brönnimann; Sample No. 3.0 (NHMW 2008z0271/0029).

Figs 7, 11: *Nannoconus globulus* Brönnimann ssp. *minor* Bralower in Bralower et al.; Samples No. 3.0 (NHMW 2008z0271/0029), 2.0 (NHMW 2008z0271/0035).

Fig. 10: *Nannoconus kamptneri minor* Bralower in Bralower et al.; Sample No. 3.0 (NHMW 2008z0271/0029).

Fig. 12: *Nannoconus* spp.; Sample No. 2.0 (NHMW 2008z0271/0035).

Fig. 13: *Nannoconus steinmanni minor* Deres & Achéritéquy; Sample No. 2.0 (NHMW 2008z0271/0035).

Fig. 14: *Nannoconus kamptneri minor* Bralower in Bralower et al.; Sample No. 2.0 (NHMW 2008z0271/0035).

Fig. 15: *Nannoconus kamptneri kamptneri* Brönnimann; Sample No. 2.0 (NHMW 2008z0271/0035).

Figs 16-18: *Nannoconus steinmanni minor* Deres & Achéritéquy; Sample No. 2.0 (NHMW 2008z0271/0035).

Figs 19-20: *Nannoconus steinmanni steinmanni* Kamptner; Sample No. 2.0 (NHMW 2008z0271/0035).

Figs 21-26: *Polycostella beckmannii* Thierstein; Samples No. 16.0 (NHMW 2008z0271/0036), 14.0 (NHMW 2008z0271/0030), 13.0 (NHMW 2008z0271/0002).

Figs 27-28: *Assipetra infracretacea* (Thierstein) Roth; Samples No. 7.0 (NHMW 2008z0271/0032), 8.0 (NHMW 2008z0271/0026).

Figs 29-30: *Hexalithus noeliae* Loeblich & Tappan; Samples No. 7.0 (NHMW 2008z0271/0032), 11.0 (NHMW 2008z0271/0008).

Light micrographs using Olympus CAMEDIA digital camera C-4000 Zoom.
Scale bars equal 1 µm.

1
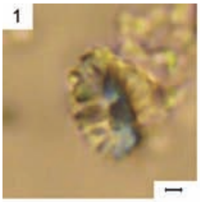
2
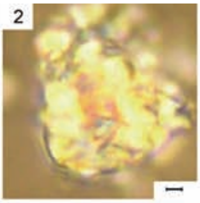
3
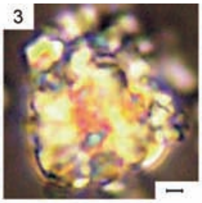
4
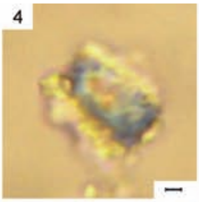
5
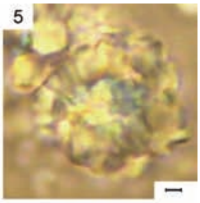
6
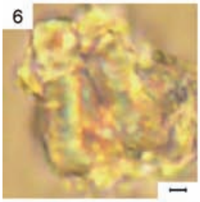
7
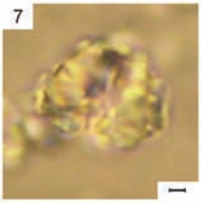
8
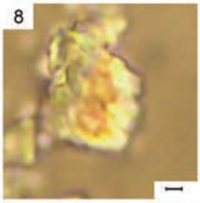
9
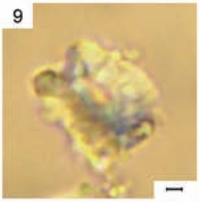
10
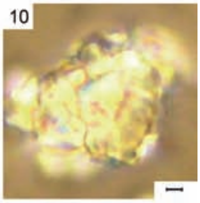
11
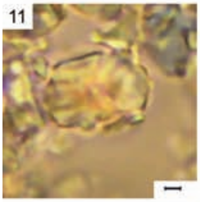
12
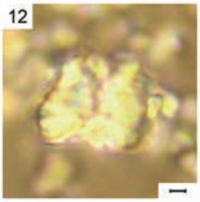
13
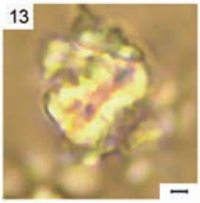
14
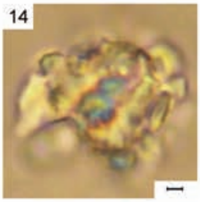
15
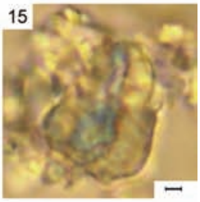
16
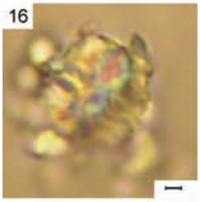
17
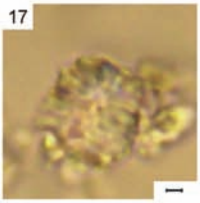
18
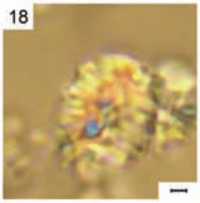
19
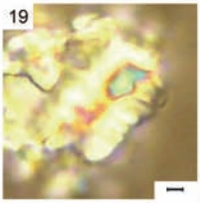
20
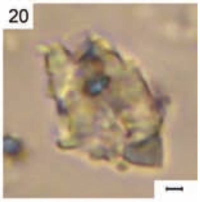
21
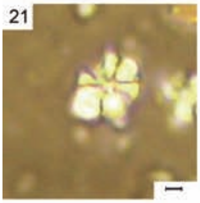
22
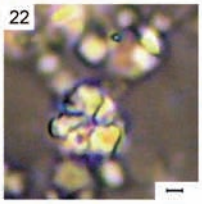
23
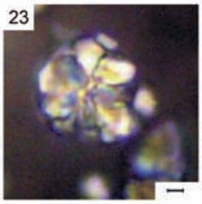
24
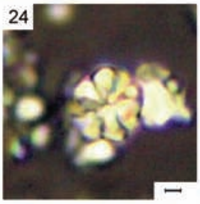
25
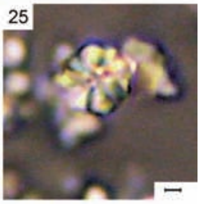
26
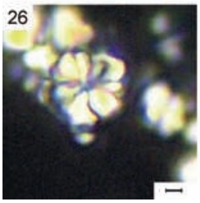
27
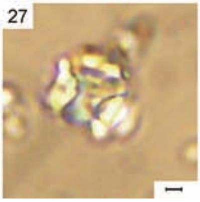
28
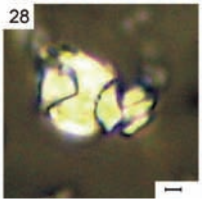
29
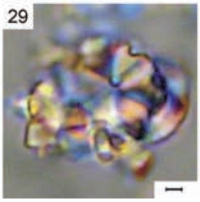
30
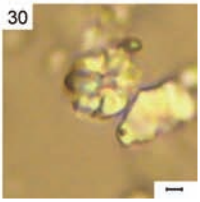

Ann. Naturhist. Mus. Wien	110 A	383–399	Wien, Jänner 2009

Crinoids from the Late Jurassic of the Nutzhof section (Lower Austria, Gresten Klippenbelt)

By Andreas KROH[1] & Alexander LUKENEDER[1]

(With 6 text-figures)

Manuscript submitted on October 5th 2008,
the revised manuscript on October 20th 2008.

Abstract

Tithonian to Berriasian sediments of the Blassenstein Formation exposed at the Nutzhof section, 5 km north of Hainfeld, in the Gresten Klippen Belt were sampled for crinoids. Only the Tithonian part of the section proved suitable for bulk sampling. Four crinoid taxa (*Balanocrinus* sp., *Saccocoma tenella* (GOLDFUSS, 1831), *Crassicoma* ? sp., and *Phyllocrinus belbekensis* ARENDT, 1974) could be documented. Among these, only *S. tenella* and probably *Crassicoma* ? sp. appear to be autochthonous; the others are interpreted as transported based on preservation and size range. The observed changes in lithology and microfauna may reflect geodynamically induced palaeogeographic changes and/or basinal deepening.

Keywords: Crinoidea, Echinodermata, Gresten Klippenbelt, Austria, Tithonian, Jurassic

Zusammenfassung

Sediment der Blassenstein-Formation aus dem Tithon bis Berrias wurden am Profil Nutzhof, 5 km nördlich von Hainfeld in der Grestener Klippenzone auf Crinoiden beprobt. Nur der Tithon-Anteil des Profils war für Schlämmproben geeignet. Vier Crinoidentaxa (*Balanocrinus* sp., *Saccocoma tenella* (GOLDFUSS, 1831), *Crassicoma* ? sp., und *Phyllocrinus belbekensis* ARENDT, 1974) konnten nachgewiesen werden. Von diese werden nur *S. tenella* und *Crassicoma* ? sp. als autochthone Elemente gedeutet. Der Erhaltungszustand und die Größensortierung der zwei anderen Formen weist auf Transport hin. Die beobachteten Änderungen von Lithologie und Mikrofauna könnten geodynamisch induzierte Veränderungen der paläogeographischen Position oder eine Vertiefung des Beckens widerspiegeln.

Schlüsselworte: Crinoidea, Echinodermata, Grestener Klippenzone, Österreich, Tithon, Jura

Introduction

Stalked crinoids were an important and diverse constituent of Palaeozoic and Mesozoic marine faunas, occurring abundantly in both shallow and deep water settings over a wide range of (palaeo-)latitudes (see HESS et al. 1999). This contrasts strongly with their modern distribution, where stalked crinoids are restricted to deeper water below 100 m. In shallow-water environments, only the stalkless comatulids, are found, with greatest abundance in the coral reefs of the tropical Indo-Pacific (MEYER & MACURDA 1976).

---

[1] Naturhistorisches Museum Wien, Burgring 7, 1010 Vienna, Austria; e-mail: andreas.kroh@nhm-wien.ac.at, alexander.lukeneder@nhm-wien.ac.at

Stalkless crinoids first evolved in the Triassic, including forms like the wide-spread osteocrinids (e.g. KRISTAN-TOLLMANN 1970; WANG et al. 2007). In the Late Jurassic to Early Cretaceous, another group of unstalked crinoids became prominent, the saccocomids. These microcrinoids were highly modified and apparently very successful, as documented by their wide-ranging occurrence (from Cuba to Japan; NICOSIA & PARISI 1979; MANNI et al. 1997) in rock-forming quantities (KEUPP & MATYSZKIEWICZ 1997; HESS 2002). Unlike most other crinoids, their abundance and brief temporal distribution accounts for their quality as index fossils for the Kimmeridgian to Tithonian (NICOSIA et al. 1979). Despite their common occurrence, their mode of life has been discussed controversially. Interpretations range from a benthic mode of life (MILSOM 1994; MILSOM & SHARPE 1995; MANNI, NICOSIA & TAGLIACOZZO 1997) to a pelagic lifestyle (JAEKEL 1892; KEUPP & MATYSZKIEWICZ 1997; HESS 1999, 2000), including active snap-swimming (SEILACHER & HAUFF 2004; SEILACHER 2005).

Research on Upper Jurassic to Lower Cretaceous deposits in the Klippen Belt southwest of Vienna led to the discovery of a succession spanning a large time interval (see LUKENEDER 2009). This section exposes strata of the Blassenstein Formation and contains marls and limestones rich in saccocomid remains as well as in other crinoids. Unlike the situation in most other occurrences, the high marl content allowed bulk sampling and extraction of the saccocomid ossicles.

Study area

The studied outcrop is located at 48°04’50’’ N, 15°47’38’’ E, in an area called Kleindurlas, 5 km north of Hainfeld and 20 km south of Böheimkirchen (fig. 1). There, strata of the Blassenstein Formation are exposed in a small, disused quarry near a farm called Nutzhof. The section comprises an 18-m-long succession of strongly tilted, inverse, well-bedded marls and limestones. At the base, marl and marly limestone bands dominate, being replaced by increasingly pure limestone towards the top. Based on preliminary data from palaeomagnetics, ammonites, and microfossils (LUKENEDER 2009; PRUNER et al. 2009; REHÁKOVÁ et al. 2009) the lower part can be assigned to the Early Tithonian and the upper part to the Middle Berriasian (fig. 2). In terms of microfacies, a change from a saccocomid facies to a calpionellid facies can be observed within the succession.

Geologically, the area belongs to the Gresten Klippen Belt, a small band of Upper Jurassic to Lower Cretaceous sediments situated north of the Northern Calcareous Alps. Adjacent units belong to the Rhenodanubian Flysch Zone.

Material & Methods

Apart from a survey of the thin sections, which were also employed to study calpionellids (REHÁKOVÁ et al. 2009), an effort was made to obtain three-dimensional specimens of the crinoids and other microfossils commonly observed in the thin sections (namely foraminifera, ostracods, rhyncholiths, small aptychi, ophiuroid remains, etc.). The older, marly part of the succession (metre 10 to 18) was sampled intensively. Wherever possible, samples were taken in marl layers adjacent to the limestone beds sampled for thin sections and palaeomagnetics (PRUNER et al. 2009). A general lack of marly horizons in

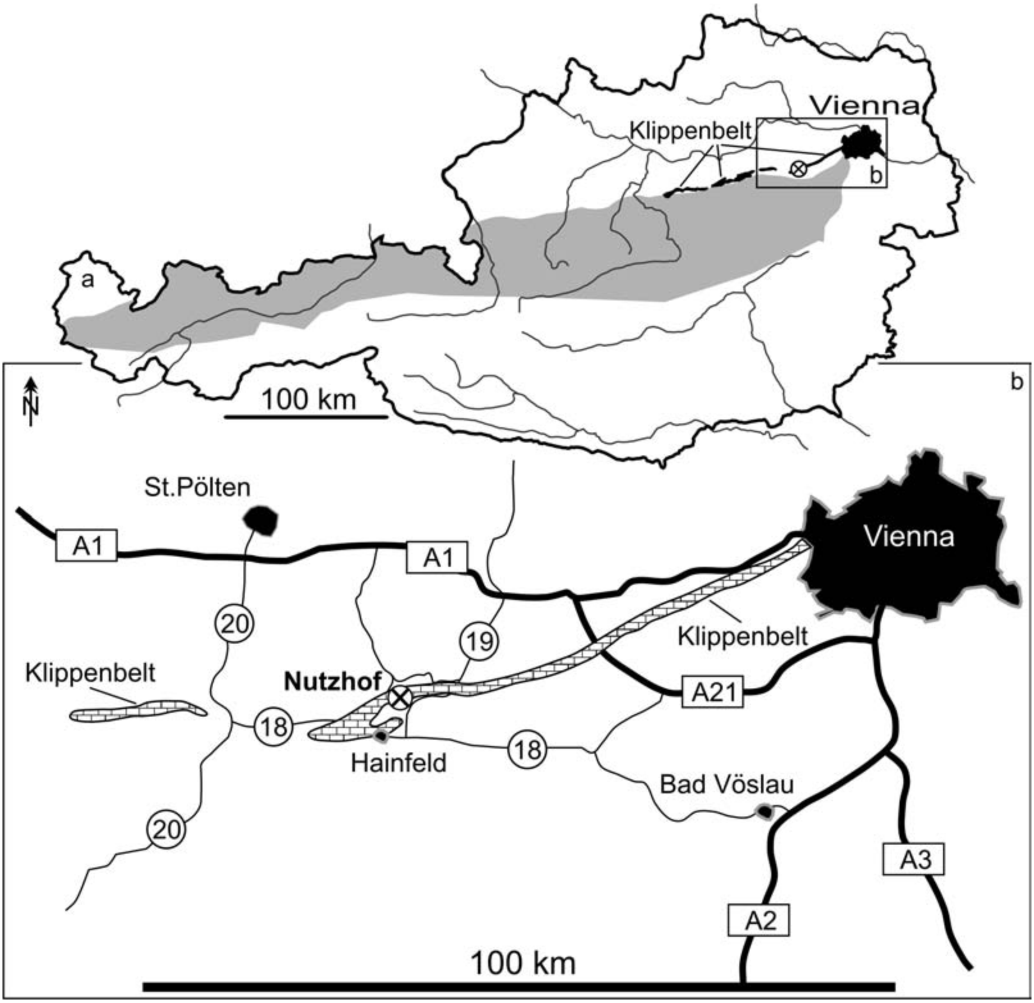

Fig. 1: Locality map of Austria with indicated position of the Klippenbelt in Lower Austria (**A**) and detailed map (**B**) of the area around Nutzhof showing the outcrop of Upper Jurassic to Lower Cretaceous sediments from the Klippenbelt (brick-structure).

part of the succession (metre 0 to 10.0) prevented bulk sampling in the younger strata. These beds were analysed by thin sections only.

Due to the high lithification of the samples traditional washing methods (hydrogen peroxide, boiling with sodium, petrol, etc.) were unsuccessful. Partial disaggregation was achieved by repetitive, combined treatment with hydrogen peroxide and the tenside Rewoquat (see LIERL 1992). Particularly well lithified aggregates that were unaffected by the treatment were removed from the samples after the first cycle. Accordingly, the quantitative data presented below are biased by lithification, but comparison with data

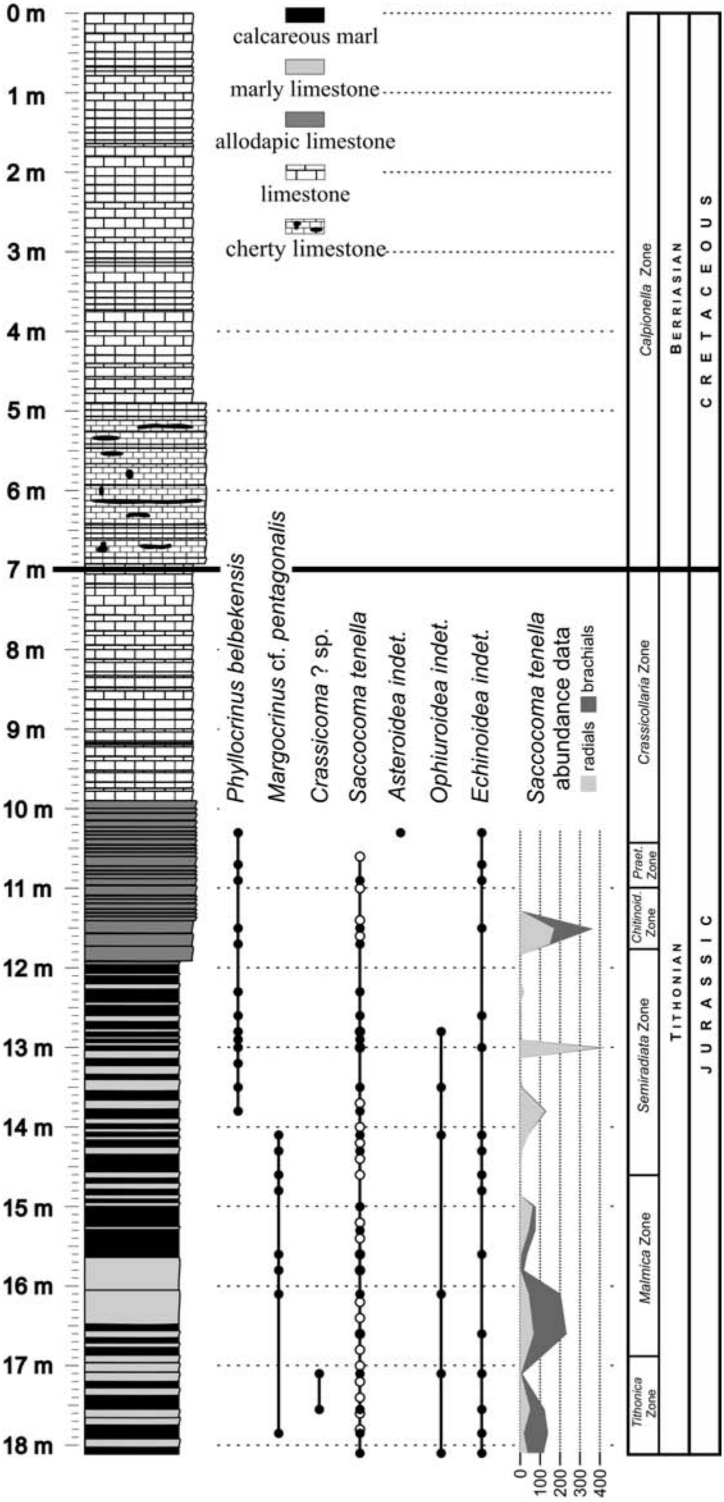

Fig. 2: Lithological log of the Nutzhof section with echinoderm ranges. Solid symbols indicate occurrences in the bulk samples, open symbols records observed in thin sections only. Note: *Saccocoma* abundance data is quantitative, but biased by sediment lithification. Stratigraphy from REHÁKOVÁ et al. (2009).

obtained form thin sections showed that this bias is small and the resulting abundance patterns largely comparable.

After disaggregation and cleaning, the microfossils were hand picked under a microscope. For the present study we used the sediment fractions ≥ 250 µm only.

All samples are stored at the Natural History Museum of Vienna, in the collection of the Department of Geology and Palaeontology. Echinoderms picked from the samples but not used in the present study are stored under the repository numbers NHMW 2008z0232/0001 to 0002 (Crinoidea indet.), 2008z0233/0001 (Asteroidea indet.), 2008z0234/0001 to 0016 (Ophiuroidea indet.), 2008z0235/0001 to 0006 (Echinoidea indet.).

Abbreviations:

NHMW – Naturhistorisches Museum Wien

Systematic part

Class Crinoidea MILLER, 1821
Order Isocrinida SIEVERTS-DORECK, 1953
Family Isocrinidae GISLEN, 1924
Genus *Balanocrinus* AGASSIZ, in DESOR, 1845

Balanocrinus sp.

(fig. 3)

Material: 13 columnals of immature (?) specimens from samples NU 14.10, 14.60, 14.80, 15.80, 16.10, and 17.85 (NHMW 2008z0228/0001, 2008z0229/0001 to 0006). Six brachial ossicles and 25 cirrals from samples NU 14.30, 14.60, 14.80, 15.60, 16.10, and 17.85 (NHMW 2008z0230/0001 to 0006, 2008z0231/0001 to 0005) are tentatively associated with the co-occurring columnals.

Description: The columnals recovered from the bulk samples are small, high and pentagonal in cross section. They are concave-sided and ornamented by small flanges on the lateral surfaces. The facets show pentaradiate symplexy with strong, but short marginal crenulae. Only a single nodal was found (sample NU 14.60), which is very similar to the internodals, apart from the synostosis on the distal facet and the large cirral facets.

Only distal and/or immature brachial ossicles were recovered. These are high, with concave sides and subequal pinnular and brachial articulation surfaces.

The proximal cirrals are short, rhomboidal in side view and bear a weak aboral rib. The distal cirrals are much longer and have a much more prominent distal rib, which is serrated.

Remarks: The present material is very scarce and consists of immature specimens. The association of columnals with brachial and cirral ossicles is mainly based on co-

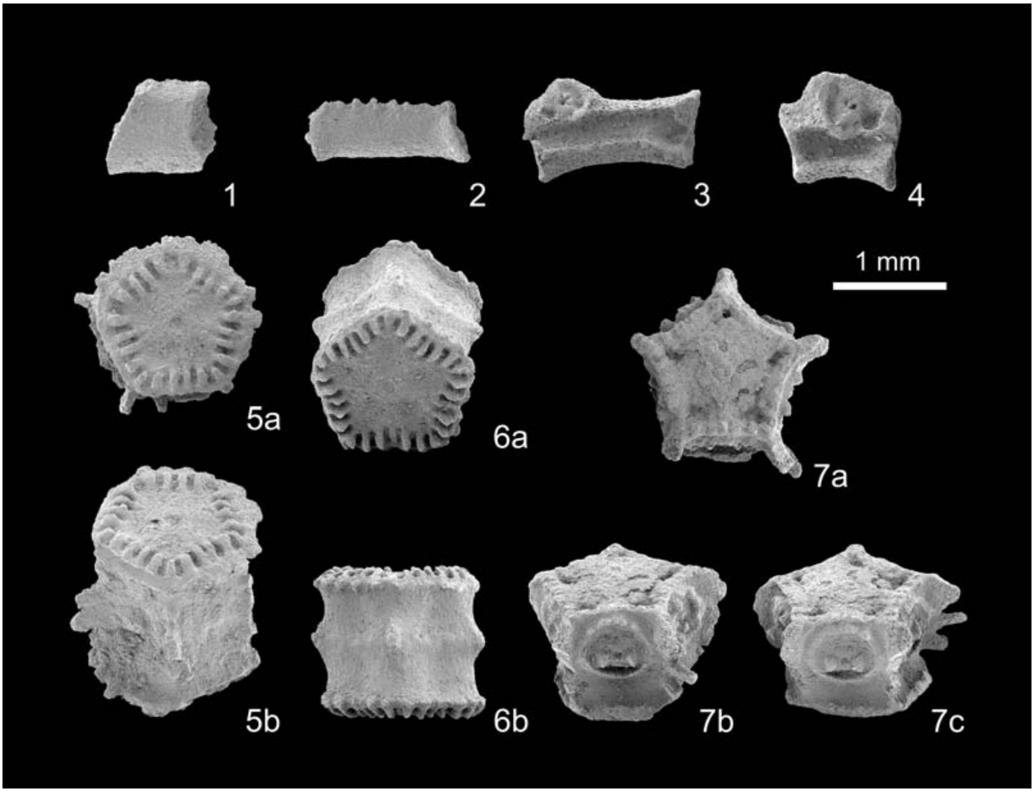

Fig. 3: *Balanocrinus* sp., Tithonian, Nutzhof, Austria (1, 2, 5: from sample NU 14.80, others from NU 14.60). **1**: proximal cirral (NHMW 2008z0230/0002); **2**: distal cirral (NHMW 2008z0230/0001); **3-4**: brachials (NHMW 2008z0230/0004, …/0005); **5-6**: internodals (NHMW 2008z0228/0001, …/0003); **7**: nodal, a = distal cryptosymplectial facet (?) (NHMW 2008z0228/0002).

occurrence. Due to the nature and scarcity of the material a specific identification is difficult. The specimens from Nutzhof are very similar to ossicles from juvenile *Balanocrinus* cf. *subterres* described by PISERA & DZIK (1979), but according to HESS (1975) and GŁUCHOWSKI (1984) a pentagonal columnal shape is more characteristic for *Balanocrinus pentagonalis*. The lateral flanges observed on the columnals, however, are unusual in *Balanocrinus* (compare e.g. HESS 1975: pl. 20, figs 1-8, 11; SALAMON & ZATOŃ 2008: fis 5e-g). Many *Isocrinus* species show rich lateral ornament, but differ by their different articular facets.

Occurrence: Early Tithonian (*Carpistomiosphaera tithonica* Zone to *Cadosina semiradiata* Zone) of Nutzhof, Klippenbelt, Austria (this study); *Balanocrinus pentagonalis* is a common member of crinoid associations in the Tithonian to Berriasian of the Pieniny Klippen Belt, Poland (GŁUCHOWSKI 1987), but has a wider range elsewhere (HESS 1975; SALAMON 2008).

Order Roveacrinida SIEVERTS-DORECK, 1953

Family Saccocomidae D'ORBIGNY, 1852

Genus *Saccocoma* AGASSIZ, 1853

***Saccocoma tenella* (GOLDFUSS, 1831)**

(fig. 4)

1892 *Comatula tenella* nobis. – GOLDFUSS: 204; pl. 62, figs 1a-d.
1892 *Comatula pectinata* nobis. – GOLDFUSS: 205; pl. 62, figs 2a-e.
1892 *Camatula* [sic!] *filiformis* nobis. – GOLDFUSS: 205; pl. 62, figs 3a-b.
1979 *Saccocoma tenella* GOLDFUSS, 1862 – PISERA & DZIK: 810-811; figs 3a-g; pl. 1, figs 8-9; pl. 2, figs 1-7; pl. 3, figs 1-3.
1980 *Saccocoma tenella* (GOLDFUSS, 1831) – HOLZER & POLTNIG: 207-215; fig. 2; pl. 1, figs 1-13; pl. 2, figs 1-16; pl. 3, figs 1-3.
1987 *Saccocoma tenella* GOLDFUSS, 1862 – GŁUCHOWSKI: 39-40; figs 13.7-10; pl. 17, figs 1, 4-6; pl. 18, figs 1-5; pl. 19, figs 1-6.
2002 *Saccocoma tenella* (GOLDFUSS, 1831) – HESS: 19; figs 12, 13.
2006 *Saccocoma tenella* (GOLDFUSS, 1831) – BRODACKI: 264-268; figs 3A-E, 4A, B, 5A-D, H, I, 6A, B, E, F, H, I.
2008 *Saccocoma tenella* (GOLDFUSS, 1831) – KROH & LUKENEDER: 46

Material: 1248 radials (NHMW 2008z0236/0001 to 0004, 0010 to 0014, 2008z0237/0001 to 0021), 971 brachials (NHMW 2008z0236/0005 to 0009, 0015 to 0023, 2008z0238/0001 to 0019) from samples NU 10.90 to NU 13.00, NU 13.50 to NU 14.30, and NU 15.00 to NU 18.10.

Description: The radials (figs 4.11-4.19) are thin and arrow-head-shaped, with distinctly serrate sides and a prominent central rib. Their outer surface is sculptured by a reticulate meshwork. The pattern formed by the meshwork varies from irregular (fig. 4.18) to oblique, well-organized sub-parallel ridges (figs 4.15, 4.16). The inner surface (fig. 4.19) is more or less smooth, with a shallow central groove tracing the position of the rib on the outer side. The articulation facet is small and preserved in few ossicles only. The aboral part of the articulation facet is rounded, knob-like and does not bear any processes (figs 4.11-4.14).

The proximal brachials (IBr2, IIBr2, IIBr4 and some of the more distal secundibrachials) bear distinct wings (figs 4.1-4.4). Although these wings are broken off in most Nutzhof specimens, they are more or less disc-shaped and subequal in size on both sides of the brachials. More distal brachials bear paired oral processes (fig. 4.5).

Remarks: The present material clearly belongs to *S. tenella*, agreeing in detail with material from the type-area Solnhofen (Bavaria, Germany; HESS 2002) and Poland (PISERA & DZIK 1979; BRODACKI 2006). The largest radials recovered from the Nutzhof bulk samples barely reach 4 mm and are thus smaller than those reported elsewhere (HOLZER & POLTNIG 1980). Nevertheless, the ontogenetic change in radial sculpture documented by HOLZER & POLTNIG (1980: 207-214) can be observed in the present material as well.

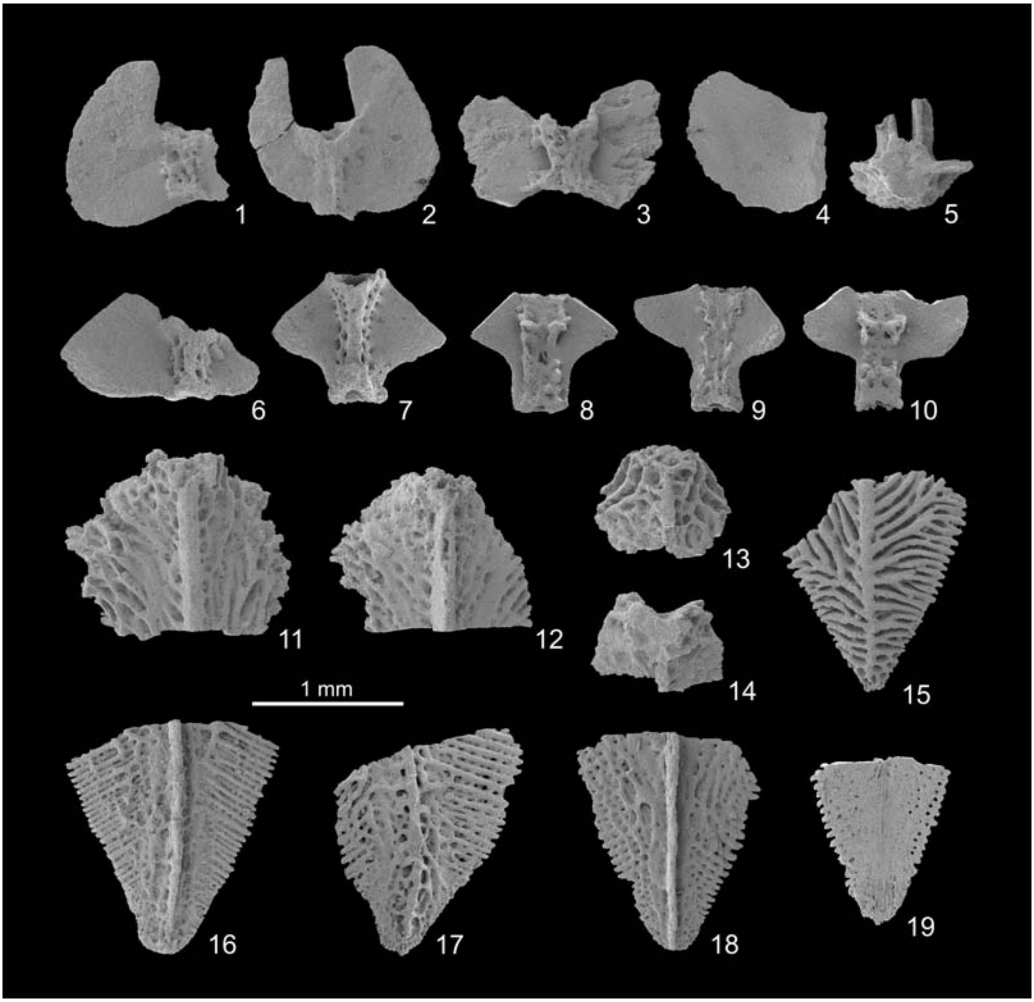

Fig. 4: *Saccocoma tenella* (GOLDFUSS, 1831), Tithonian, Nutzhof, Austria; **1-4, 6-10**: proximal brachials (1: NU 17.85; NHMW 2008z0236/0016; 2: NU 11.50; NHMW 2008z0236/0015; 3: NU 13.00; NHMW 2008z0236/0017; 4: NU 16.60; NHMW 2008z0236/0018; 6-10: NU 17.85; NHMW 2008z0236/0005 to …/0009); **5**: distal brachial (NU 15.60; NHMW 2008z0236/0019); **11-14**: parts of radials with articulation socket (11-12: NU 13.00; NHMW 2008z0236/0010, …/0011; 13-14: NU 16.10; NHMW 2008z0236/0013, …/0014); **15-18**: broken radials, outer surface (15: NU 13.00; NHMW 2008z0236/0012; 16-18: NU 17.85; NHMW 2008z0236/0002 to …/0004); **19**: broken radial, inner surface (NU 17.85; NHMW 2008z0236/0001).

S. quenstedti SIEVERTS-DORECK & HESS, in HESS, 2002 and *S. vernioryi* MANNI & NICOSIA, 1984 differ by their paired, antler-like processes attached to the aboral part of the articulation facet of the radial ossicles (two in *S. quenstedti*, four in *S. vernioryi*; HESS 2002; BRODACKI 2006). *S. longipinna* HESS, 2002 (*Saccocoma* sp. of VERNIORY 1962) differs by its highly asymmetrical proximal brachials with one strongly elongated and one rudimentary wing.

S. schwertschlageri WALTHER, 1904 is a synonym of *S. tenella* and according to MANNI & NICOSIA (1984: 183), representing cases of special preservation after total autotomy of the arms.

Occurrence: Late Kimmeridgian to Late Tithonian

Late Kimmeridgian of Dorset, UK (MILSOM 1994) and France (VERNIORY 1960); Early Tithonian of Southern Germany (JAEKEL 1892; SIEVERTS-DORECK 1955; HESS 2002); Early to Middle Tithonian of the Pieniny Klippen Belt, Poland (PISERA & DZIK 1979; GŁUCHOWSKI 1987; BRODACKI 2006); Early to Late Tithonian (*Carpistomiosphaera tithonica* Zone to *Praetintinnopsella* Zone) of Nutzhof, Klippenbelt, Austria (this study).

Genus *Crassicoma* SIEVERTS-DORECK & HESS, in HESS, 2002

***Crassicoma*? sp.**

(fig. 5)

Material: 20 brachial ossicles from samples NU 17.10 and NU 17.55 (NHMW 2008z0240/0001 to 0009).

Description: Primibrachials – the ossicle tentatively identified as IBr1 (fig. 5.4) is slightly elongated and dorso-ventrally flattened. The proximal part is slightly wider and shows a muscular articulation, the distal articulation is non-muscular and sloping. The external surface is devoid of ornamentation. The second primibrachial (IBr2 = IAx; figs 5.5-5.6) is strongly wedge-shaped with a triangular profile. It lacks both wings and oral processes. The proximal facet is non-muscular (probably a cryptosynarthry), whereas the two distal facets are muscular.

The secundibrachials (figs 5.1-5.3) are stout, dumbbell-shaped and lack wings. Instead, they possess a pair of oral projections or ridges. In profile they are distinctly triangular. One facet is muscular, the other one a horseshoe-shaped synostosis. The latter is strongly inclined in relation to the long axis of the ossicle. None of the brachials shows a pinnulae socket. Assignment to specific positions is difficult, but it appears that no IIBr1 are preserved among the material.

Distal brachials (fig. 5.7) are rectangular, slightly elongated and dorso-ventrally flattened. They bear muscular articulations on both ends, which are perpendicular to the long axis of the ossicle.

Remarks: The present brachial ossicles are distinctly larger than the *Saccocoma* brachials encountered in the same and adjacent samples. Furthermore, they lack the wings but show relatively blunt (compared to *Saccocoma*) oral projections. They are similar to proximal brachials of *Crassicoma schattenbergi* SIEVERTS-DORECK & HESS, in HESS, 2002 and *Crassicoma subornata* SIEVERTS-DORECK & HESS, in HESS, 2002 figured in HESS (1972: pl. 3, fig. 50a-b; 2002: pl. 2, fig. IIBr4; pl. 3, figs 6-9; pl. 7, fig. 19). They differ from those ossicles by lacking a reticulate ornament on the surface.

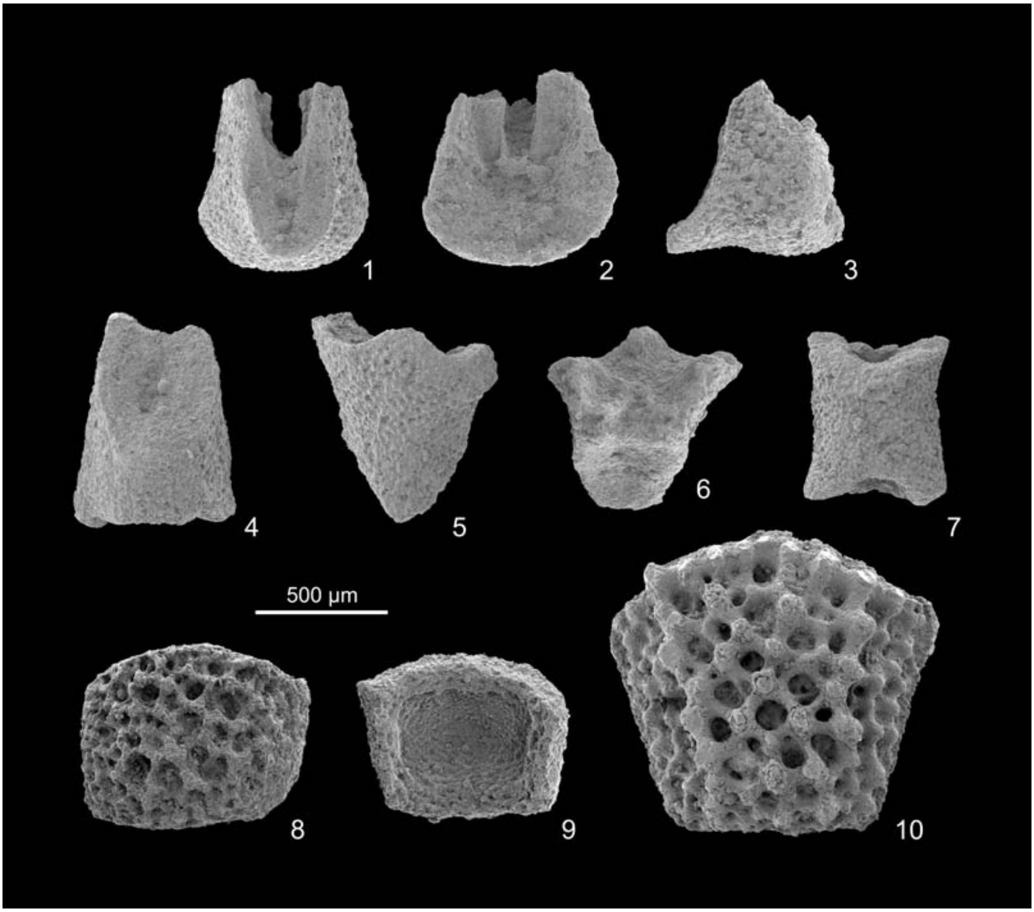

Fig. 5: 1-7: *Crassicoma*? sp., brachials, Tithonian, Nutzhof, Austria (from sample NU 17.10); **1-3**: secundibrachials (NHMW 2008z0240/0002, …/0003, …/0005); **4**: IBr1 (NHMW 2008z0240/0004); **5-6**: IBr2 (NHMW 2008z0240/0006, …/0007); **7**: distal brachial (NHMW 2008z0240/0008). **8-10**: Undetermined echinoderm ossicles (possibly radials of *Crassicoma*), Tithonian, Nutzhof, Austria (NHMW 2008z0239/0001, …/0004, …/0005).

Additionally, five echinoderm ossicles resembling *Crassicoma* radials (figs 5.8-5.10) have been recovered from samples NU 11.50, NU 11.70, NU 16.10, NU 16.60 (NHMW 2008z0239/0001 to 0005). Their external surface shows a coarse reticulate ornament much like that seen in *C. schattenbergi*. Although their general shape suggests that these may be radials, they lack a well-defined articulation facet and, thus, may not represent crinoid ossicles at all.

Occurrence: Early Tithonian (*Carpistomiosphaera tithonica* Zone to *Parastomiosphaera malmica* Zone) of Nutzhof, Klippenbelt, Austria (this study).

Order Cyrtocrinida Sieverts-Doreck, 1953

Family Phyllocrinidae Jaekel, 1907

Genus *Phyllocrinus* d'Orbigny, 1850

***Phyllocrinus belbekensis* Arendt, 1974**

(fig. 6)

1974	*Phyllocrinus belbekensis* sp.nov. – Arendt: 118-119; figs 14д-к; pl. 14, figs 1-21.
1979	*Phyllocrinus belbekensis* Arendt, 1974 – Pisera & Dzik: 824-825; figs 11c-d, 13d; pl. 4, fig. 1.
1984	*Phyllocrinus belbekensis* Arendt, 1974 – Žítt, J. & Michalík: 605-607; pl. 1, figs 1-2; pl. 2, figs 1-2; pl. 3, figs 1-2; pl. 4, figs 1-2; pl. 5, figs 1-2; pl. 6, figs 1-2, 4; pl. 7, figs 1-3.
1987	*Phyllocrinus stellaris* Zaręczny, 1876 – Głuchowski: 32-34; figs 15.3; pl. 11, figs 1-6; pl. 12, figs 1-6; pl. 13, figs 1-4.
?1987	*Phyllocrinus belbekensis* Arendt, 1974 – Głuchowski: 34; figs 15.5; pl. 14, figs 1-6.
2008	*Phyllocrinus belbekensis* Arendt, 1974 – Zatoń, Salamon & Kazmierczak: 563-564; figs 2.D_1-D_3.

Material: 32 cups and 7 cup fragments from samples NU 10.30 to NU 13.80 (NHMW 2008z0226/0001 to 0005, 2008z0227/0001 to 0013). No columnals or brachials were found that could be assigned with confidence to this taxon.

Description: Small cups with pentagonal outline, usually reaching a horizontal diameter of 1.5 mm only. Rarely, larger specimens of up to 2.4 mm were recovered from the samples. The thecal outline and shape varies from more flattened forms to forms with subequal diameter and height. In profile, the cup expands gradually upward to the proximal margin of the arm facets (figs 6.3b, 6.4a). More distally, it becomes narrower again.

The cup consists of 5 radials only; no basals are present. The sutures between the radials are poorly visible and are in broad but shallow furrows on the proximal part of the cup. The radials bear a sharp median keel on the aboral surface (fig. 6.1b). The articulation facets are small and set in a deep radial notch (fig. 6.3a), separated from the deep oral cavity by a transversal septum. Distinct ledges that are sharply separated from the remaining radial surface are situated around the arm facets (fig. 6.3a). The interradial processes are high, narrow and acute triangular. The base is very regularly pentagonal and sharply delimited. The facet to the stem shows a central elevation pierced by an axial canal (fig. 6.1a). The surface of the cup is smooth.

Remarks: The mature specimen figured by Pisera & Dzik (1979: figs 11c; pl. 4, fig. 1) differs from the present specimens by its larger stem facet. The same is true for some of the specimens figured by Arendt (1974: figs 9б, 20), but is here considered to represent natural variation by allometric growth. Otherwise, the present material is almost identical to the material of Arendt (1974).

According to Pisera & Dzik (1979: 823, 825), *P. belbekensis* differs from *Phyllocrinus stellaris* Zaręczny, 1876 by its angular radials with sharp median keel, sharply delimited ledges around arm facets and the narrow interradial processes. Specimens attributed to *P. stellaris* by Głuchowski (1987: 32-34) are unlike those described by Zaręczny

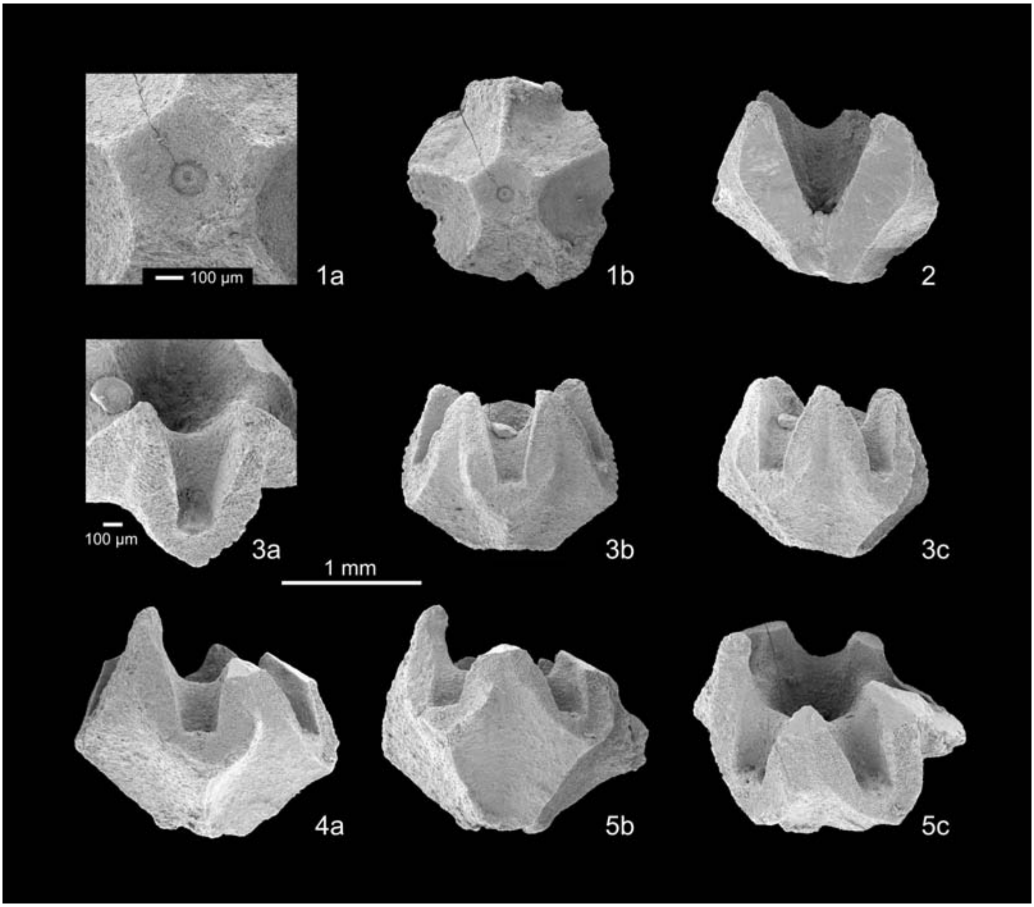

Fig. 6: Cups of *Phyllocrinus belbekensis* Arendt, 1974, Tithonian, Nutzhof, Austria (sample NU 12.30); **1**a-b: NHMW 2008z0226/0003; **2**: NHMW 2008z0226/0004; **3**a-c: NHMW 2008z0226/0001; **4**a-c: NHMW 2008z0226/0002).

(1876: 213-214, pl. 1, fig. 9) and Pisera & Dzik (1979) and are referred to *P. belbekensis* here. Under the latter name, Głuchowski (1987: pl. 14, figs 1-6) illustrated strongly corroded *Phyllocrinus* cups of questionable specific affinity. *Phyllocrinus minutus* Zaręczny, 1876 is the only other *Phyllocrinus* similar in shape, but like *P. stellaris* lacks the characteristic ledges around the arm facets of *P. belbekensis*.

Occurrence: Early to Middle Oxfordian of the epicratonic shelf deposits in southern Poland (Zatoń, Salamon & Kazmierczak 2008); Oxfordian of the Western Carpathians, Slovakia (Žítt & Michalík 1984); Early to Middle Tithonian of the Pieniny Klippen Belt, Poland (Pisera & Dzik 1979; Głuchowski 1987); Early to Late Tithonian (*Semiradiata* Zone to *Praetintinnopsella* Zone) of Nutzhof, Klippenbelt, Austria (this study); Hauterivian of Krimea, Ukraine (Arendt 1974).

Results

The crinoid fauna recovered from the bulk samples of Nutzhof is typical for Upper Jurassic strata of Central and Eastern Europe. The low diversity may be interpreted as a result of the distal position of the section, which represents a deep water facies. It seems possible, that the crinoid material, apart from the saccocomids, is of allochthonous origin. Indeed, microfacies analysis carried out by LUKENEDER (2009) indicates the presence allodapic material. This is also supported by the narrow size ranges represented by the isocrinid and phyllocrinid ossicles that could be explained by transport-induced size-sorting. Additionally, only the calyces of *Phyllocrinus* are preserved, whereas more fragile parts of the skeleton (columnals and brachials) are missing. Saccocomid remains, in contrast, do not show sorting and include abundant fragile elements. This part of the crinoid fauna is thus interpreted as being autochthonous.

Biostratigraphically, only the saccocomid remains are useful, *S. tenella* being restricted to the Late Kimmeridgian to Late Tithonian. The other species recovered, *Balanocrinus* sp. and *P. belbekensis*, have long stratigraphic ranges. From a biogeographic point of view the faunal composition indicates connections with the contemporaneous units in Eastern Europe. This is a result of the palaeogeographic position of the section on the Helvetic Shelf, on the southern slope of the European Massif (Northern Tethys Shelf; HOFMANN et al. 2002).

The replacement of saccocomid marl and limestone by calpionellid limestone in the Late Tithonian, as observed at the Nutzhof section, appears to be very characteristic. Similar successions were reported from numerous other regions in Austria (e.g. KRISTAN-TOLLMANN 1962: Gresten Klippen Belt, Frankenfels Nappe; FLÜGEL 1967: Northern Calcareous Alps; HOLZER 1968, 1980: Northern Calcareous Alps; HOLZER & POLTNIK 1980: Karawanken Mts.; REHÁKOVÁ et al. 1996: Gresten Klippen Belt, Frankenfels Nappe), Germany (LACKSCHEWITZ et al. 1989: Northern Calcareous Alps), Poland (PSZCZÓŁKOWSKI & MYCZYŃSKI 2004: Pieniny Klippen Belt) and Slovakia (VAŠIČEK et al. 1992: Western Carpathian Klippen Belt). Many of these occurrences, however, differ lithologically from the Nutzhof section. In most cases the saccocomid-bearing beds are pure, reddish limestone.

In many cases the saccocomid limestones have been interpreted as Kimmeridgian deposits (e.g. FLÜGEL 1967: 35; SAUER et al. 1992: 183; WESSELY 2008: 210, fig. 5) and have been used as a marker bed for that stage (BERNOULI 1972). Good stratigraphic evidence, however, is lacking in most cases and detailed analyses are needed to verify the supposed Kimmeridgian ages. Based on well-date sections, the major occurrences of saccocomids are of Tithonian age (NICOSIA et al. 1979; KEUPP & MATYSZKIEWICZ 1997), which holds true for the present section as well.

The distribution pattern (fig. 2) of the crinoids in the Nutzhof section is clearly non-random. *Saccocoma tenella* is restricted to the lower 6 m of the section; co-occurring with juvenile isocrinid columnals attributed to *Balanocrinus* sp. in the lower part (samples NU 17.85 to 14.10). Above (NU 13.80 to 10.30), calyces of the cyrtocrinid *Phyllocrinus belbekenis* appear, while saccocomid remains become rare and vanish (last abundant occurrence in sample 11.50). The replacement of the isocrinids by the cyrtocrinid *P. belbekensis* is clearly not a stratigraphic signal because both taxa have longer ranges elsewhere. Rather, this change reflects biotic changes in the source area of the re-deposited bioclasts. Likewise, the switch to more pure carbonates upsection and thinning of the intercalated marls may relate to changes of current patterns, possibly caused by geodynamically induced palaeogeographic changes and/or basinal deepening.

Conclusions

Four crinoid taxa were documented from the Tithonian Blassenstein Formation of the Nutzhof section: *Balanocrinus* sp., *Saccocoma tenella* (GOLDFUSS, 1831), *Crassicoma*? sp., and *Phyllocrinus belbekensis* ARENDT, 1974. Of these, only *S. tenella* is abundant. The other taxa, in particular the benthic isocrinids and phyllocrinids, are rare. The preservation state and ossicle size range of the latter groups indicate their allochthonous origin.

The saccocomid remains are restricted to the Tithonian at the Nutzhof section, the saccocomid-rich facies being replaced by calpionellid limestones upsection. Literature data suggests that this is the main interval of saccocomid distribution. The use of an abundant occurrence of saccocomids as a marker for Kimmeridgian strata appears unsuitable.

Acknowledgements

We gratefully acknowledge funding by the Austrian Science Fund (FWF project P20018-N10). The critical reviews of Hans HESS (Binningen, Switzerland) and Mariusz A. SALAMON (Sosnowiec, Poland) helped to improve this paper. Sincere thanks go to Franz ZÖCHLING, for permitting access to the section and to Hans EGGER (GBA, Vienna) for showing us the outcrop.

References

ARENDT, Y.A. (1974): [The sea lilies cyrtocrinids]. – Trudy Paleontologiceskogo Instituta Akademia Nauka SSSR, **144**: 1-251. [*in Russian*]

BERNOULI, D. (1972): North Atlantic and Mediterranean Mesozoic facies: A comparison. – Initial Reports of the Deep Sea Drilling Project, **11**: 631-643.

BRODACKI, M. (2006): Functional anatomy and mode of life of the latest Jurassic crinoid *Saccocoma*. – Acta Palaeontologica Polonica, **51**/2: 261-270.

FLÜGEL, H.W. (1967): Die Lithogenese der Steinmühl-Kalke des Arracher Steinbruches (Jura, Österreich). – Sedimentology, **9**: 23-53.

GŁUCHOWSKI, E. (1987): Jurassic and Early Cretaceous articulate crinoids from the Pieniny Klippen Belt and the Tatra Mts., Poland. – Studia Geologica Polonica, **94**: 1-102.

GOLDFUSS, A. (1826-1844): Petrefacta Germaniæ tam ea, quae in Museo Universitatis Regiae Borussicae Fridericiae Wilhelmiae Rhenanae servantur quam alia quaecunque in Museis Hoeninghusiano Muensteriano aliisque extant, Iconibus et Descriptionibus illustrata. – 1(1): i-viii+1-76; pls. 1-25 (1826); 1(2): 77-164; pls. 26-50 (1829); 1(3): 165-240; pls. 51-70 (1831); 1(4): 241-252 (1833); 2(1): i-iii+1-68; pls. 71-96 (1834); 2(2): 69-140; pls. 97-121 (1835); 2(3): 141-224; pls. 122-146 (1837); 2(4): 225-312; pls. 147-165 (1840); 3(1): i-iv+1-20; pls. 166-171 (1841); 3(2): 21-28; pls. 172-195 (1844); 3(3): 29-128; pls. 196-200 (1844) pp., Düsseldorf (Arnz & Comp.).

HESS, H. (1972): Planktonic crinoids of Late Jurassic age from Leg 11, Deep Sea Drilling Project. – Initial Reports of the Deep Sea Drilling Project, **11**: 631-643.

——— (1975): Die fossilen Echinodermen des Schweizer Juras. – Veröffentlichungen aus dem Naturhistorischen Museum Basel, **8**: 1-130.

——— (1999): Upper Jurassic Solnhofen Plattenkalk of Bavaria, Germany. – In: HESS, H., AUSICH, W.I., BRETT, C.E., & SIMMS, M.J. (eds): Fossil Crinoids. – pp. 216-224, Cambridge, MA (Cambridge University Press).

——— (2000): Saccocomen aus dem Malm Süddeutschlands und ihre Lebensweise. – Fossilien, **17**/6: 347-358.

——— (2002): Remains of Saccocomids (Crinoidea: Echinodermata) from the Upper Jurassic of southern Germany. – Stuttgarter Beiträge zur Naturkunde, Serie B (Geologie und Paläontologie), **329**: 1-57.

——— , AUSICH, W.I., BRETT, C.E., & SIMMS, M.J. (1999): Fossil Crinoids. xv+275 pp., Cambridge, MA (Cambridge University Press).

HOFMANN, T., MANDL, G., PERESSON, H., PESTAL, G., PISTOTNIK, J., REITNER, J., SCHARBERT, S., SCHNABEL, W., SCHÖNLAUB, & H.- P., KRENMAYR, H.G. (Red.) (2002): Rocky Austria: Eine bunte Erdgeschichte von Österreich . 2. Auflage. – 64 pp., Wien (Verlag der Geologischen Bundesanstalt).

HOLZER, H.-L. (1968): Stratigraphie und Lithologie der Jura-Kreide-Folge im nördlichsten Pechgraben-Steinbruch. – Mitteilungen des naturwissenschaftlichen Vereins für Steiermark, **98**: 47-57.

——— (1980): Radiolaria aus Ätzrückständen des Malm und der Unterkreide der Nördlichen Kalkalpen. – Annalen des Naturhistorischen Museum in Wien, **83**: 153-167.

——— & POLTNIG, W. (1980): Erster Nachweis einer Radialplatten-Fossillagerstätte der Schwebcrinoide *Saccocoma* im oberostalpinen Malm (Ostkarawanken, Kärnten). – Carinthia II, **170/90**: 201-216.

JAEKEL, O. (1892): Über Plicatocriniden, *Hyocrinus* und *Saccocoma*. – Zeitschrift der Deutschen Geologischen Gesellschaft, 44: 619-696.

KEUPP, H. & MATYSZKIEWICZ, J. (1997): Zur Faziesrelevanz von *Saccocoma*-Resten (Schwebcrinoiden) in Oberjura-Kalken des nördlichen Tethys-Schelfs. – Geologische Blätter für Nordost-Bayern und angrenzende Gebiete, **47**/1-4: 53-70.

KRISTAN-TOLLMANN, E. (1962): Stratigraphisch wertvolle Mikrofossilien aus dem Oberjura und Neokom der nördlichen Kalkalpen. – Erdoel-Zeitschrift, **78**: 637-549.

——— (1970): Die Osteocrinusfazies, ein Leithorizont von Schwebcrinoiden im Oberladin-Unterkarn der Tethys. – Erdöl Kohle-Erdgas-Petrochem. Verein. Brennstoff-Chem., **23**/12: 781-789.

KROH, A. & LUKENEDER, A. (2008): Crinoids from the Late Jurassic Early Cretaceous of the Nutzhof section (Lower Austria, Pieniny Klippenbelt). – In: LUKENEDER, A. (ed.): 1st International Meeting on Correlation of Cretaceous Micro- and Macrofossils 16-18 April 2008, Vienna. Scientific Program, Abstracts, Excursion Guide. – Berichte der Geologischen Bundesanstalt, **74**: 46.

LACKSCHEWITZ, K., GRÜTZMACHER, U., SUHR, J. & KIEL, R.H. (1989): Synsedimentäre Kippschollentektonik: Becken- und Schwellenfazies oberjurassischer Karbonate der Chiemgauer Alpen. – Geologisch-Paläontologische Mitteilungen Innsbruck, **16**: 163-165

LIERL, H.-J. (1992): Tenside – ihre Verwendung für die Präperation geologisch-paläontologischer Objekte. – Der Präperator, **38**/1: 12-17.

LUKENEDER, A. (2009): New biostratigraphic ammonite data from the Jurassic/Cretaceous boundary at Nutzhof (Gresten Klippenbelt, Lower Austria). – Annalen des Naturhistorischen Museum in Wien, Serie A, **110**: 313-329.

MANNI, R. & NICOSIA, U. (1984): *Saccocoma vernioryi* n. sp., a new saccocomid from the Upper Jurassic of the central Italy. – Geologica Romana, **23**: 91-97.

——— (1986): *Saccocoma schwertschlageri* WALTHER, 1904 junior synonym of *Saccocoma tenellum* (Goldfuss), 1829. Evidence of autotomy in fossil crinoids. – Bollettino della Società Paleontologica Italiana, **24**: 181-183.

MANNI, R., NICOSIA, U., & TAGLIACOZZO, L. (1997): *Saccocoma*, normal benthonic stemless crinoid: an opportunistic reply within mud dominated facies. – Palaeopelagos, **7**: 121-132.

MEYER, D.L. & MACURDA, D.B.Jr. (1977): Adaptive radiation of the comatulid crinoids. – Paleobiology, **3**: 74-82.

MILSOM, C.V. (1994): *Saccocoma*: A benthic crinoid from the Jurassic Solnhofen Limestone, Germany. – Palaeontology, **37**: 121-129.

——— & SHARPE, T. (1995): Jurassic lagoon: Salt or soup? – Geology Today, **1995**/Jan.-Feb.: 22-26.

NICOSIA, U. & PARISI, G. (1979): *Saccocoma tenella* (GOLDFUSS) – Distribuzione stratigrafica e geografica. – Bollettino della Societá Paleontologica Italiana, **18**: 320-326.

PRUNER, P., SCHNABL, P. & LUKENEDER, A. (2009): Preliminary results of magnetostratigraphic investigations across the Jurassic/Cretaceous boundary strata at Nutzhof, Austria. – Annalen des Naturhistorischen Museum in Wien, Serie A, **110**: 331-344.

PISERA, A. & DZIK, J. (1979): Tithonian crinoids from Rogoznik (Pieniny Klippen Belt, Poland) and their evolutionary relationships. – Eclogae geologicae Helvetiae, **72**: 805-849.

PSZCZÓŁKOWSKI, A. & MYCZYŃSKI, R. (2004): Ammonite-supported microfossil and nannoconid stratigraphy of the Tithonian-Hauterivian limestones in selected sections of the Branisko Succession, Pieniny Klippen Belt (Poland). – Studia Geologica Polonica, **123**: 133-197.

REHÁKOVÁ, D., HALÁSOVÁ, E. & LUKENEDER, A. (2009): The Jurassic-Cretaceous boundary in the Austrian Klippen Belt (Nutzhof, Lower Austria): Implications for Micro- and Nannofacies analysis. – Annalen des Naturhistorischen Museum in Wien, Serie A, **110**: 345-381.

——— , MICHALÍK, J. & OŽVOLDOVÁ, L. (1996): New microbiostratigraphical data from several Lower Cretaceous pelagic sequences of the Northern Calcareous Alps, Austria (Preliminary results). – Geologisch-Paläontologische Mitteilungen Innsbruck, **Sonderband 4**: 57-81.

SALAMON, M.A. (2008): The Callovian (Middle Jurassic) crinoids from northern Lithuania. – Paläontologische Zeitschrift, **82**/3: 269-278.

——— & ZATOŃ, M. (2007): A diverse crinoid fauna from the Middle Jurassic (Upper Bajocian–Callovian) of the Polish Jura Chain and Holy Cross Mountains (south-central Poland). – Swiss Journal of Geosciences, **100**/1: 153-164.

SAUER, R., SEIFERT, P. & WESSELY, G. (1992): Guidebook to excursions in the Vienna Basin and the adjacent Alpine-Carpathian Thrustbelt in Austria. Part II. – Mitteilungen der Österreichischen Geologischen Gesellschaft, **85**: 97-239.

SEILACHER, A. (2005): *Saccocoma* – Planktonfischer im Jurameer. – Fossilien, **22**/1: 48-52.

——— & HAUFF, R.B. (2004): Constructional Morphology of Pelagic Crinoids. – Palaios, **19**/1: 3-16.

SIEVERTS-DORECK, H. (1955): Die Verbreitung die Crinoidengattung *Saccocoma* im Schwäbischen Jura. – Jahreshefte des Vereins für Vaterländische Naturkunde in Württemberg, **110**: 118-120.

VAŠIČEK, Z., REHÁKOVÁ, D., MICHALÍK, J, PETERČÁKOVÁ, M. & HALÁSOVÁ, E. (1992): Ammonites, aptychi, nanno- and microplankton from the Lower Cretaceous Pieniny Formation in the "Kysuca Gate" near Žilina (Western Carpathian Klippen Belt, Kysuca Unit). – Západné Karpaty, séria paleontológia, **16**: 43-57

VERNIORY, R. (1960): Présence (et variétés) de *Saccocoma tenella* Goldfuss à Talloires (Haute-Savoie). – Archives des Sciences, **13**: 250-257.

——— (1962): Une nouvelle forme de *Saccocoma* (Montbrand, Hautes-Alpes, France). – Archives des Sciences, **15**: 391-397.

WANG, C., WANG, X., HAGDORN, H., CHEN, X., & CHENG, L. (2007): The first discovery of Triassic roveacrinids in China and its significance. – Acta Palaeontologica Sinica, **46**/3: 334-339.

WESSELY, G. (2008): Kalkalpine Schichtfolgen und Strukturen im Wienerwald. – Journal of Alpine Geology, **49**: 201-214.

ZARĘCZNY [ZARĘCZNEGO], S. (1876): Dodatek do fauny warstw tytońskich Rogoźniku i w Maruszynie. – Sprawozdanie Komisji Fizjograficznej Polska Akademia Umiejetnosci, **10**: 180-219.

ZATOŃ, M., SALAMON, M.A., & KAZMIERCZAK, J. (2008): Cyrtocrinids (Crinoidea) and associated stalked crinoids from the Lower/Middle Oxfordian (Upper Jurassic) shelfal deposits of southern Poland. – Géobios, **41**/4: 559-569.

ŽÍTT, J. & MICHALÍK, J. (1984): Upper Jurassic crinoids in the West Carpathian Klippen Belt. – Geologický Zbornik – Geologica Carpathica, **35**/5: 601-629.

Ann. Naturhist. Mus. Wien	110 A	401–421	Wien, Jänner 2009

Dinoflagellate cysts and Ammonoids from Upper Cretaceous sediments of the Pemberger Formation (Krappfeld, Carinthia, Austria)

Ali SOLIMAN[1 2], Thomas J. SUTTNER[1], Alexander LUKENEDER[3] and
Herbert SUMMESBERGER [3]

(With 3 plates, 2 figures, 1 table)

Manuscript submitted on September 8th 2008,
the revised manuscript on November 10th 2008

Abstract

Dinoflagellate cysts (dinocysts) and acritarchs are described for the first time from the Pemberger Formation of the Gosau Group (Krappfeld, Carinthia, Austria). The dinoflagellate cyst assemblage is quite diverse and well preserved and compositionally similar to those described from Upper Cretaceous strata in northern Italy, Germany and the Czech Republic. Many stratigraphically significant taxa are documented, among them *Alisogymnium nucleases*, *Cannosphaeropsis utinensis*, *Florentinia mayii*, *Isabelidinium cooksoniae* and *Xenascus ceratioides*. They support a Campanian to Maastrichtian age. Ammonoids observed in this study are instead rare within the investigated section: although several taxa were previously described to occur in this area, only *Pachydiscus* (*Pachydiscus*) *haldemsis* and some indeterminable fragments were found in the present study.

Key words: Dinoflagellata, Ammonoidea, biostratigraphy, Upper Cretaceous.

Zusammenfassung

Zysten von Dinoflagellaten (Dinozysten) und Arcritarchen werden zum ersten Mal aus der Pemberger-Formation der Gosau-Gruppe (Krappfeld, Kärnten, Österreich) beschrieben. Die beschriebene Vergesellschaftung von Dinoflagellaten-Zysten ist relativ divers und gut erhalten und in ihrer Zusammensetzung sehr ähnlich der Vergesellschaftung aus gleichaltrigen Ablagerungen von Nord-Italien, Deutschland und der Tschechischen Republik. Viele stratigraphisch signifikante Formen sind dokumentiert. Darunter finden sich Arten wie *Alisogymnium nucleases*, *Cannosphaeropsis utinensis*, *Florentinia mayii*, *Isabelidinium cooksoniae* und *Xenascus ceratioides*. Der Fossilbefund lässt auf ein Campanium bis Maastrichtium Alter schließen. Was die Makrofossilien betrifft, so konnten nur wenige Ammoniten aus dem bearbeiteten Intervall geborgen werden. Obwohl schon einige Arten aus diesem Gebiet beschrieben worden sind, wurden nur Vertreter der Art *Pachydiscus (Pachydiscus) haldemsis* sowie einige unbestimmbare Ammonitenreste entdeckt.

Schlüsselwörter: Dinoflagellata, Ammonoidea, Biostratigraphie, Oberkreide.

---

[1] University of Graz, Institute of Earth Sciences (Geology and Palaeontology), Heinrichstrasse 26, 8010 Graz, Austria; e-mail: ali.soliman@uni-graz.at; thomas.suttner@uni-graz.at

[2] Geology Department, Faculty of Science, Tanta University, Tanta, 31527, Egypt

[3] Natural History Museum Vienna, Department of Geology & Palaeontology, Burgring 7, 1010 Vienna, Austria; e-mail: alexander.lukeneder@nhm-wien.ac.at; herbert.summesberger@nhm-wien.ac.at

Introduction

Upper Cretaceous sediments of the Krappfeld in Carinthia (Austria) yield diverse dinoflagellate cysts, benthic foraminifera (SCHREIBER 1979, 1980) and some ammonoids. Earlier investigations on the micro- and macrofauna were done by THIEDIG & WIEDMANN (1976). Based on foraminifera, SCHREIBER (1980) suggested an early Maastrichtian age for these deposits belonging to the Krappfeld Group (Krappfeld Gruppe, VAN HINTE 1963). Same early Maastrichtian age was suggested for the unit by THIEDIG & WIEDMANN (1976), who dated the sequence by ammonites. These authors collected *Pseudokossmaticeras brandti*, *Pseudokossmaticeras tercense*, *Pseudokossmaticeras galicianum* and *Pachydiscus carinthiacus*. The proposed age then unfortunately was based on the incorrect use of the range of *P. brandti* which finally resulted in assigning the investigated unit to early Maastrichtian age (HANCOCK & KENNEDY 1993). Recent studies show that the ammonoid fauna (including species like *Pseudokossmaticeras tercense* (SEUNES, 1892)) indicate a Late Campanian age of the upper part of the Cretaceous at the Krappfeld. This age is largely confirmed by the micro- and macrofossils of our investigations because some of the fossil remnants hint at Late Campanian age. The rare ammonoid fauna is accompanied by lamellaptychi, belemnites, bivalves, serpulids, fish remains, trace fossils and plant debris.

This study provides new taxonomic and biostratigraphic data on dinoflagellate cysts and ammonoids from the Pemberger Formation at the Krappfeld that confirm a Campanian to Maastrichtian age for this unit. The dinoflagellate biostratigraphy is correlated with other micro- and macrofossil zonations (SUMMESBERGER et al. 1999) of the studied section and with dinoflagellate zonation schemes of Germany (KIRSCH 1991), northern Italy (RONCAGLIA and CORRADINI 1997a) and the Mediterranean area (HOEK et al. 1996).

Previous Dinoflagellate Cyst Studies

Few studies have been published on Late Cretaceous dinoflagellate cysts of Austria. KIRSCH (1991) studied 6 samples from the Waidach section near Salzburg and suggested a Late Maastrichtian age. PAVLISHINA et al. (2004) carried out a palynological study on Upper Cretaceous sediments (upper Turonian-Maastrichtian) from many sections in the Northern Calcareous Alps, focusing on sporomorphs and dinoflagellate cysts. WAGREICH et al. (2006), in an integrated study with foraminifera and calcareous nannoplankton, contributed a short note on the late Albian to early Cenomanian dinoflagellate cysts of the lower red shale interval in the Rhenodanubian Flysch (Upper Austria).

Although Austria lacks literature on Late Cretaceous dinoflagellate cysts, extensive studies from other European sections are available (e.g. ALBERTI 1961; CLARKE & VERDIER 1967; KJELLSTRÖM 1973; CORRADINI 1973; HANSEN 1977; ROBASZYNSKI et al. 1985; KIRSCH 1991; MARHEINECKE 1992; SIEGL-FARKAS & WAGREICH 1996; SIEGL-FARKAS 1997; RONCAGLIA & CORRADINI 1997a, b; TORRICELLI & AMORE 2003; SKUPIEN & MOHAMED 2008). Notable studies from the circum-Mediterranean include those of SONCINI & RAUSCHER (1990), EL BEIALY (1995), HOEK et al. (1996) and MAHMOUD & SCHRANK (2007).

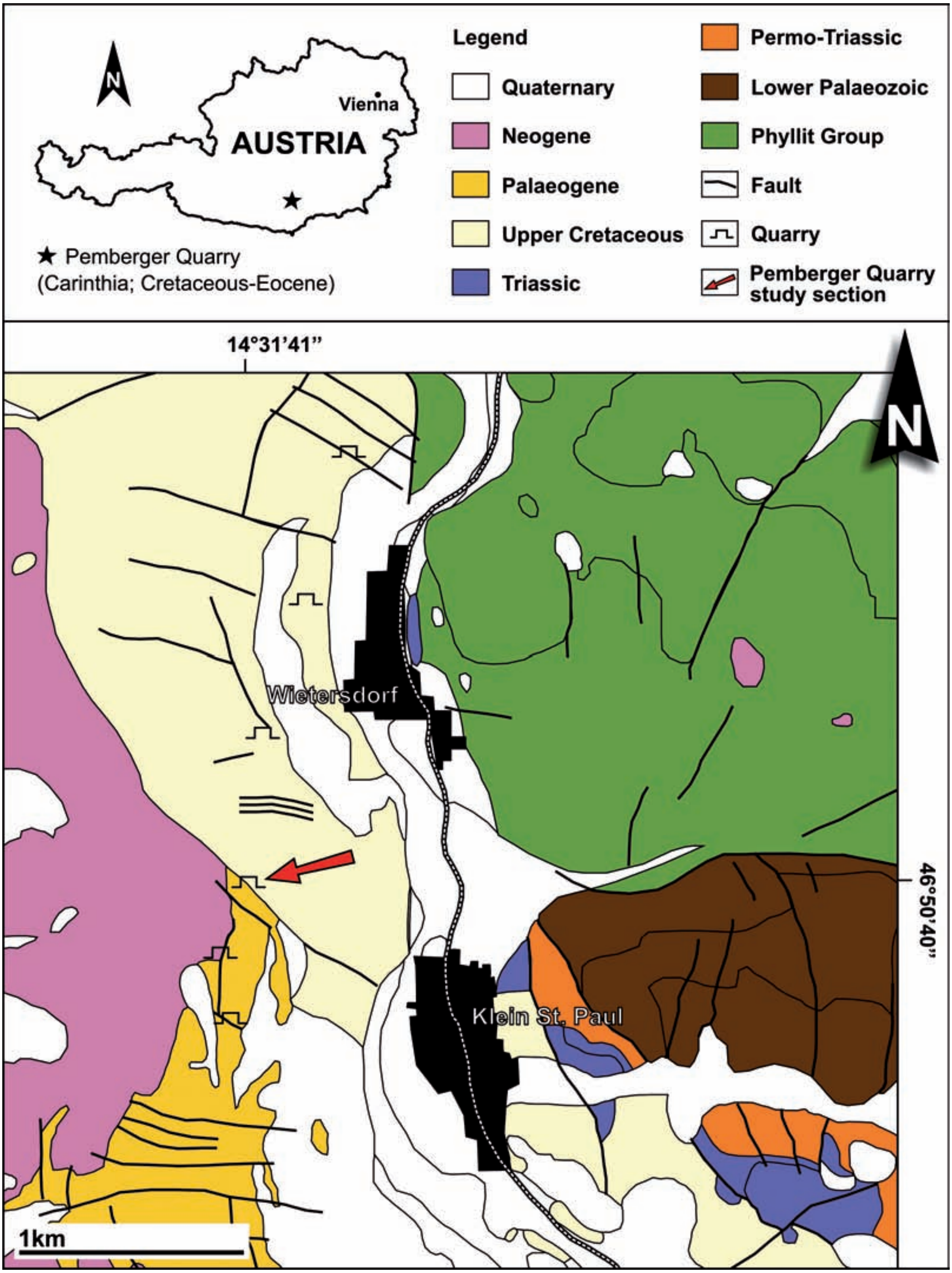

Fig. 1: Geological map of the Krappfeld area and sampling location.

Study Area

In general, the investigated deposits belong to the Gosau Group and crop out on a surface of about 100 km². These deposits are composed of flyschoid limestone and marl with a thickness up to 1500 m within the Krappfeld area (compare Tiedig & Wiedmann 1976). The Krappfeld Subgroup is incorporated into the Gosau Group, with the Pemberger Formation spanning part of the Upper Cretaceous.

The observed section within the Pemberger Quarry (fig. 1) is about 5.5 m thick and consists mainly of marl and marly limestones. Bed 24 consists of a lithoclastic breccia. The thickness of single beds is variable; usually, beds are about 10-15 cm thick and separated by thin interbeds, but at the base and top of the section, bed thickness increases to 50-80 cm. Lithologically, the beds consist of marly limestone with higher calcareous content than the interbeds; this makes them more resistent to weathering. A detailed log is provided in figure 2.

Materials and Methods

For dinoflagellate cyst analyses, nine samples were collected. Small bulk samples were processed in the Separation Laboratory of the Institute of Earth Sciences, University of Graz, following standard palynological preparation procedures (e.g. Wood et al. 1996). About 20-25 g of each sample was finely crushed and dissolved in cold hydrochloric acid (35%) and cold hydrofluoric acid (40%). Neutralization after HCl and HF was achieved by repeated decanting. A slight oxidation by diluted HNO_3 was initiated for some samples for 45 to 60 seconds, followed by washing with diluted NaOH. The remaining residue was sieved through 20 micron nylon mesh and stained with Saffranin "O". Two slides from each sample were prepared using glycerine jelly and then sealed with nail varnish for light microscopy. One SEM stub from each sample was prepared too. Residues, slides and SEM stubs are housed at the Institute of Earth Sciences, University of Graz, with labels PE-01 to PE-26 (e.g. PE-01 equates to Pemberger Quarry-bed 01).

Systematic Part

Palynofloral characteristics

All the studied samples were productive and yielded well-preserved dinocysts. The total record consisted of about 74 dinocyst taxa along with three acritarch genera (*Tarsisphaeridium*, *Paralecaniella*, ? *Cyclopsiella*) and microforaminiferal test linings (compare listing in Appendix A). Terrestrial palynomorphs are rare throughout the section. Range charts of stratigraphically significant species taxa were plotted against the lithological log of the studied section (fig. 2). There was no major change in the dinocyst assemblage throughout the studied samples. Selected taxa are illustrated on plates 1 and 2. The dinoflagellate cyst taxa listed in the present paper are fully referenced in Fensome et al. (2008).

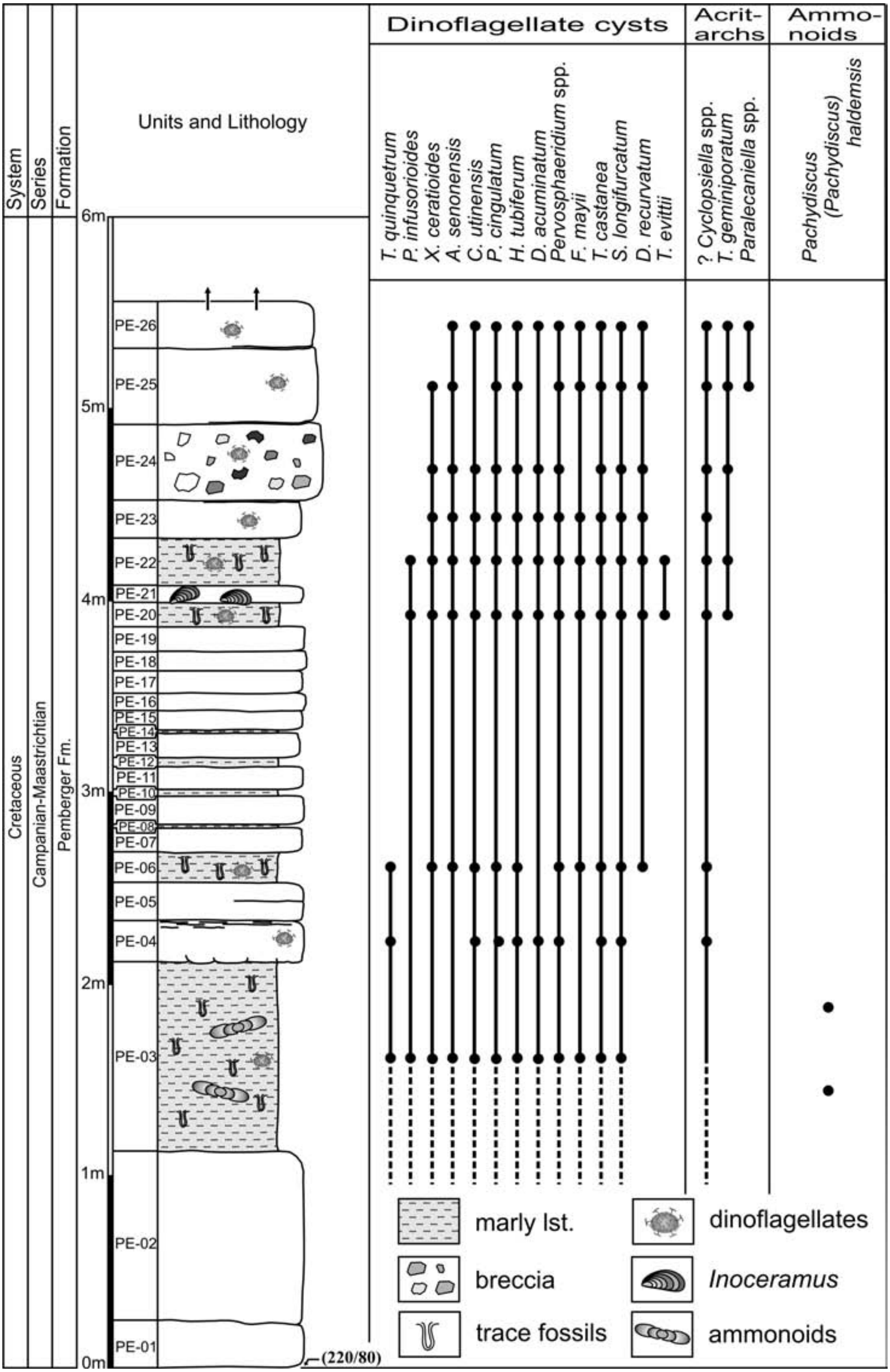

Fig. 2: Range chart of stratigraphically relevant species of palynomorphs and ammonoids.

Age assignment based on dinoflagellate cysts

Although only few samples were studied, the dinocyst assemblage is diverse and age diagnostic as many marker taxa suggesting a Late Cretaceous age have been recorded. No formal or informal zonation is proposed due to insufficient material. The recorded dinoflagellate cyst assemblage has been dated by comparison with assemblages documented from adjacent areas (ROBASZYNSKI et al. 1985; KIRSCH 1991; RONCAGLIA & CORRADINI 1997a) and especially by correlation with lowest and highest occurrences of dinocyst taxa calibrated by WILLIAMS et al. (2004).

Florentinia mayii KIRSCH, 1991 (pl. 2, fig. 4) was described from the lower Maastrichtian of Moos-Graben, Germany. However, WILLIAMS et al. (2004) calibrated its first occurrence in the northern hemisphere in the early Middle Campanian (79.0 Ma) and the last occurrence in the latest Campanian (71.86 Ma). Since this species was recorded in all of the studied samples, they cannot be older than Middle Campanian.

According to KIRSCH (1991), *Cannosphaeropsis utinensis* WETZEL, 1933 (pl. 1, fig. 3) ranges from the lower Campanian to lower Maastrichtian, yet its earliest occurrence could be as far back as the upper Santonian according to FOUCHER (1976), HARDENBOL et al. (1998: chart 5) and PRINCE et al. (1999). Furthermore, MAY (1980) suggested a latest Campanian to earliest Maastrichtian age. A record from the Campanian to lower Maastrichtian of the northern Apennines, Italy, is reported by RONCAGLIA & CORRADINI (1997a) and RONCAGLIA (2002). Closer to the study area, its highest occurrence was recorded from the upper Campanian in Hungary (SIEGL-FARKAS & WAGREICH 1996; SIEGL-FARKAS 1997).

The presence of *Xenascus ceratioides* (DEFLANDRE, 1937) LENTIN & WILLIAMS, 1973 (pl. 2, figs 2, 3), *Trichodinium castanea* (DEFLANDRE, 1935) CLARKE & VERDIER, 1967, *Surculosphaeridium*? *longifurcatum* (FIRTION, 1952) DAVEY et al., 1966 and *Palaeohystrichophora infusorioides* DEFLANDRE, 1935 (pl. 1, fig. 11) indicates a Campanian to (?) earliest Maastrichtian age (MAY 1980; TOCHER 1987; MAHMOUD & SCHRANK 2007).

Hystrichosphaeridium tubiferum (EHRENBERG, 1838) DEFLANDRE, 1937b (pl. 1 fig. 8) is a long-ranging species, a common constituent of the Late Cretaceous assemblages, and geographically widespread. Occurrences of this taxon have been recorded from the upper Turonian to Campanian of the Paris Basin (FOUCHER 1975); Campanian to Maastrichtian of the Atlantic coastal plain of New Jersey and Delaware (AURISANO 1989); ?Upper Campanian to Maastrichtian of Germany (KIRSCH 1991; MARHEINECKE 1992).

The presence of *Glaphyrocysta expansa* (CORRADINI, 1973) RONCAGLIA & CORRADINI, 1997 strongly indicates an Early Maastrichtian age (RONCAGLIA & CORRADINI 1997a). This short-ranging species was documented across the Lower/Middle Maastrichtian boundary in the northern Apennines, Italy. Its lowest occurrence delineates the *G. expansa* subzone (RONCAGLIA & CORRADINI 1997a). *Pervosphaeridium intervelum* KIRSCH, 1991 (pl. 1, fig. 13) was described from the Lower to Middle Campanian of Germany (KIRSCH 1991). It ranges from Upper Santonian (PRINCE et al. 1999) to Maastrichtian (SCHIØLER et al. 1997).

In addition to the key taxa discussed above, there are other notable taxa. Two specimens of *Apteodinium deflandrei* (pl. 2, fig. 7) were obtained from sample PE-20. This species was recorded in the Upper Campanian from the Tercis Quarry (France) by SCHIØLER &

WILSON (2001). According to WILLIAMS et al. (2004), its highest occurrence is within the lower Maastrichtian in the northern hemisphere (68.8 Ma). A Campanian-Maastrichtian age of the investigated sediments is also supported by the presence of *Dinogymnium acuminatum* EVITT et al. (1967), which is a well-known and widely distributed Late Cretaceous fossil (SCHRANK 1984, 1987; SONCINI & RAUSCHER 1990; PAVLISHINA et al. 2004).

Ammonoid taxa

Conventions: NHMW (Museum of Natural History Vienna, Austria); PIB (Institut für Paläontologie, Rheinische Friedrich-Wilhelms-Universität, Bonn, Germany); D (Diameter); Wh (Whorl height); U (Diameter of Umbilicus).

Class Cephalopoda CUVIER, 1797

Order Ammonoidea ZITTEL, 1884

Suborder Ammonitina HYATT, 1889

Superfamily Desmoceratoidea ZITTEL, 1895

Family Pachydiscidae SPATH, 1922

Genus *Pachydiscus* ZITTEL, 1884

Type species: *Ammonites neubergicus* HAUER, 1858, p. 12, pl. 2, fig. 1-3, by subsequent designation of DE GROSSOUVRE 1894.

***Pachydiscus* (*Pachydiscus*) *haldemsis* (SCHLÜTER, 1867)**
Plate 3, figs 1, 2

1867 *Ammonites haldemsis* SCHLÜTER, p. 19, pl. 3, fig. 1.
1872 *Ammonites haldemsis* SCHLÜTER, p. 70.
1894 *Pachydiscus koeneni* DE GROSSOUVRE, p. 178.
1984 *Pachydiscus* (*Pachydiscus*) *haldemsis* (SCHLÜTER, 1867) – KENNEDY & SUMMESBERGER, p. 158, pl. 4, fig. 1-5, pl. 5, fig. 1, pl. 6, fig. 2; pl. 7, fig. 1-11; pl. 13, fig. 1. With synonymy.
1997 *Pachydiscus* (*Pachydiscus*) *haldemsis* (SCHLÜTER, 1867) – KENNEDY & KAPLAN, p. 40, pl. 4, fig. 5-8; pl. 5, fig. 4; pl. 6, fig. 1,2; pl. 7, fig. 2,3; pl. 8,9; pl. 10, fig. 5,8.
1998 *Pachydiscus* (*Pachydiscus*) *haldemsis* (SCHLÜTER, 1867) – KENNEDY & JAGT, p. 158, pl. 1, fig. 2-4.
2004 *Pachydiscus* (*Pachydiscus*) *haldemsis* (SCHLÜTER, 1867) – JAGT et al., p. 575, pl. 1, fig. 9.

Lectotype is the original of SCHLÜTER (1867, p. 3, fig. 1) subsequently designated and refigured by KENNEDY & SUMMESBERGER (1984: p. 158, pl. 7, figs 3, 4).

Material: Two individuals, NHMW 2008z0276/0001 and NHMW 2008z0276/0002 from the Late Cretaceous Gosau Group of the Krappfeld in Carinthia, Austria.

Description: Two flattened, corroded and fragmented internal moulds. Measurements are exaggerated by post mortem compaction. No shell remains are preserved, fragments of sutures are visible but undecipherable. Both individuals are adult macroconchs and have parts of the body chamber preserved. The whorl section cannot be restored, whorls covering about two thirds of the preceding one. Between 25 and 30 bullae per volution give rise to strong primary ribs. Intercalatories appear in irregular distances in the outer third of the flanks. At the venter about 40 ribs per volution can be counted. Ribs are about 4 mm broad and spaced irregularly about 5 mm apart. They cross the flank in a slight flexuous curve or with a shallow concavity, sweeping finally over the venter with a shallow adapertural curvature.

	D	Wh	Wh%	U	U%
NHMW/08/276/1	160	70	43.7%	40	25%
NHMW/08/276/2	131	61.5	47%	38.4	29%
PiB 50b	147	67	45.5%	38	26.2%

Tab. 1: Measurements of the Wietersdorf specimens in comparison to the lectotype of *Pachydiscus koeneni* De Grossouvre, 1894 (PIB 50b).

Discussion: Both individuals are interpreted to be specifically identical and macroconchs of *Pachydiscus (Pachydiscus) haldemsis* (Schlüter, 1867), which were originally described as *Pachydiscus koeneni* De Grossouvre, 1894 (Kennedy & Summesberger 1984, p. 158). The co-occurring *Pachydiscus carinthiacus* Thiedig & Wiedmann 1976 (pl. 2, fig. 4) is a fragment of an adult volution which shows a distinct change in ornament from delicate and narrow standing ribs to coarse and distant ones. Co-occurring taxa of *Pseudokossmaticeras* differ by their smaller whorl height, *P. brandti* (Redtenbacher, 1873) also by its wider umbilicus (38%) and much fewer and coarser ribs (25 primaries on the last whorl of the lectotype). *Pseudokossmaticeras galicianum* (Favre, 1869) differs by its much finer ribbing.

Occurrence: *Pachydiscus* (*Pachydiscus*) *haldemsis* (Schlüter, 1867) is a widely distributed Late Campanian species. It occurs in the Northern Temperate Realm. In Austria it is described from the Late Campanian of Gams (Styria, Austria) by Summesberger et al. (1999) and from the Gschliefgraben (Kennedy & Summesberger 1984). Co-occurrence with *Pseudokossmaticeras brandti* (Redtenbacher, 1873) (Thiedig & Wiedmann 1976) in the "Krappfeld Gosau" endorses its stratigraphical position. The former use of *P. brandti* to indicate Lower Maastrichtian (Thiedig & Wiedmann 1976: 23-24) is outdated (Hancock & Kennedy 1993, p. 156). Co-occurrence with the Maastrichtian *Pachydiscus neubergicus* (Hauer) (Thiedig & Wiedmann, 1976: 23) is based upon a doubtful juvenile specimen: *Pachydiscus* sp. juv. aff. *neubergicus* (Hauer; Thiedig & Wiedmann, 1976, fig. 2A) and an earlier described adult *Pachydiscus neubergicus* (Hauer) of 10 cm diameter (Redlich 1900).

Conclusions

Dinoflagellate cysts from the Upper Cretaceous of Carinthia (Austria) are described for the first time. The encountered palynomorphs are well preserved and diversified. The identified palynofloral assemblage includes 77 species belonging to 40 genera of dinoflagellates and 3 genera of acritarchs. However, the sporomorphs (pollen and spores) are already documented but no attempt has been done, neither to identify them nor to use them as biostratigraphic tool, for dating the section. An Early Maastrichtian age was proposed for the Pemberger Formation based on foraminifera (SCHREIBER 1979, 1980) and ammonoids (THIEDIG & WIEDMANN 1976). According to this study Campanian-Early Maastrichtian age is suggested for at least the upper part of the Pemberger Formation based on the occurrence of dinoflagellate cysts like *Alisogymnium nucleases*, *Cannosphaeropsis utinensis*, *Florentinia mayii*, *Isabelidinium cooksoniae* and *Xenascus ceratioides*. Additionally, the occurrence of the newly found ammonoid taxon *Pachydiscus (Pachydiscus) haldemsis* supports the age proposed by the microflora, as it is an indicator for Late Campanian age.

Acknowledgements

We are grateful to the owners of the Pemberger Quarry, who allowed us to take samples. AS and TS wish to thank the Commission for the Palaeontological and Stratigraphical Research of Austria (CPSA) for financial support and Werner E. PILLER (Uni-Graz) for laboratory and SEM facilities. Hubert DOMANSKI and Stefan MÜLLER are gratefully acknowledged for joint field work.

Max WANK (Wolfsberg, Carinthia) is gratefully acknowledged for information about additional ammonites in Carinthian collections. Photoraphs were taken by Alice SCHUMACHER (Natural History Museum, Vienna). Thanks are due to Stefano TORRICELLI (Eni S.p.A, Exploration & Production Division), William J. KENNEDY (Oxford University of Natural History) and Petr SKUPIEN (VSB-TU Ostrava) for constructive comments and suggestions improving the manuscript.

References

ALBERTI, G. (1961): Zur Kenntnis mesozoischer und alttertiärer Dinoflagellaten und Hystrichosphaerideen von Nord- und Mitteldeutschland sowie einigen anderen europäischen Gebieten. – Palaeontographica, Abteilung A, **116**: 1-58.

AURISANO, R.W. (1989): Upper Cretaceous dinoflagellate biostratigraphy of the subsurface Atlantic Coastal Plain of New Jersey and Delaware, U.S.A. – Palynology, **13**: 143-179.

CLARKE, R.F.A. & VERDIER, J.-P. (1967): An investigation of microplankton assemblages from the Chalk of the Isle of Wight, England. – Verhandelingen der Koninklijke Nederlandse Akademie van Wetenschappen, Afdeeling Natuurkunde, Eerste Reeks, **24**/3: 1-96.

CORRADINI, D. (1973): Non-calcareous microplankton from the Upper Cretaceous of the northern Apennines. – Bollettino della Società paleontologica italiana, **11**/2: 119-197.

DE GROSSOUVRE, A. (1894): Recherches sur la Craie supérieure, 2. Paléontologie. Les ammonites de la craie supérieure. – Mémoires du Service de la Carte géologique détaillée de la France – 264 pp.

EL BEIALY, S.Y. (1995): Campanian-Maastrichtian palynomorphs from the Duwi (Phosphate) Formation of the Hamrawein and Umm E1 Hueitat mines, Red Sea Coast, Egypt. – Review of Palaeobotany and Palynology, **85**: 303-317.

FAVRE, E. (1869): Description des Mollusques fossiles de la Craie des environs de Lemberg en Galicie. – xii, 187 pp.

FENSOME, R.A., MAC RAE, R.A. & WILLIAMS, G.L. (2008): DINOFLAJ2, Version 1. – American Association of Stratigraphic Palynologists, Data Series no. **1**.

FOUCHER, J.-C. (1976): Les dinoflagellés des silex et la stratigraphie du Crétacé supérieur français. – Revue de Micropaléontologie, **18**/4: 213-220.

——— (1975): Dinoflagellés et acritarches des silex crétacés du Bassin de Paris une synthèse stratigraphique. – Annales scientifique de lUniversité de Reims et de lARERS (Association régionale pour létude et la recherche scientifiques), **13**/1-2: 8-10.

HANCOCK, J.M. & KENNEDY, W.J. (1993): The high Cretaceous ammonite fauna from Tercis, Landes, France. – Bulletin de l'Institut Royal des Sciences Naturelles de Belgique, Sciences de la Terre, **63**: 149-209.

HANSEN, J.M. (1977): Dinoflagellate stratigraphy and echinoid distribution in Upper Maastrichtian and Danian deposits from Denmark. – Bulletin of the Geological Society of Denmark, **26**: 1-26.

HARDENBOL, J., THIERRY, J., FARLEY, M.B., JACQUIN, T., DE GRACIANSKY, P.C. & VAIL, P.R. (1998): Mesozoic and Cenozoic sequence chronostratigraphic framework of European Basins. In: DE GRACIANSKY, P.C., HARDENBOL, J., JACQUIN, T. & VAIL, P.R. (eds): Mesozoic and Cenozoic sequence stratigraphy of European Basins. – SEPM Special Publications, **60**: 3-13.

HAUER, F.V. (1858): Über die Cephalopoden der Gosauschichten. – Beiträge zur Palaeontographie von Österreich, **1**: 7-14.

HINTE, J.V. (1963): Zur Stratigraphie und Mikropaläontologie der Oberkreide und des Eozäns des Krappfeldes (Kärnten). – Jahrbuch der Geologischen Bundesanstalt, Sonderband **8**: 1-147.

HOEK, R.P., ESHET, Y. & ALMOGI-LABIN, A. (1996): Dinoflagellate cyst zonation of Campanian-Maastrichtian sequences in Israel. – Micropaleontology, **42**: 125-150.

JAGT, J.W.M., WALASZCZYK, I., YAZYKOVA, E. & ZATON, M. (2004): Linking southern Poland and northern Germany: Campanian cephalopods, inoceramids and echinoids. – Acta Geologica Polonica, **54**/4: 573-586.

KENNEDY, W.J. & JAGT, J.W.M. (1998): Additional Late Cretaceous ammonite records from the Maastrichtian type area. – Bulletin de l'Institut Royal des Sciences Naturelles de Belgique, Sciences de la Terre, **68**: 155-174.

——— & KAPLAN, U. (1997): Ammoniten aus dem Campan des Stemweder Berges, Dammer Oberkreidemulde, NW-Deutschland. – Geologie und Paläontologie in Westfalen, **50**: 31-245.

——— & SUMMESBERGER, H. (1984): Upper Campanian ammonites from the Gschliefgraben (Ultrahelvetic, Upper Austria). – Beiträge zur Paläontologie von Österreich, **11**: 149-206.

KIRSCH, K.-H. (1991): Dinoflagellatenzysten aus der Oberkreide des Helvetikums und Nordultrahelvetikums von Oberbayern. – Münchner Geowissenschaftliche Abhandlungen, **22**: 1-306.

KJELLSTRÖM, G. (1973): Maastrichtian microplankton from the Höllviken Borehole No.1 in Scania, southern Sweden. – Sveriges Geologiska Undersökning, Serie C, no.688, **67**/8: 1-59.

MAHMOUD, M. & SCHRANK, E. (2007): Late Cretaceous spores, pollen and dinoflagellates from two boreholes (Nuqra-1 and 3) in the Aswan area, southeast Egypt. – Revue de Paléobiologie, **26**/2: 593-613.

MARHEINECKE, U. (1992): Monographie der Dinozysten, Acritarcha und Chlorphyta des Maastrichtium von Hemmoor (Niedersachsen). – Palaeontographica, Abteilung B, **227**: 1-173.

MAY, F.E. (1980): Dinoflagellate cysts of the Gymnodiniaceae, Peridiniaceae, and Gonyaulacaceae from the Upper Cretaceous Monmouth Group, Atlantic Highlands, New Jersey. – Palaeontographica, Abteilung B, **172**: 10-116.

PAVLISHINA, P., VERREUSSEL, R., LEEREVELD H., SUMMESBERGER, H. & WAGREICH, M. (2004): Palynological study of the Gosau Group deposits (Upper Cretaceous) of the Northern Calcareous Alps (Austria). – Annalen des Naturhistorischen Museums Wien, Serie A, **106**: 1-23.

PRINCE, I.M., JARVIS, I. & TOCHER B.A. (1999): High-resolution dinoflagellate cyst biostratigraphy of the Santonian–basal Campanian (Upper Cretaceous): new data from Whitecliff, Isle of Wight, England. – Review of Palaeobotany and Palynology, **105**: 143-169.

REDLICH, A. (1900): Die Kreide des Görtschitz- und Gurkthales. – Jahrbuch der k. k. Geologischen Reichsanstalt, **49**: 663-678.

REDTENBACHER, A. (1873): Die Cephalopodenfauna der Gosauschichten in den nordöstlichen Alpen. – Abhandlungen der k. k. Geologischen Reichsanstalt, **5**: 91-140.

ROBASZYNSKI, F., BLESS, M.J.M., FELDER, P.J., FOUCHER, J.-C., LEGOUX, O., MANIVIT, H., MEESEN, J.P.M.T. & VAN DER TUUK, L.A. (1985): The Campanian-Maastrichtian boundary in the chalky facies close to the type-Maastrichtian area. – Bulletin des Centres de recherche exploration-production Elf-Aquitaine, **9**/1: 1-113.

RONCAGLIA, L. (2002): Lower Maastrichtian dinoflagellates from the Viano Clay Formation at Viano, northern Apennines, Italy. – Cretaceous Research, **23**: 65–76.

——— & CORRADINI, D. (1997a): Upper Campanian to Maastrichtian dinoflagellate zonation in the northern Apennines, Italy. – Newsletters on Stratigraphy, **35**: 29–57.

——— & CORRADINI, D. (1997b): Dinoflagellate events with calcareous nannoplankton and planktonic foraminiferal zones in the Solignano Formation (Maastrichtian, Correlation of key dinLate Cretaceous) northern Apennines, Italy. – Review of Palaeobotany and Palynology, **97**: 177-196.

SCHIØLER, P. & WILSON, G. J. (2001): Dinoflagellate biostratigraphy around the Campanian-Maastrichtian boundary at its type section (Tercis Quarry, southwest France). In: ODIN, G.S. (ed.): The Campanian-Maastrichtian boundary: characterisation and correlation from Tercis (Landes, SW France) to Europe and other continents. – IUGS Special Publication, Monograph Series, 36, and Developments in Palaeontology and Stratigraphy, **19**: 233-246, Amsterdam (Elsevier Science Publishers).

———, BRINKHUIS, H., RONCAGLIA, L. & WILSON, G.J. (1997): Dinoflagellate biostratigraphy and sequence stratigraphy of the type Maastrichtian (Upper Cretaceous), ENCI Quarry, The Netherlands. – Marine Micropaleontology, **31**: 65-95.

SCHLÜTER, C. (1867): Beitrag zur Kenntniss der jüngsten Ammoneen Norddeutschlands. – 36 pp.

——— (1871-1876): Cephalopoden der oberen deutschen Kreide. – Palaeontographica, **21** (1871): 1-24; **21** (1872): 25-120; **24** (1876): 1-144 (121-264).

SCHRANK, E. (1984): Organic-geochemical and palynological studies of a Dakhla Shale profile (Late Cretaceous) in southeast Egypt. Part A: Succession of microfloras and depositional environment. – Berliner geowissenschaftliche Abhandlungen A, **50**: 189-207.

——— (1987): Paleozoic and Mesozoic palynomorphs from northeast Africa (Egypt and Sudan) with special reference to Late Cretaceous pollen and dinoflagellates. – Berliner geowissenschaftliche Abhhandlungen A, **75**: 249-310.

Schreiber, O.S. (1979): Heterohelicidae (Foraminifera) aus der Pemberger-Folge (Oberkreide) von Klein-Sankt Paul am Krappfeld (Kärnten). – Beiträge zur Paläontologie von Österreich, **6**: 27-59.

——— (1980): Benthonische Foraminiferen der Pemberger-Folge (Oberkreide) von Klein- Sankt Paul am Krappfeld (Kärnten). – Beiträge zur Paläontologie von Österreich, **7**: 1-206.

Seunes, J. (1892): Contribution à l'étude des cephalopodes du Crétacé supérieur de France. I. Ammonites du calcaire à *Baculites* du Cotentin (suite) II. Ammonites du Campanien de la région sous-pyrénéenne. – Départment de Landes. Mémoires de la Société Géologique de France, **2**/2: 8 – 22.

Siegl-Farkas, A. & Wagreich, M. (1996): Age and palaeoenvironment of the spherulite-bearing Polany Marl Formation (Upper Cretaceous, Hungary) on basis of palynologic and nannoplankton investigation. – Acta Biologica Szegediensis, **41**: 23-36.

——— (1997): Dinoflagellate stratigraphy of the Senonian formations of the Transdanubian Range. – Acta Geologica Hungarica, **40**: 73-100.

Skupien, P. & Mohamed, O. (2008): Campanian to Maastrichtian palynofacies and dinoflagellate cysts of the Silesian Unit, Outer Western Carpathians, Czech Republic. – Bulletin of Geosciences, **83**/2: 207-224.

Soncini, M.J. & Rauscher, R. (1990): Morphologies particulires chez les dinokystes des genres *Isabelidinium*, *Manumiella* et *Dinogymnium* dans les phosphates maastrichtiens et paléocénes du Maroc. (Unusual morphologies of dinocysts from the genera *Isabelidinium*, *Manumiella* and *Dinogymnium* in Maastrichtian and Paleocene phosphates in Morocco. – Bulletin des Centre de Recherches Exploration-Production, Elf-Aquitaine, **14**/2: 583-596.

Summesberger, H., Wagreich, M., Tröger, K.-A. & Jagt, J.W.M. (1999): Integrated biostratigraphy of the Santonian/Campanian Gosau Group of the Gams Area (Late Cretaceous; Styria, Austria). – Beiträge zur Paläontologie, **24**: 155-205.

Thiedig, F. & Wiedmann, J. (1976): Ammoniten und Alter der höheren Kreide (Gosau) des Krappfeldes in Kärnten (Österreich). – Mitteilungen des Geologisch-Paläontologischen Instituts der Universität Hamburg, **45**: 9-27.

Tocher, B.A. (1987): Campanian to Maestrichtian dinoflagellate cysts from the United States Atlantic Margin Deep Sea Drilling Project Site 612 [Leg 95]. – Initial Reports of the Deep Sea Drilling Project, **95**: 419-428.

Torricelli, S. & Amore, M.R. (2003): Dinoflagellate cysts and calcareous nannofossils from the Upper Cretaceous Saraceno Formation (Calabria, Italy): implication about the history of the Liguride Complex. – Rivista Italiana di Paleontologia e Stratigrafia, **109**/3: 499-516.

Wagreich, M., Pavlishina, P. & Malata, E. (2006): Biostratigraphy of the lower red shale interval in the Rhenodanubian Flysch Zone of Austria. – Cretaceous Research, **27**: 743-753.

Williams, G.L., Brinkhuis, H., Pearce, M.A., Fensome, R.A. & Weegink, J.W. (2004): Southern Ocean and global dinoflagellate cyst events compared: index events for the Late Cretaceous–Neogene. – In: Exon, N.F., Kennett, J.P. & Malone, M.J. (eds): Proceedings of the Ocean Drilling Program – Scientific Results, **189**: 1-98.

WOOD, G. D., GABRIEL, A.M. & LAWSON, J.C. (1996): Palynological techniques – processing and microscopy. – In: JANSONIUS, J., MCGREGOR, D.C. (eds): Palynology: Principles and Applications. – American Association of Stratigraphic Palynologists Foundation, **1**: 29-50.

Appendix

List of dinocyst species recorded

Plate and figure numbers are provided when the taxon is illustrated. Taxonomy follows FENSOME et al. (2008) and references therein.

1. *Achomosphaera ramulifera* (DEFLANDRE, 1937b) EVITT, 1963 (pl. 1, fig. 1)
2. *Actinotheca aphroditae* COOKSON & EISENACK, 1960a
3. *Alisogymnium eucleases* (COOKSON & EISENACK, 1970a) LENTIN & VOZZHENNIKOVA, 1990
4. *Apteodinium* cf. *reticulatum* SINGH, 1971 (pl. 1, fig. 6)
5. *Apteodinium deflandrei* (CLARKE & VERDIER, 1967) LUCAS-CLARK, 1987 (pl. 2, fig. 7)
6. *Areoligera coronata* (WETZEL, 1933b) LEJEUNE-CARPENTIER, 1938
7. *Areoligera flandriensis* SLIMANI, 1994
8. *Areoligera guembelii* KIRSCH, 1991
9. *Areoligera senonensis* LEJEUNE-CARPENTIER, 1938
10. *Areoligera volata* DRUGG, 1967
11. *Balcattia cirrifera* COOKSON & EISENACK, 1974
12. *Batiacasphaera compta* DRUGG, 1970
13. *Biconidinium reductum* (MAY, 1980) KIRSCH, 1991
14. *Cannosphaeropsis utinensis* WETZEL, 1933 (pl. 1, fig. 3)
15. *Codoniella campanulata* (COOKSON & EISENACK, 1960a) DOWNIE & SARJEANT, 1965
16. *Coronifera oceanica* COOKSON & EISENACK, 1958 (pl. 1, fig. 4)
17. *Cometodinium*? *whitei* (DEFLANDRE & COURTEVILLE, 1939) STOVER & EVITT, 1978; emend. MONTEIL, 1991a
18. *Cordosphaeridium fibrospinosum* DAVEY & WILLIAMS, 1966b
19. *Cribroperidinium edwardsii* (COOKSON & EISENACK, 1958) DAVEY, 1969a
20. *Cribroperidinium*? *pyrum* (DRUGG, 1967) STOVER & EVITT, 1978
21. *Cyclonephelium crassimarginatum* COOKSON & EISENACK, 1974
22. *Dinogymnium acuminatum* EVITT et al., 1967 (pl. 1, fig. 2)
23. *Dinogymnium albertii* CLARKE & VERDIER, 1967
24. *Dinogymnium curvatum* (VOZZHENNIKOVA, 1967) LENTIN & WILLIAMS, 1973
25. *Dinogymnium westralium* (COOKSON & EISENACK, 1958) EVITT et al., 1967
26. *Diphyes recurvatum* MAY, 1980 (pl. 1, fig. 5)
27. *Downiesphaeridium multispinosum* (SINGH, 1964) ISLAM, 1993
28. *Exochosphaeridium bifidum* (CLARKE & VERDIER, 1967) CLARKE et al., 1968 (pl. 1, fig. 7)
29. *Exochosphaeridium phragmites* DAVEY et al., 1966
30. *Florentinia aculeata* KIRSCH, 1991 (pl. 1, fig. 9)

31. *Florentinia mantellii* (Davey & Williams, 1966b) Davey & Verdier, 1973
32. *Florentinia mayii* Kirsch, 1991 (pl. 2, fig. 4)
33. *Glaphyrocysta espiritosantensis* (Regali et al., 1974) Arai in Fauconnier & Masure, 2004
34. *Glaphyrocysta expansa* (Corradini, 1973) Roncaglia & Corradini, 1997
35. *Glaphyrocysta ordinata* (Williams & Downie, 1966c) Stover & Evitt, 1978 (pl. 1, fig. 10)
36. *Glaphyrocysta semitecta* (Bujak in Bujak et al., 1980) Lentin & Williams, 1981
37. *Hystrichosphaeridium recurvatum* (White 1842) Lejeune-Carpentier, 1940
38. *Hystrichosphaeridium salpingophorum* (Deflandre, 1935) Deflandre, 1937b; emend. Davey & Williams, 1966b
39. *Hystrichosphaeridium tubiferum* (Ehrenberg, 1838) Deflandre, 1937b; emend. Davey & Williams, 1966b (pl. 1, fig. 8)
40. *Hystrichosphaeropsis ovum* Deflandre, 1935
41. *Isabelidinium cooksoniae* (Alberti, 1959b) Lentin & Williams, 1977a (pl. 2, fig. 1)
42. *Manumiella*? *cretacea* (Cookson, 1956) Bujak & Davies, 1983 (pl. 2, fig. 8)
43. *Nelsoniella aceras* Cookson & Eisenack, 1960a
44. *Operculodinium centrocarpum* (Deflandre & Cookson, 1955) Wall, 1967
45. *Palaeohystrichophora infusorioides* Deflandre, 1935 (pl. 1, fig. 11)
46. *Pervosphaeridium intervelum* Kirsch, 1991 (pl. 1, fig. 12)
47. *Pervosphaeridium pseudohystrichodinium* (Deflandre, 1937) Yun, 1981
48. *Phelodinium exilicornutum* Smith, 1992
49. *Phelodinium pentagonale* (Corradini, 1973) Stover & Evitt, 1978
50. *Phelodinium tricuspe* (Wetzel, 1933a) Stover & Evitt, 1978
51. *Pterodinium cingulatum* (Wetzel, 1933) Below, 1981 (pl. 1, fig. 12)
52. *Pterodinium crassimuratum* (Davey & Williams, 1966a) Thurow et al., 1988
53. *Raetiaedinium truncigerum* (Deflandre, 1937b) Kirsch, 1991
54. *Spinidinium echinoideum* (Cookson & Eisenack, 1960a) Lentin & Williams, 1976 (pl. 2, fig. 9)
55. *Spinidinium eggeri* Kirsch, 1991
56. *Spiniferites cooksoniae* Lentin & Williams, 1977b
57. *Spiniferites katatonos* Corradini, 1973
58. *Spiniferites multibrevis* (Davey & Williams, 1966a) Below, 1982c
59. *Spiniferites ramosus* (Ehrenberg, 1838) Mantell, 1854
60. *Spiniferites ramosus* subsp. *granosus* (Davey & Williams, 1966) Lentin & Williams, 1973
61. *Spiniferites scabrosus* (Clarke & Verdier, 1967) Lentin & Williams, 1975
62. *Surculosphaeridium basifurcatum* Yun, 1981
63. *Surculosphaeridium belowii* Yun, 1981
64. *Surculosphaeridium cassospinum* Yun, 1981 (pl. 2, figs 11, 12)
65. *Surculosphaeridium longifurcatum* (Firtion, 1952) Davey et al., 1966
66. *Tanyosphaeridium xanthiopyxides* (Wetzel, 1933b) Stover & Evitt, 1978; emend. Sarjeant, 1985b
67. *Trabeculidium quinquetrum* Duxbury, 1980 (pl. 2, figs 13-15)
68. *Trichodinium castanea* (Deflandre, 1935) Clarke & Verdier, 1967
69. *Trithyrodinium evittii* Drugg, 1967 (pl. 2, figs 5, 6)

70. *Trithyrodinium suspectum* (MANUM & COOKSON, 1964) DAVEY, 1969b
71. *Xenascus australensis* COOKSON & EISENACK, 1969
72. *Xenascus ceratioides* (DEFLANDRE, 1937b) LENTIN & WILLIAMS, 1973 (pl. 2, figs 2, 3)
73. *Xenascus gochtii* (CORRADINI, 1973) STOVER & EVITT, 1978
74. *Xenascus sarjeantii* (CORRADINI, 1973) STOVER & EVITT, 1978

Acritarchs

1. *Tarsisphaeridium geminiporatum* RIEGEL, 1974 (pl. 2, fig. 10)
2. *Paralecaniella* spp.
3. ? *Cyclopsiella* spp.

Plate 1

All are SEM microphotographs. The species names are followed by sample number.
Scale bars equal 20 µm.

Fig. 1: *Achomosphaera ramulifera* (Deflandre, 1937b) Evitt, 1963; sample PE-23; dorsal view.

Fig. 2: *Dinogymnium acuminatum* Evitt et al., 1967; sample PE-26; ventral view.

Fig. 3: *Cannosphaeropsis utinensis* Wetzel, 1933; sample PE-06; uncertain orientation.

Fig. 4: *Coronifera oceanica* Cookson & Eisenack, 1958; sample PE-26; ? ventral view.

Fig. 5: *Diphyes recurvatum* May, 1980; sample PE-06; ? ventral view.

Fig. 6: *Apteodinium* cf. *reticulatum* Singh, 1971; sample PE-23; dorsal view.

Fig. 7: *Exochosphaeridium bifidum* (Clarke & Verdier, 1967) Clarke et al., 1968; sample PE-23; ? apical view.

Fig. 8: *Hystrichosphaeridium tubiferum* (Ehrenberg, 1838) Deflandre, 1937; emend. Davey & Williams, 1966; sample PE-25; apical view.

Fig. 9: *Florentinia aculeata* Kirsch, 1991; sample PE-26; oblique dorsal view.

Fig. 10: *Glaphyrocysta ordinata* (Williams & Downie, 1966c) Stover & Evitt, 1978; sample PE-25; ventral view.

Fig. 11: *Palaeohystrichophora infusorioides* Deflandre, 1935; sample PE-20; lateral view.

Fig. 12: *Pterodinium cingulatum* (Wetzel, 1933) Below, 1981a; sample PE-24; antapical view.

Fig. 13: *Pervosphaeridium intervelum* Kirsch, 1991; sample PE-22; uncertain orientation.

Fig. 14: *Xenascus gochtii* (Corradini, 1973) Stover & Evitt, 1978; sample PE-06; apical view.

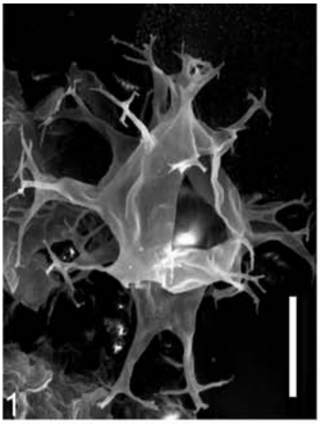
1


2

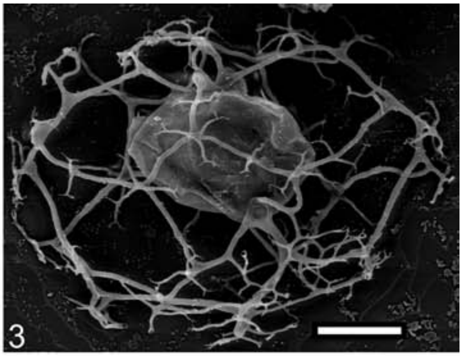
3

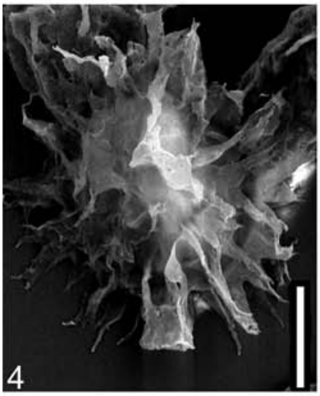
4

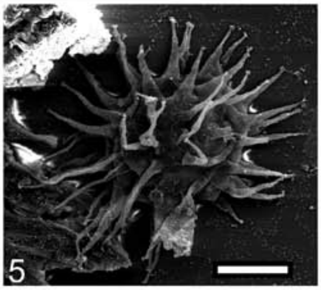
5

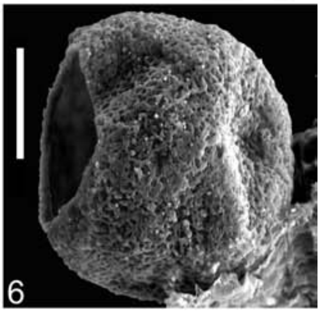
6

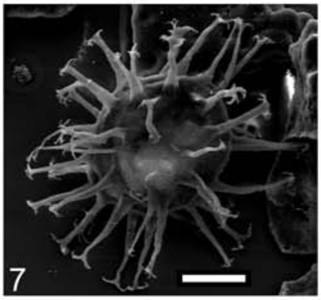
7

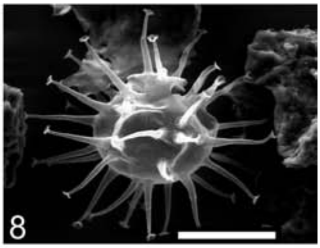
8

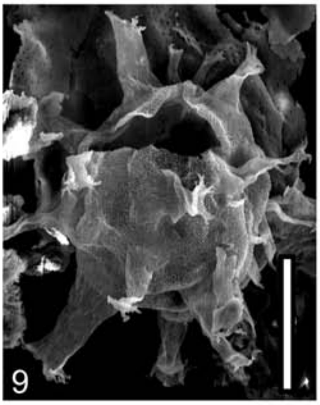
9

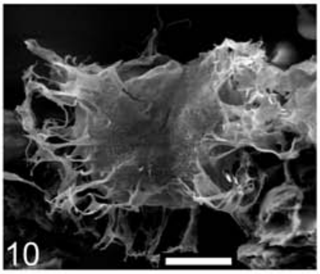
10

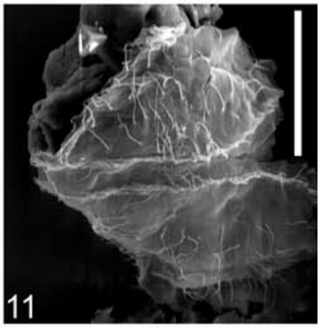
11

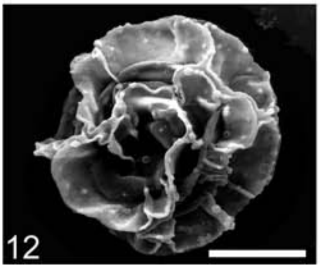
12

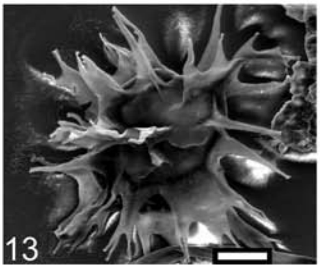
13

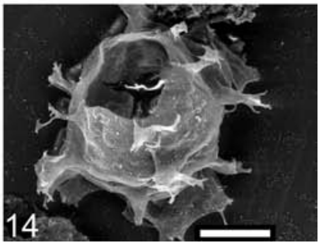
14

Plate 2

All are bright field microphotographs. The species names are followed by sample number, slide number and England Finder reference. Scale bars equal 20 µm.

Fig. 1:	*Isabelidinium cooksoniae* (Alberti, 1959b) Lentin & Williams, 1977a; sample PE-06, slide A, K54, dorsal view.
Figs. 2, 3:	*Xenascus ceratioides* (Deflandre, 1937b) Lentin & Williams, 1973; sample PE-22, slide B, S24/3, successive foci.
Fig. 4:	*Florentinia mayii* Kirsch, 1991; sample PE-20, slide A, D51, dorsal view.
Figs. 5, 6:	*Trithyrodinium evittii* Drugg, 1967; sample PE-20, slide A, G26, dorsal view.
Fig. 7:	*Apteodinium deflandrei* (Clarke & Verdier, 1967) Lucas-Clark, 1987; sample PE-20, slide A, N28/3, ? ventral view.
Fig. 8:	*Manumiella*? *cretacea* (Cookson, 1956) Bujak & Davies, 1983; sample PE-24, slide A, U55/4, dorsal view.
Fig. 9:	*Spinidinium echinoideum* (Cookson & Eisenack, 1960a) Lentin & Williams, 1976; sample PE-20, slide A, C29/3, ventral view?
Fig. 10:	*Tarsisphaeridium geminiporatum* Riegel, 1974; sample PE-22, slide A, O48, uncertain orientation.
Figs. 11, 12:	*Surculosphaeridium cassospinum* Yun, 1981; sample PE-03, slide A, E34/4, successive foci.
Figs. 13-15:	*Trabeculidium quinquetrum* Duxbury, 1980; sample PE-04, slide B, O70/1, successive foci.

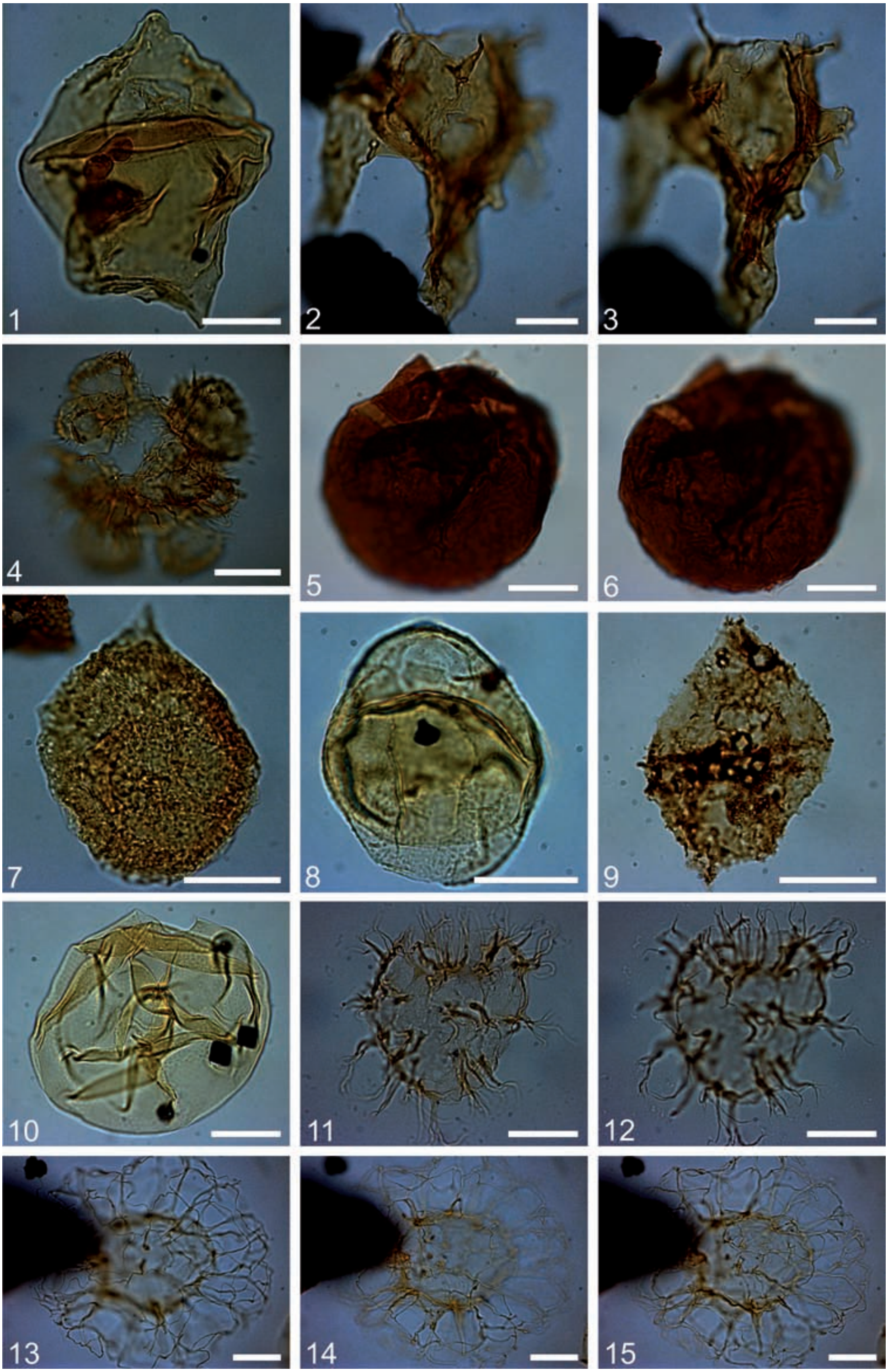
1
2
3
4
5
6
7
8
9
10
11
12
13
14
15

Plate 3

Fig. 1, 2: *Pachydiscus* (*Pachydiscus*) *haldemsis* (SCHLÜTER, 1867); sample PE-03; lateral view, NHMW 2008z0276/0001-2.


1

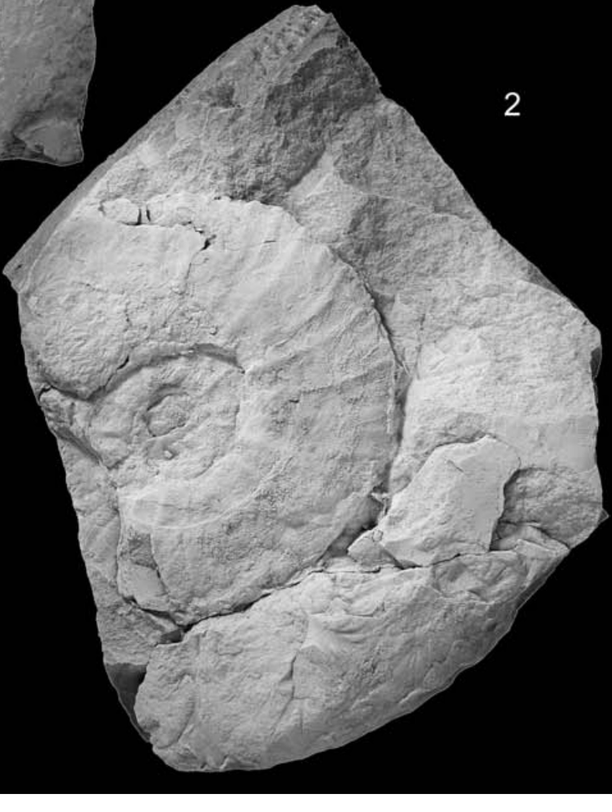
2

Ann. Naturhist. Mus. Wien | 110 A | 423–442 | Wien, Jänner 2009

Foraminifera and sequence stratigraphy of the lower part of the Speeton Clay Formation (Lower Cretaceous) in N. E. England

Malcolm B. Hart[1], Gregory D. Price[1] & Christopher W. Smart[1]

(With 9 figures)

Manuscript submitted on July 8th 2008,
the revised manuscript on November 5th 2008

Abstract

The Speeton Clay Formation is exposed in the cliffs north of Flamborough Head in N. E. England. The formation ranges in age from Ryazanian to the Albian but is often poorly exposed in the sea cliffs and on the foreshore. In the lower part of the succession (Ryazanian – Barremian) the foraminiferal assemblage is dominated by long-ranging nodosariids although, at some levels, the fauna is dominated by monospecific assemblages of epistominiids. The diversity of the total foraminiferal assemblage varies throughout the succession, with the maximum diversity being recorded in the Late Hauterivian. Using information from (i) diversity, (ii) distribution of epistominiids, (iii) glauconite and (iv) pyrite it is possible to identify potential sequence boundaries in the Late Ryazanian (~138 Ma), Early Valanginian (~136 Ma), mid-Hauterivian (~129 Ma) and Early Barremian. These four events are very close in age to the events (K20, K30, K40 and K50) originally described by Sharland and co-workers in Arabia.

Keywords: Foraminifera, Speeton Clay Formation, Sequence Stratigraphy, taphonomy.

Introduction

The Speeton Clay Formation is about 100 metres thick at its type locality in Filey Bay (Fig. 1) but thickens inland to ~360 m in the Fordon No. 1 borehole about 4.4 km west of Speeton (Dilley, in discussion of Neale 1968). South of the present outcrop, seismic data indicate a thickness of ~1 km before thinning towards the Market Weighton High (Kirby & Swallow 1987; Rawson 2006). Off-shore, in the North Sea Basin thicknesses of 100–170 m are normally recorded (Rawson et al. 1978; Cameron et al. 1992, fig. 79) although <900 m are recorded near the Dowsing Fault Line (Cameron et al. 1992). In the well-known Filey Bay succession all six Lower Cretaceous stages are represented although the Valanginian, Aptian and Albian successions are much reduced by non-sequences and erosional features. The dominantly argillaceous succession is badly affected by folding, faulting and landslides, and surfaces are frequently obscured by downwash. The most reliable sections are found on the foreshore when a combination of favourable tides and wind has removed beach sand and shingle.

---

[1] School of Earth, Ocean & Environmental Sciences, University of Plymouth, Drake Circus, Plymouth PL4 8AA, United Kingdom Corresponding author: Malcolm B. Hart (mhart@plymouth.ac.uk)

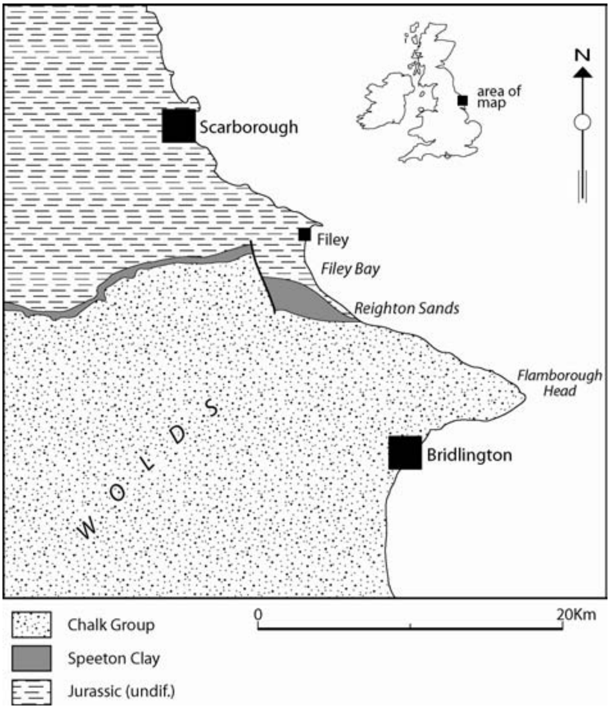

Fig. 1: Location of the Filey Bay succession of the Speeton Clay Formation in N. E. England.

Within the overall clay succession are thin, phosphatic nodule beds and concentrations of glauconite which may represent significant pauses in sedimentation. Some of the clays are distinctly mottled (by chondritiform burrow systems), while in places there are silt layers and distinctive colour changes. Some of these pale (more calcareous)/dark (less calcareous) rhythmic alternations are best seen in the top C Beds and lowest B Beds (near the Hauterivian/Barremian boundary) and may represent Milankovitch precession cycles (22,300 years: see RAWSON & MUTTERLOSE 1983).

One of the earliest descriptions of the Speeton Clay Formation was by LECKENBY (1859), closely followed by JUDD in 1868. Late in the nineteenth century LAMPLUGH (1889) subdivided the succession into four units, each of which was represented by a letter (A – D, with the D Beds at the bottom and the A Beds at the top). Each of the identified units was recognised by the presence of a diagnostic belemnite and so this lettering scheme was not a genuine lithostratigraphical sub-division of the formation. Bed E was identified as the thin phosphatic "Coprolite Bed" that forms the base of the succession and which rests non-conformably on the Kimmeridge Clay Formation (Upper Jurassic). Subsequent work by ENNIS (1937), NEALE (1960a, 1962a), KAYE (1964) and FLETCHER (1969) has refined the lithological subdivisions of the lettered units. The ammonite fauna has been described by LAMPLUGH (1924), NEALE (1962a), RAWSON (1971a, b, 1975), RAWSON et al. (1978), KEMPER et al. (1981) and DOYLE (1989) but taxa are relatively rare except in the Hauterivian. Belemnites, however, are relatively common throughout the succession and have been described by LAMPLUGH (1889, 1924),

SWINNERTON (1936), SPAETH (1971), PINCKNEY & RAWSON (1974), PINCKNEY (1975), RAWSON & MUTTERLOSE (1983), MUTTERLOSE et al. (1987) and MUTTERLOSE (1990).

The first systematic description of the foraminifera was by SHERLOCK (1914), who compared the fauna with the Gault Clay Formation of Folkestone (Kent, S. E. England), the Hils Clay of Germany (HECHT 1938; BARTENSTEIN & BETTENSTAEDT 1962), the Gault Clay Formation of Montcley, France (BERTHELIN 1880) and the Recent foraminifera collected during the HMS *Challenger* Expeditions. A later paper by KHAN (1962) compared the foraminifera of the Speeton Clay Formation with comparable successions in Germany, but the imprecise location of the samples used in this investigation has rendered this work of limited value.

The ostracod fauna, which is quite diverse and abundant, has been described by NEALE (1960b, 1962b, 1968, 1973, 1978). The calcareous nannofossil assemblage has been described by BLACK (1971), SISSINGH (1977), PERCH-NIELSEN (1979) and TAYLOR (1978a, b, 1982).

Distribution of the foraminifera

It has been suggested that water depths during the deposition of the lower part of the Speeton Clay Formation may have been less than 100 m (RAWSON 2006, p. 375). Some horizons, in the D Beds (e.g., D5) may either have been shallower as suggested by the presence of *Lingula*, or almost anoxic as indicated by the presence of abundant pyrite (including infilled burrow systems). In such shallow shelf successions the foraminiferal morphogroups present do not show the variability seen in, for example, the Brazilian Continental Margin (KOUTSOUKOS & HART 1990). Analysis of the fauna using alpha diversity and triangular diagrams (MURRAY 1991, pp. 313-322) has also proven to be ineffective in this succession. The dominant assemblage is one of relatively long-ranging nodosariids (especially *Lenticulina* and *Citharina*) with smaller numbers of agglutinated taxa. In some horizons the assemblage can, however, contain ~95 % *Epistomina* and/or *Hoeglundina*.

Our knowledge of the foraminifera is limited with the only major investigation being that of FLETCHER (1966) which remains largely unpublished. FLETCHER (1973) provided a summary of his research, presenting data on the distribution of the foraminifera in the Speeton Clay Formation (bed-by-bed), though no taxa were illustrated. Some of this information was used by HART et al. (1982, 1989) in a summary of Cretaceous foraminifera, which was supplemented by some additional collecting by MBH in 1977 and a study of borehole material in the collections of the late Professor J. W. NEALE (Hull University). The material used by FLETCHER, in the collections of Hull University, has also been consulted and this provided some of the specimens used to illustrate HART et al. (1982, 1989). The diversity information presented here is based on the species identifications of MBH, after consultation with Dr B. N. FLETCHER and Prof. J. W. NEALE. The samples prepared by FLETCHER were washed on a 75µm sieve, while the additional samples prepared by MBH used the “white spirit” method (BRASIER 1980) and were also washed on a 75µm sieve (the norm in the 1960s and 1970s). In 1988 CRITTENDEN (in an unpublished PhD thesis) described the fauna of the Speeton Clay Formation in the Southern North Sea Basin, although the bulk of the fauna was not illustrated by SEM photographs. BANNER & DESAI (1988) have described the planktic foraminifera from the Aptian and

Albian succession in N. E. England, although planktic taxa have not been described from the Ryazanian (Berriasian) to Barremian part of the Speeton Clay Formation.

Sequence Stratigraphy

Sequence stratigraphy was developed in the 1970s and, initially, used for the interpretation of seismic profiles. Vail et al. (1977) developed the concept, extending it to allow the inclusion of borehole and outcrop data. The hypothesis was that short-term fluctuations in sea level generate "sequences" or "genetically related strata bounded by uncomformities or their correlative conformities" (Van Wagoner et al. 1988, p. 39). Sequence stratigraphy quickly developed a relatively complicated terminology of systems tracts. This "Exxon Model" of a sequence must not be confused with the "Galloway Model", which uses the Maximum Flooding Surface (rather than the Sequence Boundary) as the key to sequence identification (Galloway 1989a, b) or the "Einsle Model" which is based on the recognition of transgressive/regressive cycles (Einsle & Bayer 1991).

The "Exxon Model" was used by Emery & Myers (1996) in their interpretation of sequences and the palaeontological signal that would be left in the fossil record (Fig. 2). As there are no planktic taxa in the lower levels of the Speeton Clay Formation in the Filey Bay section only the pattern left by the benthic taxa is relevant. In this, parts of the Lowstand Systems Tract (LST) would have a reduced diversity while the maximum diversity would be expected around the Maximum Flooding Surface (MFS) or "Zone of Maximum Flooding" (*sensu* Montanez & Osleger 1993; Strasser et al. 1994,

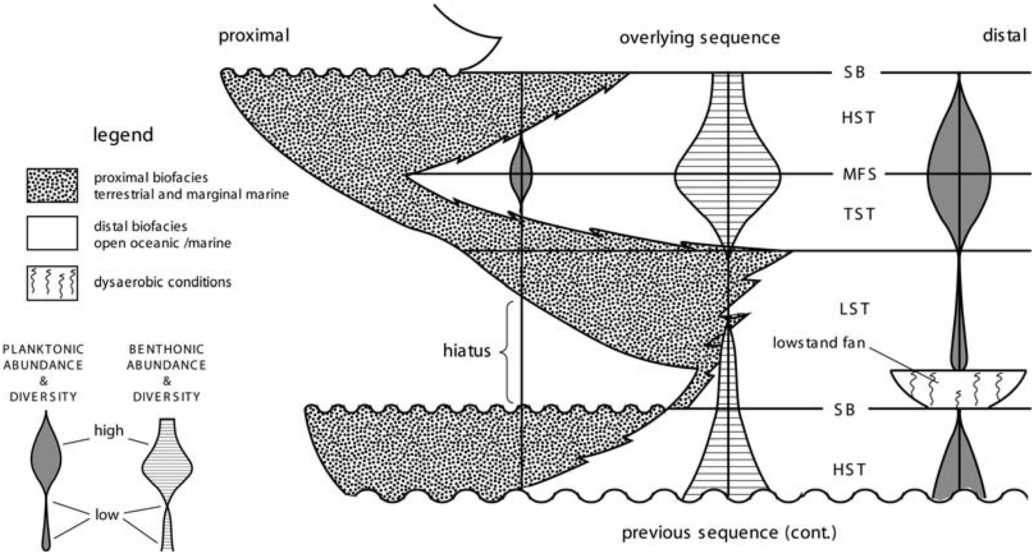

Fig. 2: The "Exxon Model" of a sequence (based on Emery & Myers 1996, fig. 6.14a) and the hypothetical distribution of benthic and planktic foraminifera. The planktic foraminifera are most abundant (and diverse) in the region of the MFS with deeper-water morphotypes being found in more distal regions while only surface-water morphotypes are to be found in more proximal environments.

1999; Oliver 1998). The MFS coincides with the most landward distribution of diverse, open marine, plankton and a diversity maximum of benthic taxa. This approach has been used effectively in younger rocks, most notably in the Cenozoic sediments of the Gulf of Mexico (Shaffer 1987, 1990; Armentrout 1987, 1991; Armentrout & Clement 1990; Armentrout et al. 1990, 1999; Pacht et al. 1990; Vail & Wornardt, 1990; Van der Zwan & Brugman 1999). Recently a number of other authors have extended this approach to the interpretation of Mesozoic successions (Olsson 1988; Cubaynes et al. 1990; Simmons et al. 1991; Powell 1992; Hart 1997, 2000; Henderson 1997; Henderson & Hart 2000; Oxford et al 2000, 2004; Sharland et al. 2000).

The Speeton Clay Formation has been investigated, often indirectly, for its record of Early Cretaceous sequences and changes in sea level. Some of this research (Mitchell & Underwood 1999; Underwood & Mitchell 1999; Rückheim et al. 2006) has been focussed on the upper part of the formation which is Barremian to Albian in age. The lower part of the formation (Berriasian to Barremian in age) has been studied by Rawson & Riley (1982), Copestake et al. (2003) and Hoedemaeker & Herngreen (2003). The interpretations of the latter authors appear to have been driven by parallel work on the Río Argos (S. E. Spain) succession by Hoedemaeker (1995) and Hoedemaeker & Leereveld (1995). The Río Argos succession investigated by Hoedemaeker (and P. R. Vail – though not listed as a co-author on the 1995 paper) is a very complete, fossiliferous succession dominated by limestone/marlstone cycles that are driven by Milankovitch periodicities (Ten Kate & Sprenger 1989). It is quite difficult to follow the reasoning behind Hoedemaeker's selection of systems tracts and, in the paper with Leereveld, there is no indication of the sequence boundaries that appear in Hoedemaeker (1995, fig. 1). This interpretation identified major (= long term) sequence boundaries in the early to mid-Berriasian, late Berriasian, mid-Valanginian, mid-Hauterivian, late Hauterivian and early to mid-Barremian. These major events appear to be those used by Hoedemaeker & Herngreen (2003, foldout chart). Hoedemaeker & Herngreen (2003, p. 261) also indicate that Hoedemaeker had used the foraminiferal data of Fletcher (1973) and the ostracod data of Neale (1962b) in his (Hoedemaeker 1998, 2002) interpretation of the D Beds of the Speeton Clay Formation. This appears to be the only reference to the use of microfossils in the interpretation of the sequence stratigraphy in the lower part of the Speeton Clay Formation.

The MFS is usually identified as the most clay-rich part of the sequence (Emery & Myers 1996), often identified in well logs by the presence of a higher gamma-ray record. This clay-rich environment will leave a very different faunal signal, compared with silts or sands elsewhere in the succession. How this faunal signal is interpreted is now described.

Interpretation of the benthic fauna

Any fauna recorded in geological samples is the result of:

- The initial fauna that was living on or within the sediment;
- Post-mortem taphonomy (including transport in and transport out);
- Diagensis and compaction;
- Changes during burial and geological time; modern weathering and exhumation (if not collected from the subsurface); and
- Errors introduced during sampling, processing and analysis.

In order to understand the processes involved in the distribution of benthic foraminifera within sequences we have investigated the controls on a modern assemblage and then attempted to understand the anticipated post-depositional changes.

Plymouth Sound – a modern analogue

In Plymouth Sound, a large drowned valley system on the Devon/Cornwall boundary in S. W. England we have, over a number of years, collected sea floor samples from fixed sites and documented the changes in the benthic foraminifera from1973 onwards and over annual cycles (1994–1996 and 2007–2008). All samples collected in this on-going project were placed in buffered formalin on the boat and then washed and stained with rose Bengal (to identify the "living" foraminifera) within a few hours. In Figure 3 it can be seen that the sites cover a range of substrates, including sand, sand waves, shell gravel, mixed mud/sand/gravel and mud. When the diversity and annual production are calculated for these sample sites the data are quite interesting (Fig. 4). Sample 9

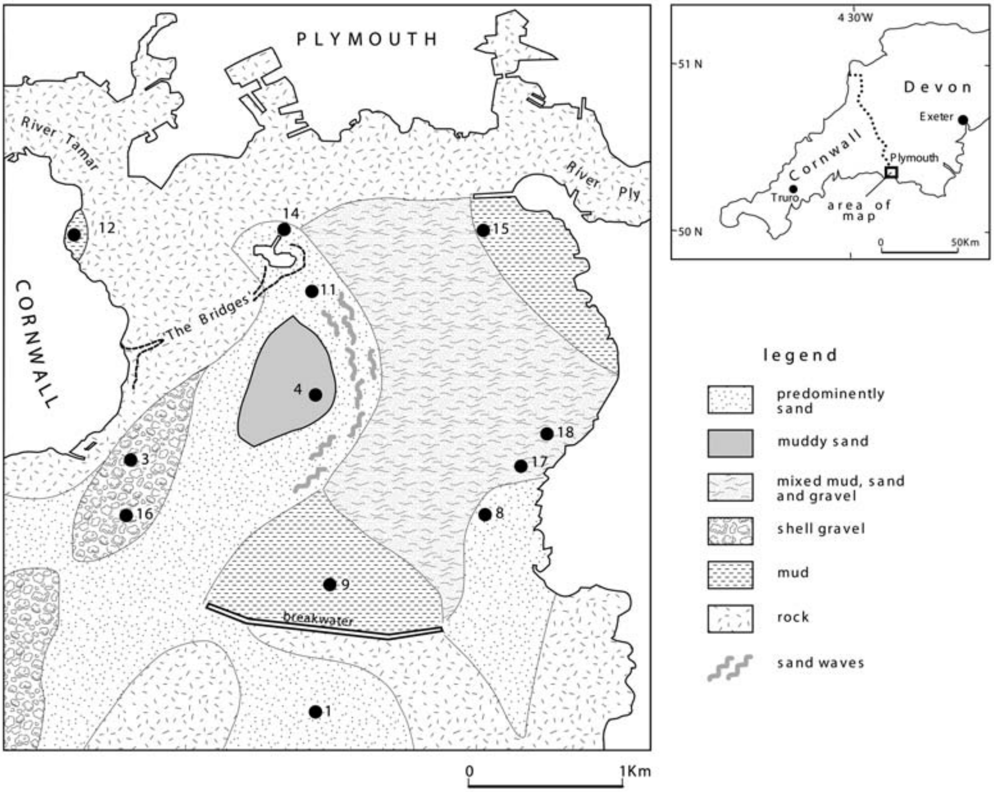

Plymouth Sound with station locations showing idealised sediment type and distribution.
Based on mapping carried out by Fiona Fitzpatrick (1991)

Fig. 3: Sediment distribution map of Plymouth Sound and the location of some of the sampling sites used in the monthly analysis (1994–1996) of the benthic foraminifera (after CASTIGNETTI et al. 2000)

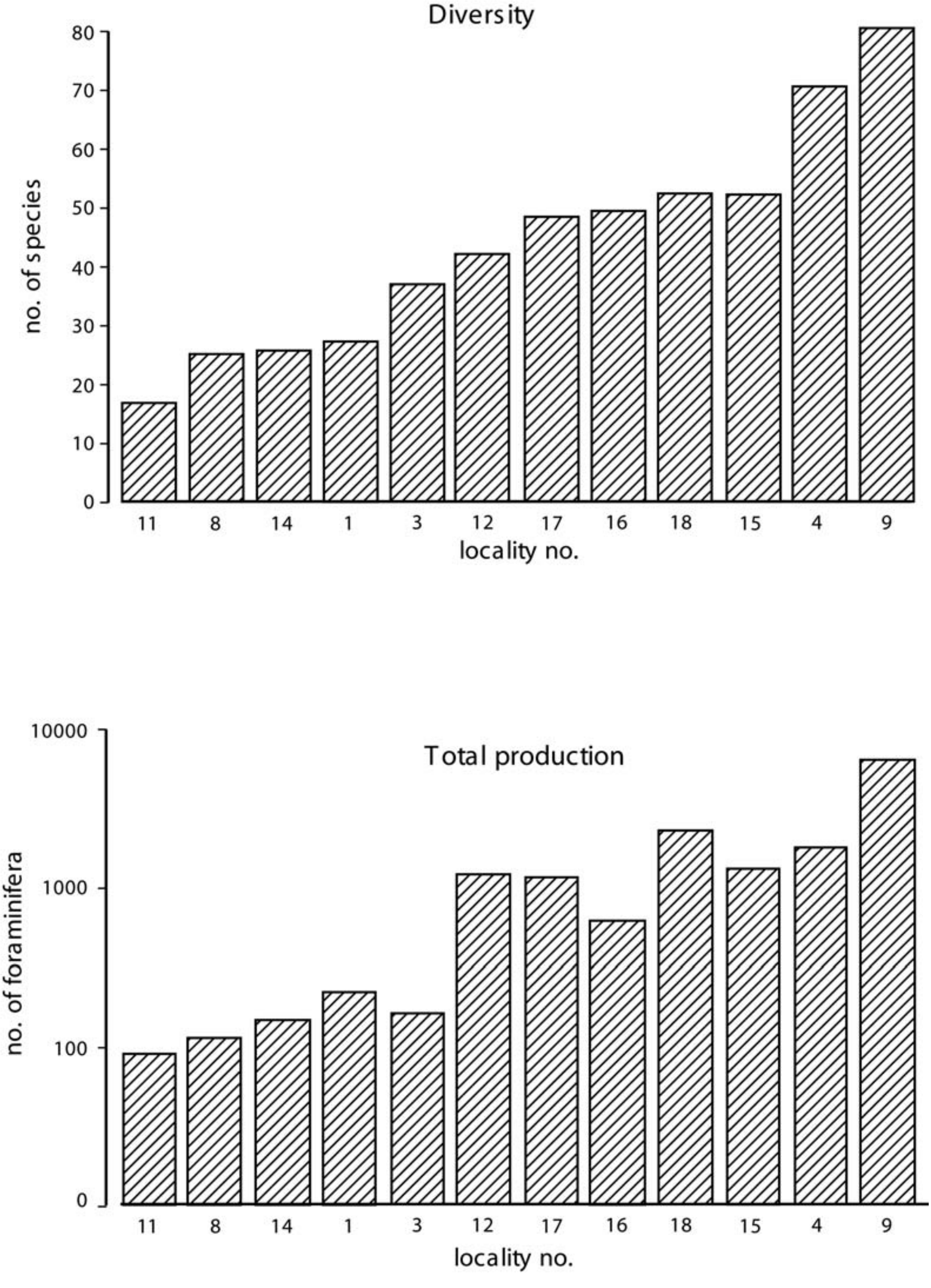

Fig. 4: Graphical plots of annual species diversity and annual total production of benthic foraminifera for the sites indicated in Figure 3 (after CASTIGNETTI 1997). Note the logarithmic scale for the numbers of foraminifera in the graph for Total Production.

(mud) records the highest diversity while the sand wave environment is the lowest with other sand environments also recording low values. The graphs for total annual production, though not quite identical, provide a very similar pattern between the mud (highest) and sands (lowest).

As in all ecological studies the controls on the fauna are complex but it is clear that in the nutrient-rich clays there is an abundant, diverse fauna with the nutrient-poor sands supporting only a poor, *in-situ* living fauna. It is also clear that the faunas in the clay-rich environments will be enhanced by the slow rate of sedimentation and that any micropalaeontological sample from a geological succession must include a significant number of yearly standing crops compared with the dilution effect of the higher rates of sedimentation in the more sand-rich environments. Compaction will further accentuate this situation with clays often being subjected to 50 % reduction in thickness as water is removed. This compaction can be evidenced in the Speeton Clay Formation by the generally compressed nature of the agglutinated taxa (e.g., *Ammobaculites*, *Haplophragmoides*, etc.).

In recent years a number of investigations of the preservation potential of foraminifera have been undertaken by MURRAY (1989), ALVE & MURRAY (1995) and MURRAY & ALVE (2000). It is particularly noted by MURRAY & ALVE (2000) that high diversity agglutinated assemblages can be derived from high diversity assemblages dominated by calcareous taxa through the selective dissolution of the calcareous component over time. This process will particularly impact on the aragonitic taxa and, in the Jurassic and Cretaceous, the epistominids will often only be recorded in the dense, clay-rich parts of the succession that have acted as aquacludes to ground water movement (Fig. 5). In some parts of this, and other, clay successions epistominids are also preserved as pyrite steinkerns or, even when the outer test survives, an infilling of pyrite. Deposition of pyrite within the tests of foraminifera is normally limited to organic-rich clay environments.

Using the model shown in Figure 5 it is relatively simple to argue that the EMERY & MYERS (1996, fig. 6.14a) interpretation of faunas in an idealised sequence is correct and that, in geological settings, we should expect both variation in diversity, quality of preservation (including collapsed agglutinated taxa) and a presence/absence of aragonitic taxa.

Foraminifera in the Speeton Clay Formation

As indicated above, the lower part of the Speeton Clay Formation contains a quite diverse assemblage of benthic foraminifera. The fauna is dominated by *Lenticulina* spp. many of which are well-known across Eastern England, the North Sea Basin (CRITTENDEN 1988) and North Germany (see HECHT 1938; BARTENSTEIN & BETTENSTAEDT 1962). Other wide-ranging, diagnostic taxa are members of the Superfamily Ceratobuliminacea (*Epistomina* and *Hoeglundina*); both of which have aragonitic tests. As shown in Figure 6, many of these aragonitic species are relatively well-preserved, although many are in-filled with pyrite (also an indicator of organic-rich, clay environments).

When the species diversity data for the lower part of the Speeton Clay Formation are plotted (Fig. 7) it is evident that there are two main “cycles”. One is Lower to mid-

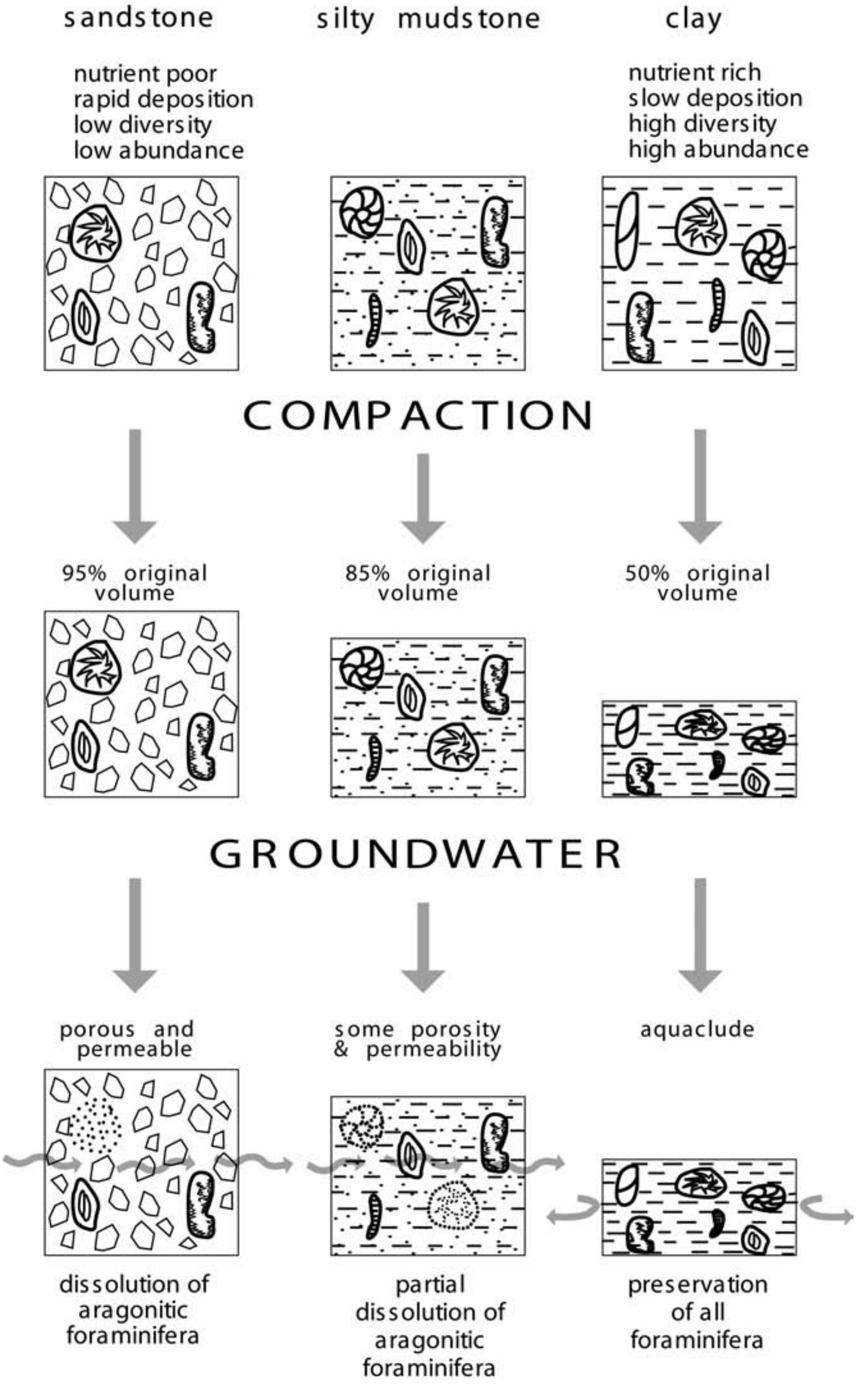

Fig. 5: Theoretical model for the history of a "sample" from deposition to final collection, showing the effects of taphonomy, compaction and dissolution by groundwater flow (after OXFORD et al. 2004).

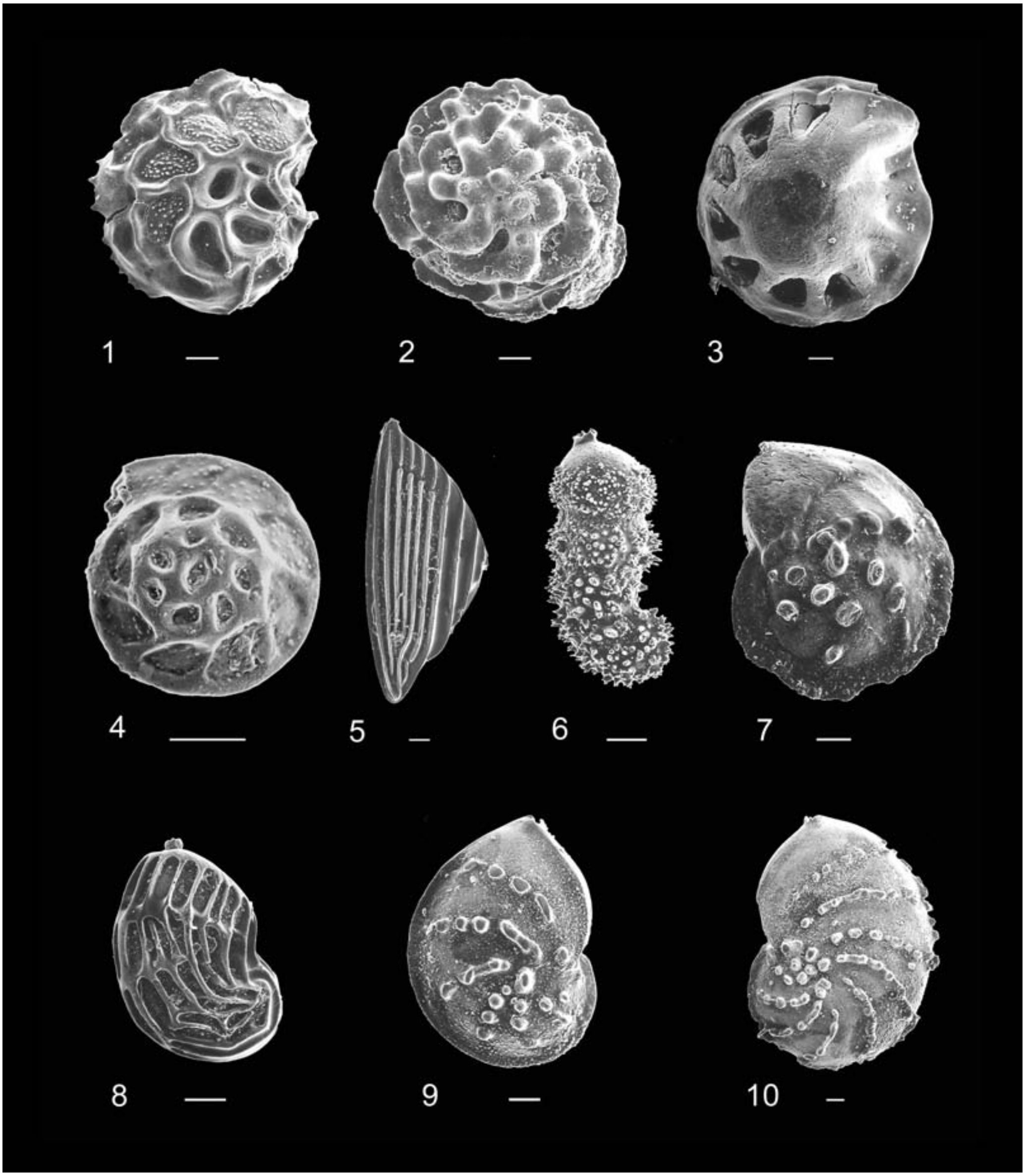

Fig. 6: Representative species of foraminifera from the Speeton Clay Formation, Filey Bay, N. E. England. (1) *Epistomina ornata* (ROEMER), Hauterivian (Bed C4); (2) *Epistomina ornata* (ROEMER), Hauterivian (Bed C4); (3) *Hoeglundina caracolla* (ROEMER), Barremian (Bed LB4D); (4) *Epistomina hechti* BARTENSTEIN & BOLLI, Barremian (Bed LB2); (5) *Citharina harpa* (ROEMER), Hauterivian (Bed C4E); (6) *Marginulinopsis foeda* (REUSS), Hauterivian (Bed C4C); (7) *Lenticulina eichenbergi* BARTENSTEIN & BRAND, Hauterivian (Bed C7); (8) *Lenticulina schreiteri* (EICHENBERG), Hauterivian (Bed C2F); (9) *Lenticulina guttata* (TEN DAM); and (10) *Lenticulina guttata* (TEN DAM), Hauterivian (Bed C3). All of the scale bars represent 100 µm. The figured specimens (and other material from the Speeton Clay Formation) are in the Micropalaeontology Collections (under the heading “Stratigraphic Index of Fossil Foraminifera”) of the University of Plymouth.

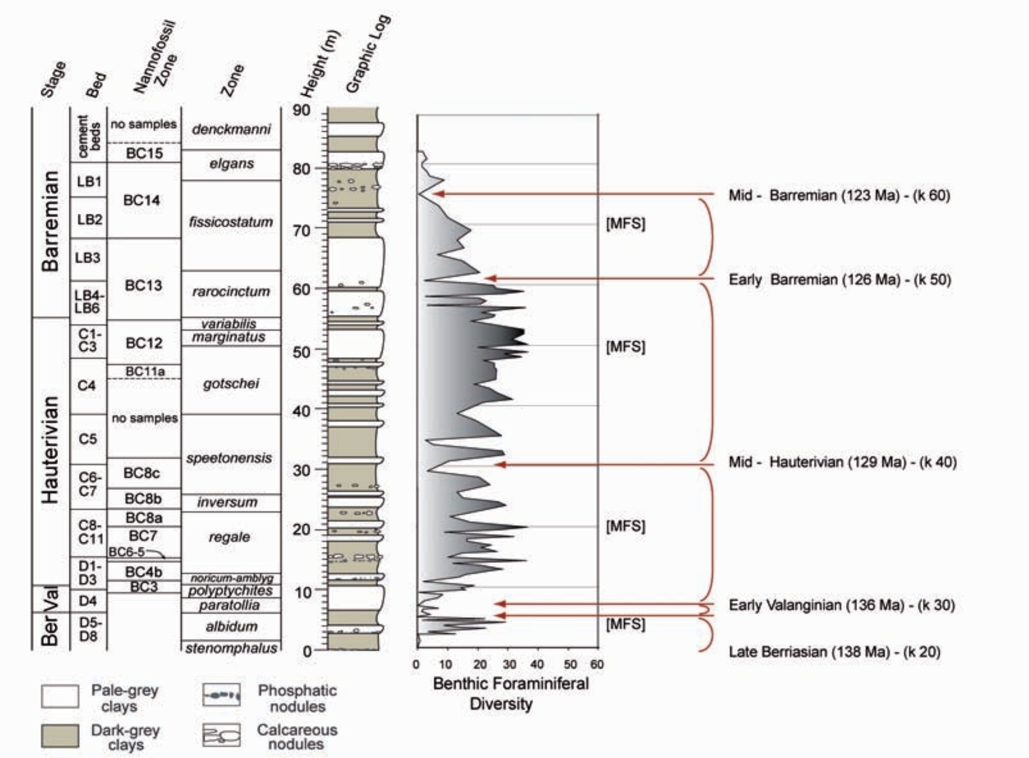

Fig. 7: The Speeton Clay Formation in the Filey Bay succession, including lithostratigraphy, biostratigraphy, species diversity of benthic foraminifera and interpretation of the sequence stratigraphy. The “no samples” marked in the calcareous nannofossil column refers (here and in Figs 8, 9) to samples solely for nannofossil work and not samples for stable isotopes or foarminifera.

Hauterivian with another in the mid-Upper Hauterivian, with a (?) sequence boundary in the mid-Hauterivian (~129 Ma) which appears close to the SHARLAND et al. (2001) K40 event. This is, almost certainly, the mid-Hauterivian event identified by RAWSON & RILEY (1982) and close to the mid-Hauterivian discontinuity identified by HOEDEMAEKER & HERNGREEN (2003). The end of the upper cycle appears to be in the Early Barremian (~126 Ma), with another sequence boundary a little higher in the mid-Barremian (~123 Ma). Both of these events appear to be close to K50 and K60 of the SHARLAND et al. (2001) model and some of the sequence boundaries and maximum flooding events identified by COPESTAKE et al. (2003).

There is a fairly prominent maximum flooding event in the latest Berriasian/Ryazanian (*Peregrinoceras albidum* Zone) followed by a regression or sequence boundary in the earliest Valanginian (~136 Ma = K30). While we have no desire to overplay what the foraminiferal distribution tells us, it does appear to be the case that the major cycles (sequences) are in some agreement with other Lower Cretaceous data. The pattern recorded by the foraminifera also confirms why the ammonites are largely seen in the Hauterivian as that appears to be the most “open” marine part of the succession

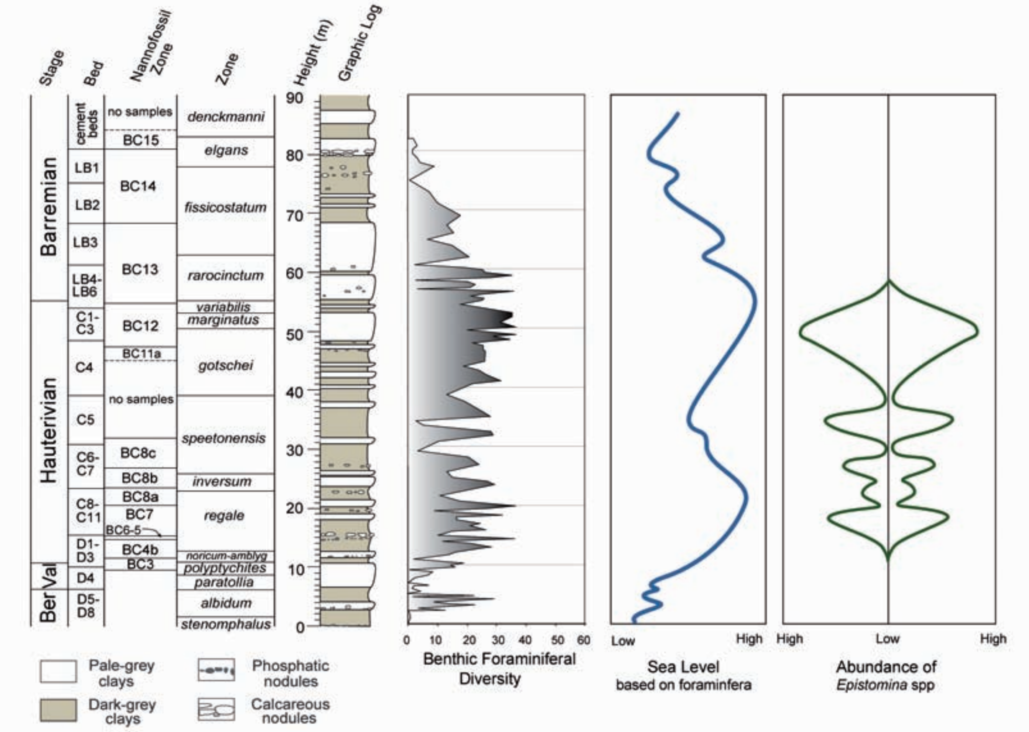

Fig. 8: The Speeton Clay Formation in the Filey Bay succession, including lithostratigraphy, biostratigraphy, diversity of benthic foraminifera, suggested sea level changes and schematic distribution of *Epistomina* and *Hoeglundina*.

(Fig. 8). This is supported by the distribution of the aragonitic foraminifera, which reach their maximum levels of abundance in the Hauterivian and earliest Barremian. The distribution of *Epistomina* and *Hoeglundina* in the sequences identified here is comparable to that recorded by OXFORD et al. (2004) in the Oxfordian (Jurassic). Using the diversity data and the known distribution of taxa (FLETCHER 1973; HART et al. 1989) it is possible to interpret the sea level changes in a general way (Fig. 7). There is, in this interpretation, a relatively close correspondence with some of the transgressive/regressive cycles identified by DE GRACIANSKY et al. (1998, chart 4).

Stable isotope stratigraphy

Figure 9 shows the $\delta^{18}O$ and $\delta^{13}C$ data (from PRICE et al. 2000; MCARTHUR et al. 2003), together with the diversity curve. The carbon isotope profile shows a clear trend through the studied section from $\delta^{13}C$ values around 0.0‰ during the early Valanginian (*Paratollia–Polyptychites* beds) to more positive values during the early Hauterivian interval. Such an abrupt change in $\delta^{13}C$ values, a characteristic feature of a stratigraphic break, maybe correlated with the late Valanginian-early Hauterivian positive carbon isotope event observed by WEISSERT (1989). The Valanginian positive carbon isotope excursion has been related to episodes of platform drowning within Tethys whereby the leaching of nutrients on coastal lowlands during a rise in sea-level resulted in increased ocean fertilization, productivity and an expansion of the oxygen minimum zone (e.g., WEISSERT 1989). This, in turn, leads to global sea-waters enriched in δ^{13}C. Such a trend is consistent with the sea level curve based on foramiferal diversity data and the known distribution of taxa. What is more difficult to reconcile is the oxygen isotope data and sea level curve. Increasingly negative δ^{18}O carbonate values can be related to elevated temperatures in environmental settings where continental ice volume is at a minimum and evaporation or freshwater input are minor factors. Hence assuming that these conditions apply, from the Valanginian through into the Hauterivian oxygen isotope values become more positive, possibly indicative of cooling and decrease to more negative values in the Barremian (i.e., warming). The postulated sea level curve would, however, appear to suggest the opposite and this discrepancy has yet to be resolved. It may simply be a function of the scale of the relatively minor sea level changes involved. The mid-Barremian is also a time of plate re-adjustment in North West Europe (e.g., opening of the Bay of Biscay).

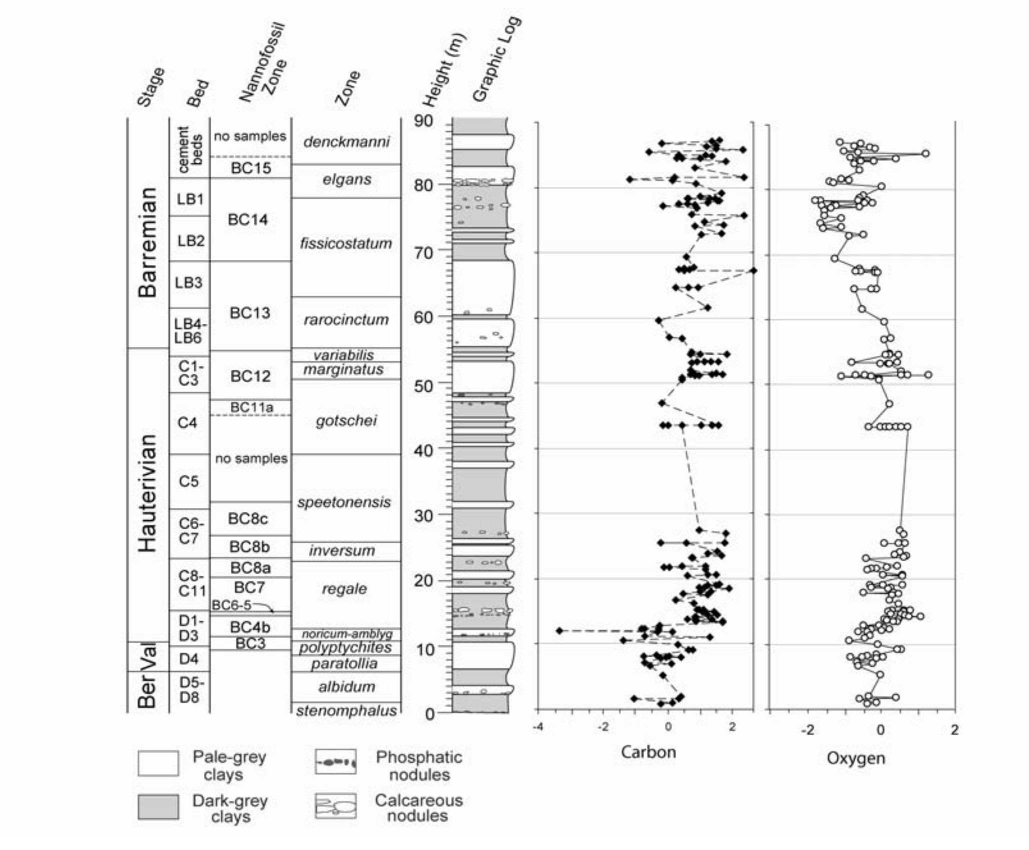

Fig. 9: The Speeton Clay Formation in the Filey Bay succession, including lithostratigraphy, biostratigraphy and the carbon and oxygen stable isotope data (from PRICE et al. 2000; MCARTHUR et al. 2003).

Summary

The distribution of benthic foraminifera in the Speeton Clay Formation does appear to record the major sequences (sequence boundaries and "zones" of maximum flooding). While not perfect, the resulting pattern does seem to show some agreement with other interpretations of the succession. The recorded pattern has been discussed in the light of on-going research on modern environments and a model is presented for discussion. The very "spiky" nature of the diversity curve is what was found by OXFORD et al. (2004) in Oxfordian strata on the Dorset Coast and it either represents "noise" in the diversity graph or, more significantly, parasequences that would require very close sampling to resolve.

Acknowledgements

The authors wish to thank Dr Brian Fletcher and the late Professor John Neale for their advice and wise counsel on the stratigraphy and micropalaeontology of the Speeton Clay Formation. The helpful suggestions of two reviewers (Prof. P. Rawson and Dr C. Underwood) are also acknowledged. Mr John Abraham is thanked for the production of some of the figures.

References

ALVE, E. & MURRAY, J.W. (1995): Experiments to determine the origin and palaeoenvironmental significance of agglutinated foraminiferal assemblages. – In: KAMINSKI, M.A., GEROCH, S. & GASINSKI, M.A. (eds): Proceedings of the Fourth International Workshop on Agglutinated Foraminifera, Grzybowski Foundation Special Publication, **3**: 1-11.

ARMENTROUT, J.M. (1987): Integration of biostratigraphy and seismic stratigraphy: Pliocene – Pleistocene, Gulf of Mexico. – In: Gulf Coast Section, Society of Economic Paleontologists and Mineralogists, Eighth Annual Research Conference, 6-14.

––– (1991): Paleontologic constraints on depositional modelling; examples of integration of biostratigraphy and seismic stratigraphy, Gulf of Mexico. – In: WEIMER, P. & LINK, M.H. (eds): Seismic facies and sedimentary processes of submarine fans and turbidite systems. – pp. 137-170, Berlin (Springer-Verlag).

––– & CLEMENT, J.F. (1990): Biostratigraphic correlation of depositional cycles: a case study in High Island-Galveston-East Breaks areas, offshore Texas. – In: Gulf Coast Section, Society of Economic Paleontologists and Mineralogists, Eleventh Annual Research Conference: 21-51.

––– , ECHOLS, R.C. & LEE, T.D. (1990): Patterns of foraminiferal abundance and diversity: implications for sequence stratigraphic analysis. – In: Gulf Coast Section, Society of Economic Paleontologists and Mineralogists, Eleventh Annual Research Conference: 53-58.

––– , FEARN, B., RODGERS, K., ROOT, S., LYLE, W.D., HERRICK, D.C., BLOCH, R.B., SNEDDEN, J.W. & NWANKO, B. (1999): High-resolution sequence biostratigraphy of a lowstand prograding delta wedge: Oso Field (late Miocene), Nigeria. – In: JONES, R.W. & SIMMONS, M.D. (eds): Biostratigraphy in Production and Development Geology. – Geological Society, London, Special Publications, **152**: 259-290.

BANNER, F. T. & DESAI, D. (1988): A review and revision of the Jurassic – Early Cretaceous Globigerinina, with especial reference to the Aptian assemblages of Speeton, (North Yorkshire, England). – Journal of Micropalaeontology, **7**: 143-185.

BARTENSTEIN, H. & BETTENSTAEDT, F. (1962): Marine Unterkreide (Boreal und Tethys). -In: SIMON, W. & BARTENSTEIN, H. (eds): Leitfossilien der Mikropaläontologie – pp. 225-297, Berlin (Gebruder Borntraeger).

BERTHELIN, G. (1880): Mémoire sur les Foraminifères de l'Étage Albien de Montcley (Doubs). – Mémoire Société géologique de France, **1**(5): 1-84.

BLACK, M. (1971): Coccoliths of the Speeton Clay and Sutterby Marl. – Proceedings of the Yorkshire Geological Society, **38**: 381-424.

BRASIER, M. D. (1980): Microfossils. – 193 p., London (George Allen & Unwin).

CAMERON,T. D. J., CROSBY, A., BALSON, P. S., JEFFERY, D. H., LOTT, G. K., BULAT, J. & HARRISON, D. J. (1992): The geology of the southern North Sea. United Kingdom Offshore Regional Report, British Geological Survey. London (HMSO).

CASTIGNETTI, P. (1997): Population dynamics and facies association of Recent foraminifera from a nearshore marginal marine environment: Plymouth Sound. Unpublished Ph.D. Thesis, University of Plymouth [2 volumes].

——, HART, M.B. & MANLEY, C.J. (2000): *Technitella* (Norman, 1878) from Plymouth Sound, South Devon, U.K. – In: HART, M.B., KAMINSKI, M.A. & SMART, C.W. (eds): Proceedings of the Fifth International Workshop on Agglutinated Foraminifera. – Grzybowski Foundation Special Publication, **7**: 81-88.

COPESTAKE, P., SIMS, A. P., CRITTENDEN, S., HAMAR, G. P., INESON, J. R., ROSE, P. T. & TRINGHAM, M. E. (2000): Lower Cretaceous. – In: EVANS, D., GRAHAM, C., ARMOUR, A. & BATHURST, P. (eds): The Millenium Atlas: Petroleum Geology of the Central and Northern North Sea. – pp. 191-211, London (Geological Society).

CRITTENDEN, S. (1988): The Lithostratigraphy and Biostratigraphy (Foraminifera) of the Early Cretaceous of the Southern North Sea Basin. – Unpublished PhD Thesis, University of Plymouth: 416 pp.

CUBAYNES, R., REY, J., RUGET, C., COURTINAT, B. & BODEGAT, A.M. (1990): Relations between systems tracts and micropalaeontological assemblages on a Toarcian carbonate shelf (Quercy, southwest France). – Bulletin, Société Géologique de France, **8**: 989-993.

DE GRACIANSKY, P.-C., HARDENBOL, J., JACQUIN, T. & VAIL, P. R. (1998): Mesozoic and Cenozoic Sequence Stratigraphy of European Basins. – Society of Economic Paleontologists and Mineralogists (SEPM), Tulsa, Oklahoma, Special Publication **60**: 786 pp.

DOYLE, J. C. (1989): The stratigraphy of a late Lower Hauterivian horizon in the Speeton Clay formation (Lower Cretaceous) of East Yorkshire. – Proceedings of the Geologists' Association, **100**: 175-182.

EINSLE, G. & BAYER, U. (1991): Asymmetry in transgressive-regressive cycles in shallow seas and passive continental margin settings. – In: EINSLE, G., RICKEN, W. & SEILACHER, A. (eds): Cycles and Events in Stratigraphy. – pp. 660-681, Berlin (Springer-Verlag).

EMERY, D. & MYERS, K.J. (1996): Sequence Stratigraphy. – Blackwell Science, Oxford, 297 pp.

ENNIS, W. C. (1937): The Upper Beds of the Speeton Clay. – Transactions of the Hull Geological Society, **7**(5): 130-138.

FITZPATRICK, F. (1991): Studies of sediments in a tidal environment. – Unpublished PhD Thesis, Polytechnic South West (now University of Plymouth).

FLETCHER, B. N. (1966): Lower Cretaceous foraminifera from the Speeton Clay of Yorkshire. – Unpublished PhD Thesis, University of Hull, 428 pp.

––– (1966): A lithological subdivision of the Speeton Clay C Beds (Hauterivian), East Yorkshire. – Proceedings of the Yorkshire Geological Society, **37**: 323-327.

––– (1973): The distribution of Lower Cretaceous (Berriasian-Barremian) Foraminifera in the Speeton Clay. – In: CASEY, R. & RAWSON, P.F. (eds): The Boreal Lower Cretaceous – Geological Journal, Special Issue No. **5**: 161-168.

GALLOWAY, W. E. (1989a): Genetic stratigraphic sequences in basin analysis. 1: Architecture and genesis of flooding surface bounded depositional units. – American Association of Petroleum Geologists, Bulletin, **73**: 125-142.

––– (1989b): Genetic stratigraphic sequences in basin analysis. ll: Application to northwest Gulf of Mexico Cenozoic basin. – American Association of Petroleum Geologists, Bulletin, **73**: 143-154.

HART, M.B. (1997): The application of micropalaeontology to sequence stratigraphy: an example from the chalk of south-west England. – Proceedings of the Ussher Society, **9**: 158-163.

––– (2000): Foraminifera, sequence stratigraphy and regional correlation; an example from the uppermost Albian of Southern England. – Revue de Micropaléontologie, **43**: 27-45.

––– , BAILEY, H. W. CRITTENDEN, S., FLETCHER, B. N., PRICE, R. J. & SWIECICKI, A. (1982): Cretaceous. – In: JENKINS, D. G. & MURRAY, J. W. (eds): Stratigraphical Atlas of Fossil Foraminifera [1st Edition]. – pp. 149-227, Chichester (Ellis Horwood Ltd).

––– , BAILEY, H. W. CRITTENDEN, S., FLETCHER, B. N., PRICE, R. J. & SWIECICKI, A. (1989): Cretaceous. – In: JENKINS, D. G. & MURRAY, J. W. (eds): Stratigraphical Atlas of Fossil Foraminifera [2nd Edition]. – pp. 273-371, Chichester (Ellis Horwood Ltd).

HECHT, F. E. (1938): Standard Gleiderung der Nordwestdeutschen Unterkreide nach Foraminifera. – Abhandlungen Senckenberg Naturforschende Gesellschaft, **443**: 1-42.

HENDERSON, A. S. (1997): The palaeoecology and biostratigraphy of the Foraminifera from the Oxfordian of North Dorset. – Unpublished PhD Thesis, University of Plymouth, 385 pp.

––– & HART, M. B. (2000): The distribution of Foraminiferida in the Oxfordian sequences of North Dorset. – GeoResearch Forum, **6**: 311-320.

HOEDEMAEKER, P. J. (1995): Ammonite evidence for long-term sea-level fluctuations between the 2nd and 3rd order in the lowest Cretaceous. – Cretaceous Research, **16**: 231-241.

––– (1998): A Tethyan-Boreal correlation of pre-Aptian Cretaceous strata: correlating the uncorrelatables. – Geologica Carpathica, **50**: 101-124.

––– (2002): Correlating the uncorrelatables: a Tethyan-Boreal correlation of pre-Aptian Cretaceous strata. – In: MICHALÍK, J. (ed.): Tethyan/Boreal Cretaceous Correlation. Mediterranean and Boreal Cretaceous palaeobiogeographic areas in Central and Eastern Europe. – pp. 235-284, Bratislava (Publishing House of the Slovak Academy of Sciences).

––– & LEEREVELD, H. (1995): Biostratigraphy and sequence stratigraphy Of the Berriasian-lowest Aptian (Lower Cretaceous) of the Río Argos succession, Caravaca, SE Spain. – Cretaceous Research, **16**: 195-230.

––– & HERNGREEN, G. F. W. (2003): Correlation of Tethyan and Boreal Berriasian – Barremian strata with emphasis on strata in the subsurface of the Netherlands. – Cretaceous Research, **24**: 253-275.

JUDD, J. W. (1868): On the Speeton Clay. – Quarterly Journal of the Geological Society of London, **24**: 218-250.

KAYE, P. (1964): Observations on the Speeton Clay (Lower Cretaceous). – Geological Magazine, **101**: 340-356.

KEMPER, E., RAWSON, P. F. & THIEULOY, J.–P. (1981): Ammonites of Tethyan ancestry in the early Lower Cretaceous of north–west Europe. – Palaeontology, **24**: 251-311.

KIRBY, G. A. & SWALLOW, P. (1987): Tectonism and sedimentation in the Flamborough Head region of north-east England. – Proceedings of the Yorkshire Geological Society, **46**: 301-309.

KOUTSOUKOS, E. A. M. & HART, M. B. (1990): Cretaceous foraminiferal morphogroup distribution patterns, palaeocommunities and trophic structures; a case study from the Sergipe Basin, Brazil. – Transactions of the Royal Society of Edinburgh: Earth Sciences, **81**: 221-246.

KHAN, M. H. (1962): Lower Cretaceous index foraminifera from northwestern Germany and England. – Micropaleontology, **8**: 385-390.

LAMPLUGH, G. W. (1889): On the subdivisions of the Speeton Clay. – Quarterly Journal of the Geological Society of London, **52**: 575-618.

——— (1924): A review of the Speeton Clays. – Proceedings of the Yorkshire Geological Society, **20**: 1-31.

LECKENBY, J. (1859): Note on the Speeton Clay of Yorkshire. – Geologist, **2**: 9-11.

MCARTHUR, J.M., MUTTERLOSE, J., PRICE, G.D., RAWSON, P.F., RUFFELL, A.H. & THIRLWALL, M.F. (2004): Belemnites of Valanginian, Hauterivian and Barremian age: Sr-isotope stratigraphy, composition (^{87}Sr/^{86}Sr, δ^{13}C, δ^{18}O,Na, Sr, Mg), and palaeo-oceanography. – Palaeogeography, Palaeoclimatology, Palaeoecology, **202**: 253-272.

MITCHELL, S. F. & UNDERWOOD, C. J. (1999): Lithological and faunal stratigraphy of the Aptian and Albian (Lower Cretaceous) of the type Speeton Clay, Speeton, N. E. England. – Proceedings of the Yorkshire Geological Society, **52**: 277-296.

MONTANEZ, I. P. & OSLEGER, D. A. (1993): Parasequence stacking patterns, third-order accommodation events, and sequence stratigraphy of Middle to Upper Cambrian platform carbonates, Bonanza King Formation, southern Great Basin. – In: LOUCKS, R.G. & SARG, J.F. (eds): Carbonate sequence stratigraphy: Recent developments and applications. – American Association of Petroleum Geologists, Memoir, **57**: 305-326.

MURRAY, J.W. (1989): Syndepositional dissolution of calcareous foraminifera in modern shallow-water sediments. – Marine Micropaleontology, **15**: 117-121.

——— (1991): Ecology and Palaeoecology of Benthic Foraminifera. – 397 p. Harlow, England (Longman Scientific & Technical, Longman Group UK Limited).

——— & ALVE, E. (2000): Do calcareous dominated shelf foraminiferal assemblages leave worthwhile ecological information after their dissolution? – In: HART, M.B., KAMINSKI, M.A. & SMART, C.W. (eds): Proceedings of the Fifth International Workshop on Agglutinated Foraminifera. – Grzybowski Foundation Special Publication, **7**: 311-331.

MUTTERLOSE, J. (1990): A belemnite scale for the Lower Cretaceous. – Cretaceous Research, **11**: 1-16.

MUTTERLOSE, J., PINCKNEY, G. & RAWSON, P. F. (1987): The belemnite Acroteuthis in the Hibolites beds (Hauterivian – Barremian) of North West Europe. – Palaeontology, **30**: 635-645.

NEALE, J. W. (1960a): The subdivision of the Upper D Beds of the Speeton Clay of Speeton, East Yorkshire. – Geological Magazine, **97**: 353-362.

——— (1960b): Marine Lower Cretaceous Ostracoda from Yorkshire, England. – Micropaleontology, **6**: 203-224.

——— (1962a): Ammonoidea from the Lower D Beds (Berriasian) of the Speeton Clay. – Palaeontology, **5**: 272-296.

——— (1962b): Ostracoda from the type Speeton Clay (Lower Cretaceous) of Yorkshire. – Micropaleontology, **8**: 425-484.

——— (1968): Biofacies and lithofacies of the Speeton Clay D Beds, E. Yorkshire. – Proceedings of the Yorkshire Geological Society, **36**: 309-335.

——— (1973): Ostracoda as a means of correlation in the Boreal Lower Cretaceois, with special reference to the British marine Ostracoda. – In: CASEY, R. & RAWSON, P. F. (eds): The Boreal Lower Cretaceous – Geological Journal, Special Issue No. **5**: 169-184.

——— (1978): The Cretaceous. – In: BATE, R. H. & ROBINSON, E. (eds): A Stratigraphical Index of British Ostracoda – Geological Journal, Special Issue No. **8**: 325-384.

OLIVER, G.M. (1998): High resolution sequence stratigraphy and diagenesis of mixed carbonate/siliciclastic successions. – Unpublished Ph.D. Thesis, University of Plymouth.

OLSSON, R.K. (1988): Foraminiferal modelling of sea-level change in the Late Cretaceous of New Jersey. – In: WILGUS, C.K. et al. (eds): Sea-level change: an integrated approach. – Society of Economic Paleontologists and Mineralogists Special Publication, **42**: 289-298.

OXFORD, M.J., HART, M.B. & WATKINSON, M.P. (2000): Micropalaeontological investigations of the Oxford Clay – Corallian succession of the Dorset Coast. – Geoscience in south-west England, **10**: 9-13.

——— , HART, M.B. & WATKINSON, M.P. (2004): Foraminiferal characterisation of Mid-Upper Jurassic sequences in the Wessex Basin (United Kingdom). – Rivista Italiana di Paleontologia e Stratigrafia, **110**: 209-218.

PACHT, J.A., BOWEN, B.E., BEARD, J.H. & SHAFFER, B.L. (1990): Sequence stratigraphy of Plio-Pleistocene depositional facies in the offshore Louisiana south additions. – Gulf Coast Association of Geological Societies, Transactions, **40**: 1-18.

PERCH-NIELSEN, K. (1979): Calcareous nannofossils from the Cretaceous between the North Sea and the Mediterranean. – In: WEIDMANN, J. (ed.): Aspekte der Kreide Europas. – International Union of Geological Sciences, Series A, No. **6**, 223-272, Stuttgart (E. Schweizerbart'sche Verlagsbuchhandlung).

PINCKNEY, G. & RAWSON, P. F. (1974): Acroteuthis assemblages in the Upper Jurassic and Lower Cretaceous of northwest Europe. – Newsletters in Stratigraphy, **3**: 193-204.

PINCKNEY, G. (1975): The belemnite genus Acroteuthis in the Late Jurassic and early Lower Cretaceous of northwest Europe. – Unpublished PhD Thesis, University of London, 239 pp.

POWELL, A. J. (1992): Making the most of microfossils. – Geoscientist, **2**: 12-16.

PRICE, G.D., RUFFELL, A.H., JONES, C.E., KALIN, R.M. & MUTTERLOSE, J. (2000): Isotopic evidence for temperature variation during the early Cretaceous (late Ryazanian-mid Hauterivian). – Journal of the Geological Society, London, **157**: 335-344.

RAWSON, P. F. (1971a): Lower Cretaceous ammonites from north-east England: the Hauterivian genus Simbirskites. – Bulletin of the British Museum Natural History (Geology), **20**: 25-86.

——— (1971b): The Hauterivian (Lower Cretaceous) biostratigraphy of the Speeton Clay of Yorkshire, England. – Newsletters in Stratigraphy, **1**: 61-75.

——— (1975): Lower Cretaceous ammonites from north-east England: the Hauterivian heteromorphy *Aegocrioceras*. – Bulletin of the British Museum Natural History (Geology), **26**: 129-159.

——— (2006): Cretaceous: sea levels peak as the North Atlantic opens. – In: BRENCHLEY, P. J. & RAWSON, P. F. (eds): The Geology of England and Wales. – pp. 365-393, London (Geological Society).

——— & MUTTERLOSE, J. (1983): Stratigraphy of the Lower B and basal Cement Beds (Barremian) of the Speeton Clay, Yorkshire, England. – Proceedings of the Geologists' Association, **94**: 133-146.

——— & RILEY, L. A. (1982): Latest Jurassic-Early Cretaceous events and the 'Late Cimmerian Unconformity in the North Sea area. – American Association of Petroleum Geologists, Bulletin, **66**: 2628-2648.

——— , CURRY, D., DILLEY, F. C., HANCOCK, J. M., KENNEDY, W. J., NEALE, J. W., WOOD, C. J. & WORSSAM, B. C. (1978): A correlation of Cretaceous rocks in the British Isles. – Geological Society of London, Special Report No. **9**, 70 pp.

RÜCKHEIM, S., BORNEMANN, A. & MUTTERLOSE, J. (2006): Integrated stratigraphy of an Early Cretaceous (Barremian–Early Albian) North Sea borehole (BGS 81/40). – Cretaceous Research, 27: 447-463.

SHAFFER, B.L. (1987): The potential of calcareous nannofossils for recognising Plio-Pleistocene climatic cycles and sequence boundaries on the shelf. – Gulf Coast Section of the Society of Economic Paleontologists and Mineralogists, Eighth Annual Research Conference: 142-145.

——— (1990): The nature and significance of condensed sections in Gulf Coast late Neogene stratigraphy. – Gulf Coast Association of Geological Societies, Transactions, **40**: 186-195.

SHARLAND, P.R., ARCHER, R., CASEY, D.M., DAVIES, R.B., HALL, S.H., HEWARD, A.P., HORBURY, A.D. & SIMMONS, M.D. (2001): Arabian Plate Sequence Stratigraphy. – GeoArabia Special Publication **2**, Bahrain (Gulf PetroLink).

SHERLOCK, R. L. (1914): The foraminifera of the Speeton Clay of Yorkshire. – Geological Magazine, **6**: 216-222, 255-265, 289-296.

SIMMONS, M.D., WILLIAMS, C.L. & HART, M.B. (1991): Sea level changes across the Albian-Cenomanian boundary in south-west England. – Proceedings of the Ussher Society, **7**: 408-412.

SISSINGH, W. (1977): Biostratigraphy of Cretaceous calcareous nannoplankton. – Geologie en Mijnbouw, **56**: 37-65.

SPAETH, C. (1971): Untersuchungen an Belemniten des Formenkreises um Neohibolites minimus (Miller 1826) aus dem Mittel- und Ober-Alb Nordwestdeutschlands. – Geologisches Jahrbuch, **100**: 127 pp.

STRASSER, A., PITTET, B. & PASQUIER, J.-B. (1994): Multiplication of maximum-flooding surfaces, sequence boundaries, and transgressive surfaces as a response to high- frequency sea-level fluctuations. – 14th International Sedimentological Congress, Rio de Janeiro, Abstracts: 70-72.

——— , PITTET, B., HILLGÄRTNER, H. & PASQUIER, J.-B. (1999): Depositional Sequences in shallow carbonate-dominated sedimentary systems: concepts for a high-resolution analysis. – Sedimentary Geology, **128**: 201-221.

SWINNERTON, H. H. (1936-1955): A monograph of British Lower Cretaceous Belemnites. – Palaeontographical Society Monograph, 86 pp.

TAYLOR, R. J. (1978a): The distribution of calcareous nannofossils in the Speeton Clay (Lower Cretaceous) of Yorkshire. – Proceedings of the Yorkshire Geological Society, **42**: 195-209.

——— (1978b): The biostratigraphy of Lower Cretaceous calcareous nannoplankton from northwest Europe and North Africa. – Unpublished PhD Thesis, University of London, 362 pp.

——— (1982): Lower Cretaceous (Ryazanian to Albian) calcareous nannofossils. – In: LORD, A. R. (ed.): A Stratigraphical Index of Calcareous Nannofossils. – pp. 40-80, Chichester (Ellis Horwood Ltd).

TEN KATE, W. G. & SPRENGER, A. (1989): On the periodicity in a calcilutite-marl succession (S. E. Spain). – Cretaceous Research, **10**: 1-31.

UNDERWOOD, C. J. & MITCHELL, S. F. (1999): Mid-Cretaceous onlap history of the Market Weighton structural high, northeast England. – Geological Magazine, **136**: 681-696.

VAIL, P. R., MITCHUM, R. M., TODD, R. G., WIDMIER, J. M., THOMPSON, S., SANGREE, J. B., BUBB, J. N. & HATLEID, W. G. (1977): – Seismic stratigraphy and global changes in sea-level. – In: PAYTON, C. E. et al. (eds): Seismic stratigraphy – applications to hydrocarbon exploration. – American Association of Petroleum Geologists, Memoir **26**: 49-62.

——— & WORNARDT, W. W. (1990): Well-log seismic stratigraphy: an integrated tool for the 1990's. – In: Sequence Stratigraphy as an Exploration Tool: concepts and practices in the Gulf Coast, Gulf Coast Section of the Society of Economic Paleontologists and Mineralogists, Eleventh Annual Research Conference, Houston: 3789-397.

VAN DER ZWAN, C. J. & BRUGMAN, W. A. (1999): Biosignals from the EA Field, Nigeria. – In: JONES, R. W. & SIMMONS, M. D. (eds): Biostratigraphy in production and development geology. – Geological Society, London, Special Publications, **152**: 291-301.

VAN WAGONER, J. C., POSAMENTIER, H. W., MITCHUM, R. M., VAIL, P. R., SARG, J. F., LOUTIT, T. S. & HARDENBOL, J. (1988): An overview of the fundamentals of sequence stratigraphy and key definitions. – In: WILGUS, C. K. & al. (eds): Sea- level changes : an integrated approach. – Society of Economic Paleontologists and Mineralogists, Memoir **42**: 39-45.

WEISSERT, H. (1989): C-isotope stratigraphy, a monitor of palaeoenvironmental change: acase study from the early Cretaceous. – Surveys in Geophysics, **10**: 1–161.